

# Coding for Gaussian Two-Way Channels: Linear and Learning-Based Approaches

Junghoon Kim, Taejoon Kim, Anindya Bijoy Das, Seyyedali Hosseinalipour, David J. Love,  
and Christopher G. Brinton

## Abstract

Although user cooperation cannot improve the capacity of Gaussian two-way channels (GTWCs) with independent noises, it can improve communication reliability. In this work, we aim to enhance and balance the communication reliability in GTWCs by minimizing the sum of error probabilities via joint design of encoders and decoders at the users. We first formulate general encoding/decoding functions, where the user cooperation is captured by the coupling of user encoding processes. The coupling effect renders the encoder/decoder design non-trivial, requiring effective decoding to capture this effect, as well as efficient power management at the encoders within power constraints. To address these challenges, we propose two different *two-way coding* strategies: linear coding and learning-based coding. For linear coding, we propose optimal linear decoding and discuss new insights on encoding regarding user cooperation to balance reliability. We then propose an efficient algorithm for joint encoder/decoder design. For learning-based coding, we introduce a novel recurrent neural network (RNN)-based coding architecture, where we propose *interactive* RNNs and a power control layer for encoding, and we incorporate bi-directional RNNs with an attention mechanism for decoding. Through simulations, we show that our two-way coding methodologies outperform conventional channel coding schemes (that do not utilize user cooperation) significantly in sum-error performance. We also demonstrate that our linear coding excels at high signal-to-noise ratios (SNRs), while our RNN-based coding performs best at low SNRs. We further investigate

This work was supported in part by ONR under grant N000142112472 and by NSF under grants ITE2226447, CNS2225577, CNS2212565, EEC1941529, and CNS2146171. A part of this work was presented at 58th Annual Allerton Conference on Communication, Control, and Computing (Allerton) in 2022 [1].

J. Kim, A. B. Das, D. J. Love, and C. G. Brinton are with the Department of Electrical and Computer Engineering, Purdue University, West Lafayette, IN, 47907 USA (e-mail: {kim3220, das207, djlove, cgb}@purdue.edu).

T. Kim is with the Department of Electrical Engineering and Computer Science, University of Kansas, KS, 66045 USA (email: taejoonkim@ku.edu).

S. Hosseinalipour is with the Department of Electrical Engineering, University at Buffalo-SUNY, NY, 14260 USA (email: alipour@buffalo.edu).

our two-way coding strategies in terms of power distribution, two-way coding benefit, different coding rates, and block-length gain.

### Index Terms

Gaussian two-way channels, communication reliability, user cooperation, linear coding, neural coding

## I. INTRODUCTION

Most of the modern communication systems, including cellular networks, WiFi networks, satellite communications, and social media platforms, facilitate two-way interaction, enabling users to exchange messages in both directions [2], [3]. This interactive capability promotes a seamless exchange of information and feedback, supports real-time communication, and fosters effective collaboration among users. The input-output model that allows for the bidirectional exchange of information is referred to as *two-way channels*, which was studied by Shannon in [4]. A practically relevant two-way channel model is the Gaussian two-way channel (GTWC), where Gaussian-distributed noise is added independently to each direction of the two-way channel between the users [5]. Earlier studies on GTWCs have been mostly focused on analyzing the channel capacity region of GTWCs. An important result was obtained by Han in [5], which revealed that incorporating the previously received symbols (i.e., feedback information) into generating transmit symbols at the users does not increase the capacity of GTWCs. In other words, the channel capacity for GTWCs is achieved when the two-way channel is considered as two independent one-way channels, i.e., when two users do not cooperate with each other.

In addition to channel capacity, communication reliability or error probability is another important metric in information/communication theory. Currently, some researchers are focusing on examining GTWCs in terms of communication reliability. In [6], Palacio-Baus and Devroye defined error exponents for GTWCs and showed how cooperations between the two users, or using previously received symbols into creating transmit symbols, can improve the error exponents in comparison to the non-cooperative case. In [7], Vasal suggested a dynamic programming (DP)-based methodology for encoding to improve the communication reliability for GTWCs. Despite ongoing efforts to improve the communication reliability for GTWCs, the existing works still lack in providing a specific coding method and its performance evaluation under a finite block-length regime.

To the best of our knowledge, there is no framework for designing practical codes in GTWCs, which is the main motivation behind this study. A foundational coding strategy for GTWCs is to carry out a *linear* processing for encoding and decoding in order to simplify the system model of GTWCs and mitigate

the coding complexity. It is important to note that GTWCs can be thought of as an expanded system model of feedback-enabled Gaussian one-way channels (GOWCs), where a linear coding framework for GOWCs with feedback has been well developed. The seminal work done by Schalkwijk and Kailath in [8] introduced a simple linear encoding for GOWCs that can achieve doubly exponential decay in the probability of error upon having noiseless feedback information. In [9], Butman introduced a general framework for linear coding, in which the noise may be colored, nonstationary, and correlated in GOWCs. In [10], Chance and Love proposed a linear encoding scheme for GOWCs with noisy feedback, which is further analyzed and revealed to be an optimal structure under some conditions for linear encoding by [11]. There have been attempts to view the linear code design in feedback-enabled GOWCs as feedback stabilization in control theory [12] and optimal DP [13]. Overall, despite the availability of well-developed frameworks of linear coding for feedback-enabled GOWCs, such a linear framework has not been developed for GTWCs, which is one of the main motivations of this work. Linear processing offers the significant advantage of low complexity for encoding/decoding with a simplified system model. However, a significant limitation of linear coding is its inherent constraint on producing optimal codes because of the linearity.

To tackle the issues of linear processing, we further develop *non-linear* coding for GTWCs to provide higher degrees of flexibility in designing the codes. It is important to note that there have been research efforts on designing non-linear codes in feedback-enabled GOWCs. Along these lines, Kim. *et al.* [14] proposed Deepcode, which exploits recurrent neural networks (RNNs) for non-linear coding in feedback-enabled GOWCs, and showed performance improvements in the error probability across many noise scenarios as compared to linear coding. In [15], Safavi. *et al.* proposed deep extended feedback (DEF) codes that generalizes Deepcode to improve the spectral efficiency and error performance. In [16], Ozfatura. *et al.* proposed generalized block attention feedback (GBAF) codes that exploit self-attention modules to incorporate different neural network architectures. They showed that GBAF codes can outperform the existing solutions, especially in the noiseless feedback scenario. Kim. *et al.* [17] proposed a novel RNN-based feedback coding methodology through state propagation-based encoding, which incorporates efficient power control, an attention mechanism, and block-level classification of the messages. The proposed methodology greatly enhances the error performance in practical noise regions as compared to the existing coding schemes. While there have been many successful attempts to develop non-linear codes via deep learning for feedback-enabled GOWCs, to the best of our knowledge, no such efforts have been made yet for GTWCs.

In this paper, we aim to bridge the gaps between the two pieces of literature on GOWCs and GTWCs. The design of coding schemes for GTWCs faces the three following challenges.

(C-1) *Coupling of user encoding processes.* In GTWCs, each user generates a transmit symbol at each time step using its encoder. The encoding process utilizes its own message and the previously received symbols from the other user. Here, using the receive symbols as feedback information can enhance communication reliability, as demonstrated in feedback-enabled GOWCs [8], [10], [14], [17]. The generated transmit symbols are then exchanged between the users over time, resulting in a coupling effect in their encoding processes. This coupling intertwines the encoding and decoding operations of the users, ultimately affecting the overall system behavior.

(C-2) *Requirement of effective decoding to capture the coupling effect.* It is crucial for the decoding process at each user to effectively capture the coupling effect introduced by the encoders. This requirement necessitates a joint design of encoders and decoders for both users, adding complexity and posing a significant challenge in the design of decoders.

(C-3) *Need for efficient power management within power constraints.* Power management faces significant challenges due to the coupled encoding processes and the consideration of average power constraints for each user. Furthermore, when designing encoding schemes that utilize feedback information, power control over the sequence of transmit symbols becomes crucial for achieving robust error performance, as demonstrated in feedback-enabled GOWCs [8], [10], [14], [17]. Therefore, it is essential to incorporate an effective power control strategy into the encoder design for both users.

In light of the aforementioned challenges, we propose two distinct *two-way coding* strategies for GTWCs: (i) linear coding, which is based on tractable mathematical derivations, and (ii) non-linear coding, which is inspired by recent advancements in deep learning. The major contributions of the paper are summarized below.

- We first introduce a general functional form of encoding and decoding for two-way channels, where each user generates the transmit symbols by encoding both its own message and the past received symbols from the other user. Using the defined encoding/decoding functions, we then formulate an optimization problem for minimizing the sum of the error probabilities of the users under each user's power constraint, aiming to improve and balance the communication reliability in two-way channels.
- We propose a *linear* coding scheme for GTWCs. We first formulate a signal model for linear coding that captures the coupling of encoders to address (C-1). We then derive an optimal form of linear decoding at each user as a function of encoding schemes of the users, which addresses (C-2). To obtain a tractable solution, we convert the sum-error minimization problem to the weighted sum-power minimization problem. In weighted sum-power minimization, we provide new insights on user cooperation by exploring the relationship between the channel noise ratio and the weight coefficient

imposed in weighted sum-power minimization. Building upon the insights presented in [6] that a user with lower channel noise can act as a helper by providing feedback, our work extends this concept to address weighted sum problems. In particular, whether a user would act as a helper is affected not only by the channel ratio but also the weight coefficient. We then develop an efficient algorithm for joint encoder-decoder design under power constraints for (C-3). Lastly, we discuss how to extend our linear coding approach to medium/long block-lengths.

- We propose a novel *learning-based* coding architecture via RNN to capture the three aforementioned challenges of (C-1), (C-2), and (C-3). Specifically, to address (C-1), we construct a pair of *interactive* RNNs for encoding, where the previous output of one user's RNN is fed into the other user's RNN as a current input. The interactive RNNs effectively capture user cooperation in GTWCs through a novel utilization of RNNs, inspired by the successful application for feedback utilization in GOWCs [17]. To address (C-3), we introduce a power control layer at each user's encoder, which we prove satisfies all power constraints asymptotically. To address (C-2), we adopt bi-directional RNNs with an attention mechanism to fully exploit correlation among receive symbols, in which the encoders' coupling behavior is implicitly captured as a form of symbols. To address all these three challenges jointly in the coding architecture, we train the overall encoders/decoders at the users via auto-encoder.
- We analyze the computational complexity of the proposed linear and non-linear coding schemes. Through numerical simulations, we show that our two-way coding strategies outperform conventional channel coding schemes (that do not utilize user cooperation) by wide margins in terms of sum-error performance. For linear coding, we introduce an enhancement strategy by transmitting messages in alternate channel uses, which is motivated by the solution behavior. Under asymmetric channels, linear coding performs best when the channel signal-to-noise ratios (SNRs) of both users are high, while RNN-based coding excels when either of the channel SNRs is low. For RNN-based coding, we observe that when the difference between the channel SNRs of the users is larger than some threshold, the user with higher channel SNR sacrifices some of its error performance to improve the other user's error performance, which in turn improves the sum-error performance. This behavior is consistent with the understanding presented in [6] that a user with lower channel noise can function as a helper. We further provide information-theoretic insights on power distribution at the users, where both linear and RNN-based coding schemes allocate more power to early channel uses in asymmetric channels. This behavior is aligned with power distribution for feedback-enabled GOWCs [10], [17]. Lastly, we demonstrate that our coding schemes support higher coding rates and study the block-length gain of RNN-based coding.

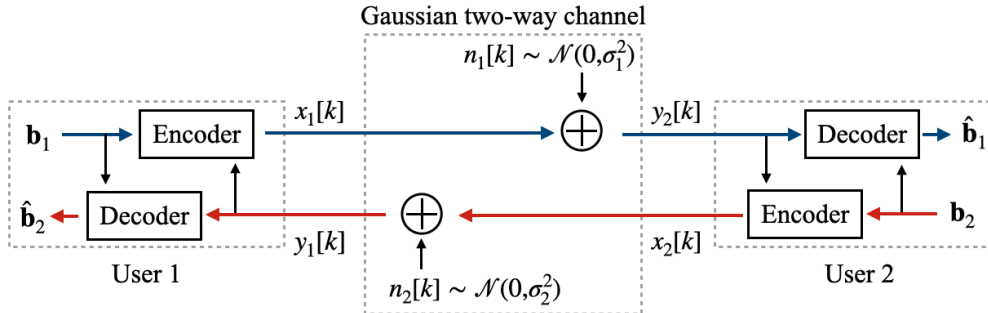


Fig. 1: System model for Gaussian two-way channels. The goal is to successfully convey the messages  $\mathbf{b}_i$  to each other by exchanging transmit symbols  $x_i[k]$  between the users. The users employ encoders and decoders to ensure successful message transmissions, where the two-way interaction between the users should be captured.

- We highlight the new contributions made in this work, in contrast to our previous study [1]. Overall, we introduce both linear and non-linear coding approaches, while our prior work focused only on linear coding. For non-linear coding, we propose a new neural coding methodology based on deep learning. Also, we shift our focus towards enhancing reliability by minimizing sum-errors within power limitations as opposed to weighted sum-power minimization in our prior study, and then establish the connection between the optimization of the two minimization problems. Building upon the tractable solution framework for weighted sum-power minimization in our previous work, we propose a new linear coding solution for sum-error minimization. Furthermore, we add discussions on the extension to medium/long block-lengths, the effect of different modulation orders, and user cooperation under asymmetric channels. Also, we analyze the computational complexity of our linear and non-linear coding schemes. Finally, we conduct extensive performance evaluations, including sum-error performance, two-way coding benefits, varying coding rates, and block-length gain, as well as power distribution mainly discussed in our prior work.

## II. SYSTEM MODEL AND OPTIMIZATION PROBLEM FOR CODING

In this section, we first present a transmission model for GTWCs in Sec. II-A. Then, we provide a general functional form of encoding and decoding at the users in Sec. II-B. Lastly, we formulate an optimization problem for sum-error minimization in Sec. II-C.

### A. Transmission Model

We consider a two-way channel between two users, User 1 and User 2, with additive white Gaussian noise (AWGN), as shown in Fig. 1. This channel model is referred to as a GTWC. We assume that

transmission occurs over  $N$  channel uses (or timesteps). Let  $k \in \{1, \dots, N\}$  denote the channel use index, and  $x_1[k] \in \mathbb{R}$  and  $x_2[k] \in \mathbb{R}$  represent the transmit symbols of User 1 and User 2, respectively, at time  $k$ . Subsequently, the receive symbols at User 2 and User 1, respectively, at time  $k$  are given by

$$y_2[k] = x_1[k] + n_1[k] \in \mathbb{R}, \quad y_1[k] = x_2[k] + n_2[k] \in \mathbb{R}, \quad (1)$$

where  $n_1[k] \sim \mathcal{N}(0, \sigma_1^2)$  and  $n_2[k] \sim \mathcal{N}(0, \sigma_2^2)$  are Gaussian noises, which are independent of each other and across the channel use index  $k$ . We consider an average power constraint for transmission at the users as

$$\mathbb{E} \left[ \sum_{k=1}^N x_i^2[k] \right] \leq NP, \quad i \in \{1, 2\}, \quad (2)$$

where  $P$  denotes the average transmit power constraint per channel use at each user. The distribution of variables over which the expectation in (2) is taken will be specified in (6).

### B. Functional Form of Encoding and Decoding

The goal of exchanging transmit symbols among the users is to transmit a *message* available at each user to the other. As shown in Fig. 1, we consider that each User  $i$ ,  $i \in \{1, 2\}$ , aims to transmit a unique message represented by a bit vector,  $\mathbf{b}_i \in \{0, 1\}^{K_i}$ , to the other user, where  $K_i$  is the number of source bits at User  $i$ . We first provide a general functional form of encoding and decoding at the users.

1) *Encoding*: User  $i$  encodes the bit vector  $\mathbf{b}_i \in \{0, 1\}^{K_i}$  to generate the  $N$  transmit symbols,  $\{x_i[k]\}_{k=1}^N$ . The coding rate at User  $i$  is defined by  $r_i = K_i/N$ . Rather than encoding the bit vector  $\mathbf{b}_i$  solely to generate the transmit symbols  $\{x_i[k]\}_{k=1}^N$ , we consider a joint encoding scheme that leverages both the bit vector and the receive symbols in GTWCs. The utilization of receive (or feedback) symbols in generating transmit symbols has been demonstrated to effectively enhance communication reliability in feedback-enabled GOWCs [8], [10], [14], [17]. This observation inspires us to utilize feedback in the framework of GTWC encoding. In particular, at time  $k$ , the encoding at User  $i$  is described as a function of the bit vector  $\mathbf{b}_i$  and the  $k-1$  receive symbols  $\{y_i[j]\}_{j=1}^{k-1}$  in (1). We denote an encoding function of User  $i$  at time  $k$  as  $f_{i,k} : \mathbb{R}^{K_i+k-1} \rightarrow \mathbb{R}$ . We can subsequently represent the encoding of User  $i$  at time  $k$  as

$$x_i[k] = f_{i,k}(\mathbf{b}_i, y_i[1], \dots, y_i[k-1]), \quad k = 1, \dots, N. \quad (3)$$

The encoding functions  $\{f_{i,k}\}_{i,k}$  can be linear or non-linear depending on design choices. In this work, we address both cases, linear coding in Sec. III and non-linear coding in Sec. IV.

2) *Decoding*: Once the  $N$  transmissions are completed, Users 1 and 2 compute estimates of the bit vector of the other user, respectively,  $\hat{\mathbf{b}}_2 \in \{0, 1\}^{K_2}$  and  $\hat{\mathbf{b}}_1 \in \{0, 1\}^{K_1}$ . For decoding, User  $i$  can utilize the  $N$  receive symbols,  $\{y_i[k]\}_{k=1}^N$  in (1), and its own bit vector  $\mathbf{b}_i$ . Specifically, its own bit vector  $\mathbf{b}_i$  can be used as side information for decoding at User  $i$  since the receive symbols  $\{y_i[k]\}_{k=1}^N$  contain not only the other user's bit vector information but also its own bit vector information due to the causal encoding processes in (3) and the subsequent symbol exchange in (1). We denote the decoding functions of User 1 and 2 as  $g_1 : \mathbb{R}^{N+K_1} \rightarrow \{0, 1\}^{K_2}$  and  $g_2 : \mathbb{R}^{N+K_2} \rightarrow \{0, 1\}^{K_1}$ , respectively. We can then represent the decoding processes conducted by User 1 and User 2, respectively, as

$$\hat{\mathbf{b}}_2 = g_1(\mathbf{b}_1, y_1[1], \dots, y_1[N]), \quad \hat{\mathbf{b}}_1 = g_2(\mathbf{b}_2, y_2[1], \dots, y_2[N]). \quad (4)$$

The decoding functions  $\{g_i\}_i$  can be either linear or non-linear. We address linear coding in Sec. III and non-linear coding in Sec. IV.

### C. Optimization of Encoders and Decoders

Since our goal is to design practical codes with finite block-lengths, we consider error probability as our main performance indicator. To quantify the error probability, we consider two different metrics of interest. The first metric is block error rate (BLER), which is the ratio of the number of incorrect bit vectors to the total number of bit vectors. Formally, the BLER of User  $i$ 's bit vector is defined as  $\text{BLER}_i = \Pr[\{\mathbf{b}_i \neq \hat{\mathbf{b}}_i\}]$ ,  $i \in \{1, 2\}$ . The other metric is bit error rate (BER), which is the ratio of the number of incorrect bits to the total number of bits in bit vectors. We first represent the  $\ell$ -th entry of  $\mathbf{b}_i$  and  $\hat{\mathbf{b}}_i$  as  $b_i[\ell] \in \{0, 1\}$  and  $\hat{b}_i[\ell] \in \{0, 1\}$ , respectively. Then, the BER of  $b_i[\ell]$  is defined by  $\text{BER}_{i,\ell} = \Pr[\{b_i[\ell] \neq \hat{b}_i[\ell]\}]$ ,  $i \in \{1, 2\}$  and  $\ell \in \{1, \dots, K_i\}$ . It is worth noting that BER values can differ for each individual bit entry, i.e.,  $\text{BER}_{i,\ell} \neq \text{BER}_{i,m}$  for  $\ell \neq m$ , depending on the design of encoding/decoding functions in (3)-(4). To achieve the goal of minimizing BERs across all entries, our objective is to minimize the average BER over all entries. Formally, we define the average BER of User  $i$ 's bit vector as  $\text{BER}_i = (1/K_i) \sum_{\ell=1}^{K_i} \text{BER}_{i,\ell} = (1/K_i) \sum_{\ell=1}^{K_i} \Pr[\{b_i[\ell] \neq \hat{b}_i[\ell]\}]$ . In this work, we assume that all bits in  $\mathbf{b}_1$  and  $\mathbf{b}_2$  are independent and identically distributed (i.i.d.) to one another.

For generalization, we assume User  $i$  uses an error probability metric denoted by  $\mathcal{E}_i(\{f_{1,k}\}_{k=1}^N, \{f_{2,k}\}_{k=1}^N, g_i, P, \sigma_1^2, \sigma_2^2, K_1, K_2, N)$ , which can represent either  $\text{BLER}_i$  or  $\text{BER}_i$  depending on design choices. Here,  $\bar{i}$  denotes the index of the counterpart of User  $i$ , i.e.,  $\bar{i} = 2$  if  $i = 1$  while  $\bar{i} = 1$  if  $i = 2$ . In this work, we aim to design the encoding and decoding functions when the values of  $P, \sigma_1^2, \sigma_2^2, K_1, K_2$ , and  $N$  are given. We thus simplify the dependency as  $\mathcal{E}_i(\{f_{1,k}\}_{k=1}^N, \{f_{2,k}\}_{k=1}^N, g_i)$ . The objective in this



work is to minimize the error probability of both users, while balancing the communication reliability in two-way channels. Accordingly, we formulate the following optimization problem:

$$\underset{\{f_{1,k}\}_{k=1}^N, \{f_{2,k}\}_{k=1}^N, g_1, g_2}{\text{minimize}} \quad \mathcal{E}_1(\{f_{1,k}\}_{k=1}^N, \{f_{2,k}\}_{k=1}^N, g_2) + \mathcal{E}_2(\{f_{1,k}\}_{k=1}^N, \{f_{2,k}\}_{k=1}^N, g_1) \quad (5)$$

$$\text{subject to} \quad \mathbb{E}_{\mathbf{b}_1, \mathbf{b}_2, \mathbf{n}_1, \mathbf{n}_2} \left[ \sum_{k=1}^N x_i^2[k] \right] \leq NP, \quad i \in \{1, 2\}, \quad (6)$$

where  $\mathbf{n}_i = [n_i[1], \dots, n_i[N]]^\top$ ,  $i \in \{1, 2\}$ . The expectation in (6) is taken over the distributions of the bit vectors,  $\mathbf{b}_1$  and  $\mathbf{b}_2$ , and the noise terms,  $\mathbf{n}_1$  and  $\mathbf{n}_2$ ; the transmit symbol  $x_i[k]$  in (6) is the encoding output as a function of its local bit vector  $\mathbf{b}_i$  and the receive symbols,  $y_i[1], \dots, y_i[k-1]$ , shown in (3). The receive symbols,  $y_i[1], \dots, y_i[k-1]$ , are dependent on the noises  $\mathbf{n}_1$  and  $\mathbf{n}_2$  and the other user's encoding process, i.e., the bit vector of the other user  $\mathbf{b}_{\bar{i}}$ , through the successive encoding operation of the both users as shown in (1) and (3).

Solving (5)-(6) is non-trivial and challenging since the encoding processes of both the users (in (3)) are coupled to each other in a causal manner, and the coupling effect should be incorporated into the design of the encoders/decoders of both users. To address these challenges, we propose two distinct *two-way coding* approaches. First, we propose a *linear* coding approach with low complexity for designing the encoders/decoders in Sec. III. Despite the low design complexity, however, the linear assumption on coding may limit the performance due to limited degrees of flexibility in the design of encoders/decoders. To allow higher degrees of freedom for coding, we propose a *non-linear* coding approach based on deep learning in Sec. IV.

### III. LINEAR CODING: FRAMEWORK AND SOLUTION

In this section, we first formulate a signal model for linear coding in Sec. III-A. We then derive the optimal linear decoding scheme in Sec. III-B. To obtain a tractable solution, we convert the original sum-error minimization problem to the weighted sum-power minimization problem in Sec. III-C. We next analyze encoders' behaviors and further reduce the design complexity of encoders in Sec. III-D. Afterwards, we propose a solution method for the weighted sum-power minimization in Sec. III-E, based on which we provide an overall algorithm for the sum-error minimization in Sec. III-F. Lastly, we discuss how to extend our linear coding approach to long block-lengths in Sec. III-G.

#### A. Signal Model for Linear Coding

To conduct linear coding for GTWCs in Fig. 1, we consider a message symbol  $m_i \in \mathbb{R}$ , where User  $i$ ,  $i \in \{1, 2\}$ , converts the bit vector  $\mathbf{b}_i \in \{0, 1\}^{K_i}$  to the message symbol  $m_i$  through  $2^{K_i}$ -ary pulse

amplitude modulation (PAM) [18]. Note that  $\mathbb{E}[m_i] = 0$  and  $\mathbb{E}[m_i^2] = 1$ . We represent the  $N$  receive symbols at User  $i$  (in (1)) in vector form as  $\mathbf{y}_i = [y_i[1], \dots, y_i[N]]^\top \in \mathbb{R}^{N \times 1}$ . Then, we can rewrite the expressions in (1) as

$$\mathbf{y}_2 = \mathbf{x}_1 + \mathbf{n}_1, \quad \mathbf{y}_1 = \mathbf{x}_2 + \mathbf{n}_2, \quad (7)$$

where  $\mathbf{x}_i = [x_i[1], \dots, x_i[N]]^\top$ ,  $i \in \{1, 2\}$ . Note that we refer to the vector form of the symbols as signals, i.e.,  $\mathbf{x}_i$  as the transmit signal and  $\mathbf{y}_i$  as the receive signal,  $i \in \{1, 2\}$ .

We consider that User  $i$ ,  $i \in \{1, 2\}$ , employs the message encoding vector  $\tilde{\mathbf{g}}_i \in \mathbb{R}^{N \times 1}$  for encoding the message  $m_i$  and the feedback encoding matrix  $\tilde{\mathbf{F}}_i \in \mathbb{R}^{N \times N}$  for encoding the receive symbols. Note that  $\tilde{\mathbf{F}}_i$ ,  $i \in \{1, 2\}$ , is strictly lower triangular (i.e., the matrix entries are zero on and above the diagonal) due to the causality of the system. To avoid feeding back redundant information under limited transmit power, we consider that each user removes the contribution of its known prior transmit symbols from the receive symbols to generate its future transmit symbols, similar to linear coding for feedback-enabled GOWCs [8]–[10]. For the case of User 1, the transmit signal  $\mathbf{x}_1$  is transmitted across the channel to User 2, who encodes a noisy version of  $\mathbf{x}_1$ , i.e.,  $\mathbf{y}_2$ , by using  $\tilde{\mathbf{F}}_2$  to generate  $\mathbf{x}_2$ . User 2 then transmits  $\mathbf{x}_2$  to User 1, who receives a noisy version of  $\mathbf{x}_2$ , i.e.,  $\mathbf{y}_1$ . In short,  $\mathbf{y}_1$  contains some information of  $\mathbf{x}_1$  to which the feedback encoding matrix  $\tilde{\mathbf{F}}_2$  is applied. Therefore, User 1 subtracts its signal portion  $\mathbf{x}_1$  from the receive signal  $\mathbf{y}_1$  as  $\mathbf{y}_1 - \tilde{\mathbf{F}}_2 \mathbf{x}_1$ . Similarly, User 2 subtracts its signal portion  $\mathbf{x}_2$  from  $\mathbf{y}_2$  and obtains the modified feedback information  $\mathbf{y}_2 - \tilde{\mathbf{F}}_1 \mathbf{x}_2$ . The transmit signals of the users are then given by

$$\mathbf{x}_1 = \tilde{\mathbf{g}}_1 m_1 + \tilde{\mathbf{F}}_1 (\mathbf{y}_1 - \tilde{\mathbf{F}}_2 \mathbf{x}_1), \quad (8)$$

$$\mathbf{x}_2 = \tilde{\mathbf{g}}_2 m_2 + \tilde{\mathbf{F}}_2 (\mathbf{y}_2 - \tilde{\mathbf{F}}_1 \mathbf{x}_2). \quad (9)$$

Since each user transmits the signals encapsulating the received signals from the other user over multiple channel uses in a causal manner, a *coupling* occurs between the transmit signals of the users. Since this coupling occurs successively across time, it intertwines the encoding/decoding operations and impacts the overall system behavior. To mitigate the coupling effects in the signal representation, we rewrite the signal model in (8)-(9) as

$$\mathbf{x}_1 = \mathbf{g}_1 m_1 + \mathbf{F}_1 (\mathbf{y}_1 - \mathbf{F}_2 \mathbf{x}_1), \quad (10)$$

$$\mathbf{x}_2 = \mathbf{g}_2 m_2 + \mathbf{F}_2 \mathbf{y}_2, \quad (11)$$

by expressing  $\mathbf{g}_1$ ,  $\mathbf{F}_1$ ,  $\mathbf{g}_2$ , and  $\mathbf{F}_2$  as functions of  $\tilde{\mathbf{g}}_1$ ,  $\tilde{\mathbf{F}}_1$ ,  $\tilde{\mathbf{g}}_2$ , and  $\tilde{\mathbf{F}}_2$ . The detailed derivation of the functional expressions is provided in Appendix A. Given the functional expressions, both  $\mathbf{F}_1$  and  $\mathbf{F}_2$  are strictly lower triangular.

Based on the equivalent conversion from (8)-(9) to (10)-(11), we aim to design  $\mathbf{g}_1$ ,  $\mathbf{F}_1$ ,  $\mathbf{g}_2$ , and  $\mathbf{F}_2$  and focus on the signal representation in (10)-(11). By putting the expressions of  $\mathbf{x}_2$  and  $\mathbf{x}_1$  (obtained in (10)-(11)) into (7), we can rewrite (7) as

$$\mathbf{y}_1 = \mathbf{g}_2 m_2 + \mathbf{F}_2 \mathbf{y}_2 + \mathbf{n}_2, \quad (12)$$

$$\begin{aligned} \mathbf{y}_2 &= \mathbf{g}_1 m_1 + \mathbf{F}_1 (\mathbf{y}_1 - \mathbf{F}_2 \mathbf{x}_1) + \mathbf{n}_1 \\ &= \mathbf{g}_1 m_1 + \mathbf{F}_1 \mathbf{g}_2 m_2 + (\mathbf{I} + \mathbf{F}_1 \mathbf{F}_2) \mathbf{n}_1 + \mathbf{F}_1 \mathbf{n}_2. \end{aligned} \quad (13)$$

To obtain the equality in the second line in (13), we put the expression of  $\mathbf{y}_1$  (given in (12)) into  $\mathbf{y}_1$  in the first line in (13).

We insert the expressions of  $\mathbf{y}_1$  and  $\mathbf{y}_2$  (obtained in (12)-(13)) back into (10)-(11), and rewrite the transmit signals  $\mathbf{x}_1$  and  $\mathbf{x}_2$  in (10)-(11) as

$$\mathbf{x}_1 = \mathbf{g}_1 m_1 + \mathbf{F}_1 (\mathbf{g}_2 m_2 + \mathbf{F}_2 \mathbf{n}_1 + \mathbf{n}_2), \quad (14)$$

$$\begin{aligned} \mathbf{x}_2 &= \mathbf{g}_2 m_2 + \mathbf{F}_2 (\mathbf{g}_1 m_1 + \mathbf{F}_1 \mathbf{g}_2 m_2 + (\mathbf{I} + \mathbf{F}_1 \mathbf{F}_2) \mathbf{n}_1 + \mathbf{F}_1 \mathbf{n}_2) \\ &= (\mathbf{I} + \mathbf{F}_2 \mathbf{F}_1) \mathbf{g}_2 m_2 + \mathbf{F}_2 \mathbf{g}_1 m_1 + \mathbf{F}_2 (\mathbf{I} + \mathbf{F}_1 \mathbf{F}_2) \mathbf{n}_1 + \mathbf{F}_2 \mathbf{F}_1 \mathbf{n}_2. \end{aligned} \quad (15)$$

Note that the transmit signals in (14)-(15) are represented as the sum of messages and noises. Using (14)-(15), we formulate the transmit power of the users as

$$\mathbb{E}[\|\mathbf{x}_1\|^2] = \|\mathbf{g}_1\|^2 + \|\mathbf{F}_1 \mathbf{g}_2\|^2 + \|\mathbf{F}_1 \mathbf{F}_2\|_F^2 \sigma_1^2 + \|\mathbf{F}_1\|_F^2 \sigma_2^2, \quad (16)$$

$$\mathbb{E}[\|\mathbf{x}_2\|^2] = \|(\mathbf{I} + \mathbf{F}_2 \mathbf{F}_1) \mathbf{g}_2\|^2 + \|\mathbf{F}_2 \mathbf{g}_1\|^2 + \|\mathbf{F}_2 (\mathbf{I} + \mathbf{F}_1 \mathbf{F}_2)\|_F^2 \sigma_1^2 + \|\mathbf{F}_2 \mathbf{F}_1\|_F^2 \sigma_2^2, \quad (17)$$

where the messages and the noises are assumed to be uncorrelated to each other.

### B. Optimal Linear Decoding

Since the decoding is conducted at each of the users independently, we can use a similar technique used in feedback-enabled GOWCs to find the optimal linear decoding scheme [10], [11]. After the  $N$  channel uses, each user aims to estimate the message of the other user. We first consider the decoding process at User 1. User 1 estimates  $m_2$  with the receive signal  $\mathbf{y}_1$  by using a linear combining vector  $\mathbf{w}_2 \in \mathbb{R}^{N \times 1}$ . We note that  $\mathbf{y}_1 = \mathbf{x}_2 + \mathbf{n}_2 = \mathbf{F}_2 \mathbf{g}_1 m_1 + (\mathbf{I} + \mathbf{F}_2 \mathbf{F}_1) \mathbf{g}_2 m_2 + \mathbf{F}_2 (\mathbf{I} + \mathbf{F}_1 \mathbf{F}_2) \mathbf{n}_1 + (\mathbf{I} + \mathbf{F}_2 \mathbf{F}_1) \mathbf{n}_2$ , where  $\mathbf{x}_2$  is given in (15). Rather than using  $\mathbf{y}_1$  directly, we consider the following two pre-processing stages: (i) User 1 obtains  $\mathbf{z}_1 = \mathbf{y}_1 - \mathbf{F}_2 \mathbf{g}_1 m_1 = (\mathbf{I} + \mathbf{F}_2 \mathbf{F}_1) \mathbf{g}_2 m_2 + (\mathbf{I} + \mathbf{F}_2 \mathbf{F}_1) \mathbf{F}_2 \mathbf{n}_1 + (\mathbf{I} + \mathbf{F}_2 \mathbf{F}_1) \mathbf{n}_2$  by subtracting its message contribution,  $\mathbf{F}_2 \mathbf{g}_1 m_1$ , from  $\mathbf{y}_1$ ; (ii) User 1 subsequently defines  $\tilde{\mathbf{y}}_1 = (\mathbf{I} + \mathbf{F}_2 \mathbf{F}_1)^{-1} \mathbf{z}_1 = \mathbf{g}_2 m_2 + \mathbf{F}_2 \mathbf{n}_1 + \mathbf{n}_2$ . Using  $\mathbf{y}_1$  is equivalent to using  $\tilde{\mathbf{y}}_1$  in terms of estimating  $m_2$ , since  $\tilde{\mathbf{y}}_1$  is a linear

function of  $\mathbf{y}_1$ . Using the result of pre-processing, User 1 obtains the message estimate as  $\hat{m}_2 = \mathbf{w}_2^\top \tilde{\mathbf{y}}_1$ . Since  $\tilde{\mathbf{y}}_1 = \mathbf{g}_2 m_2 + \mathbf{F}_2 \mathbf{n}_1 + \mathbf{n}_2$ , we represent  $\hat{m}_2 = \mathbf{w}_2^\top \mathbf{g}_2 m_2 + \mathbf{w}_2^\top (\mathbf{F}_2 \mathbf{n}_1 + \mathbf{n}_2)$ , where the first term is the message portion, while the second terms denotes the effective noise. The effective noise,  $\mathbf{w}_2^\top (\mathbf{F}_2 \mathbf{n}_1 + \mathbf{n}_2)$ , still follows a Gaussian distribution due to the linear processing of the Gaussian noise variables,  $\mathbf{n}_1$  and  $\mathbf{n}_2$ . The distribution of the effective noise is given by  $\mathcal{N}(0, \mathbf{w}_2^\top \mathbf{Q}_2 \mathbf{w}_2)$ , where

$$\mathbf{Q}_2 = \mathbf{F}_2 \mathbf{F}_2^\top \sigma_1^2 + \sigma_2^2 \mathbf{I}. \quad (18)$$

The SNR used to estimate  $m_2$  is correspondingly defined by

$$\text{SNR}_2 = \frac{|\mathbf{w}_2^\top \mathbf{g}_2|^2}{\mathbf{w}_2^\top \mathbf{Q}_2 \mathbf{w}_2}. \quad (19)$$

Similarly, we consider that User 2 estimates  $m_1$  using the receive signal  $\mathbf{y}_2$  via a linear combining vector  $\mathbf{w}_1 \in \mathbb{R}^{N \times 1}$ . In pre-processing, User 2 subtracts its message contribution,  $\mathbf{F}_1 \mathbf{g}_2 m_2$ , from  $\mathbf{y}_2$  in (13), and obtains  $\tilde{\mathbf{y}}_2 = \mathbf{y}_2 - \mathbf{F}_1 \mathbf{g}_2 m_2 = \mathbf{g}_1 m_1 + (\mathbf{I} + \mathbf{F}_1 \mathbf{F}_2) \mathbf{n}_1 + \mathbf{F}_1 \mathbf{n}_2$ . User 2 then obtains the message estimate as  $\hat{m}_1 = \mathbf{w}_1^\top \tilde{\mathbf{y}}_2$ . By using the expression of  $\tilde{\mathbf{y}}_2$  obtained above, we obtain  $\hat{m}_1 = \mathbf{w}_1^\top \mathbf{g}_1 m_1 + \mathbf{w}_1^\top ((\mathbf{I} + \mathbf{F}_1 \mathbf{F}_2) \mathbf{n}_1 + \mathbf{F}_1 \mathbf{n}_2)$ , where the first and second terms are the message portion and the effective noise, respectively. The effective noise term,  $\mathbf{w}_1^\top ((\mathbf{I} + \mathbf{F}_1 \mathbf{F}_2) \mathbf{n}_1 + \mathbf{F}_1 \mathbf{n}_2)$ , follows the Gaussian distribution with  $\mathcal{N}(0, \mathbf{w}_1^\top \mathbf{Q}_1 \mathbf{w}_1)$ , where

$$\mathbf{Q}_1 = (\mathbf{I} + \mathbf{F}_1 \mathbf{F}_2)(\mathbf{I} + \mathbf{F}_1 \mathbf{F}_2)^\top \sigma_1^2 + \mathbf{F}_1 \mathbf{F}_1^\top \sigma_2^2. \quad (20)$$

The corresponding SNR to estimate  $m_1$  is defined by

$$\text{SNR}_1 = \frac{|\mathbf{w}_1^\top \mathbf{g}_1|^2}{\mathbf{w}_1^\top \mathbf{Q}_1 \mathbf{w}_1}. \quad (21)$$

Given  $\mathbf{g}_1$ ,  $\mathbf{F}_1$ ,  $\mathbf{g}_2$ , and  $\mathbf{F}_2$ , the optimal combining vector (that minimizes the error probability for message estimation) is obtained by maximizing the SNRs in (19) and (21) [10], [11], [19], given by

$$\mathbf{w}_i^* = \frac{\mathbf{Q}_i^{-1} \mathbf{g}_i}{\mathbf{g}_i^\top \mathbf{Q}_i^{-1} \mathbf{g}_i}, \quad i \in \{1, 2\}. \quad (22)$$

Plugging (22) in (19) and (21), we obtain the following SNR expression

$$\text{SNR}_i = \mathbf{g}_i^\top \mathbf{Q}_i^{-1} \mathbf{g}_i, \quad i \in \{1, 2\}. \quad (23)$$

The optimal combining vector for decoding in (22) is represented as a function of the encoding schemes of the users, i.e.,  $\mathbf{g}_1$ ,  $\mathbf{F}_1$ ,  $\mathbf{g}_2$ , and  $\mathbf{F}_2$ . Accordingly, the SNR expression in (23) is also a function of the encoding schemes. Thus, the joint design of the encoding and decoding schemes is equivalent to the design of the encoding schemes only with the derived form of SNRs in (23).

### C. Conversion of Optimization Problem

For linear coding, we can represent the error probability metric  $\mathcal{E}_i$  in (5) as a function of SNR, i.e.,  $\mathcal{E}_i(\text{SNR}_i)$ , since the formula of  $\text{SNR}_i$  given in (23) captures both the encoding and decoding schemes.<sup>1</sup> This modified input-output relationship in error probability makes it more convenient to analyze linear coding. We note that  $\mathcal{E}_i$  is either  $\text{BLER}_i$  or  $\text{BER}_i$ ; with  $2^{K_i}$ -ary PAM,  $\text{BLER}_i$  is equivalent to symbol error rate (SER) of the message  $m_i$ , i.e.,

$$\text{BLER}_i = \frac{2^{K_i+1} - 2}{2^{K_i}} Q\left(\sqrt{\frac{3\text{SNR}_i}{2^{2K_i} - 1}}\right), \quad (24)$$

where  $Q(x) = \frac{1}{\sqrt{2\pi}} \int_x^\infty (-\frac{u^2}{2}) du$  denotes the tail distribution function of the standard normal distribution. For BER, we can approximately obtain  $\text{BER}_i \approx \text{BLER}_i / K_i$  when Gray coding is used for modulation and SNR is high [20]. In low SNR regime, we can calculate BER from a known relationship among SNR and the modulation order  $2^{K_i}$  [18]. With the functional form  $\mathcal{E}_i(\text{SNR}_i)$ , we rewrite the optimization problem (5)-(6) as

$$\begin{aligned} & \underset{\mathbf{g}_1, \mathbf{F}_1, \mathbf{g}_2, \mathbf{F}_2}{\text{minimize}} && \mathcal{E}_1(\text{SNR}_1) + \mathcal{E}_2(\text{SNR}_2) \\ & \text{subject to} && \mathbb{E}[\|\mathbf{x}_1\|^2] \leq NP, \quad \mathbb{E}[\|\mathbf{x}_2\|^2] \leq NP, \end{aligned} \quad (25)$$

where  $\text{SNR}_i$  and  $\mathbf{x}_i$ ,  $i \in \{1, 2\}$ , are functions of the variables,  $\mathbf{g}_1$ ,  $\mathbf{F}_1$ ,  $\mathbf{g}_2$ , and  $\mathbf{F}_2$ , and the expectation is taken over the distributions of  $m_1$ ,  $m_2$ ,  $\mathbf{n}_1$ , and  $\mathbf{n}_2$ . However, it is intractable to directly solve the optimization problem in (25) due to (i) the coupling between the encoding schemes and the SNR expression in (23) and (ii) the power constraints in (25). We thus propose to transform it into a more tractable optimization problem through several steps as explained below. We start by stating the following remark.

**Remark 1.** *The sum-error metric,  $\mathcal{E}_1(\text{SNR}_1) + \mathcal{E}_2(\text{SNR}_2)$ , is a decreasing function of  $P$ .*

We further discuss the validity of Remark 1 within our linear coding framework in Appendix B. Based on the relationship between sum-error and power in Remark 1, we introduce an alternative optimization problem to (25), which aims to minimize the maximum transmit power, given by

$$\begin{aligned} & \underset{\mathbf{g}_1, \mathbf{F}_1, \mathbf{g}_2, \mathbf{F}_2}{\text{minimize}} && \bar{P} \\ & \text{subject to} && \mathcal{E}_1(\text{SNR}_1) + \mathcal{E}_2(\text{SNR}_2) = \omega \end{aligned}$$

<sup>1</sup> $\mathcal{E}_i$  is a function of  $P$ ,  $\sigma_1^2$ ,  $\sigma_2^2$ ,  $K_1$ ,  $K_2$ , and  $N$ , in addition to the encoding and decoding schemes, as discussed in Sec. II-C. In this work, we focus on the dependency of the encoding and decoding schemes on the error probability, since  $P$ ,  $\sigma_1^2$ ,  $\sigma_2^2$ ,  $K_1$ ,  $K_2$ , and  $N$  are given.

$$\mathbb{E}[\|\mathbf{x}_1\|^2] \leq N\bar{P}, \quad \mathbb{E}[\|\mathbf{x}_2\|^2] \leq N\bar{P}, \quad (26)$$

where  $\bar{P}$  denotes the objective value which is distinguished from the average power constraint value  $P$ . We consider that  $w$  is given, i.e., not a variable, in solving (26), and thus the two problems in (25) and (26) are not equivalent. However, the optimal solutions for (25) can be obtained by solving (26) through adjusting the value of  $w$  based on Lemma 1; if the obtained objective value  $\bar{P}$  in (26) is smaller than  $P$ , we keep decreasing the value of  $w$  and solve the above problem until  $\bar{P}$  reaches  $P$ . However, it is still challenging to solve (26) under the sum-error equality constraint, since there may exist multiple pairs of  $\text{SNR}_1$  and  $\text{SNR}_2$  that satisfy the constraint. Therefore, we consider individual constraints on  $\text{SNR}_1$  and  $\text{SNR}_2$  for optimization rather than the sum-error constraint. We subsequently reformulate (26) and obtain

$$\begin{aligned} & \underset{\mathbf{g}_1, \mathbf{F}_1, \mathbf{g}_2, \mathbf{F}_2}{\text{minimize}} && \bar{P} \\ & \text{subject to} && \text{SNR}_1 = \eta_1, \quad \text{SNR}_2 = \eta_2. \\ & && \mathbb{E}[\|\mathbf{x}_1\|^2] \leq N\bar{P}, \quad \mathbb{E}[\|\mathbf{x}_2\|^2] \leq N\bar{P}, \end{aligned} \quad (27)$$

where  $\eta_i \in \mathbb{R}^+$  is the target SNR for the message  $m_i$ ,  $i \in \{1, 2\}$ . The two problems (26) and (27) become equivalent when  $\mathcal{E}_1(\eta_1) + \mathcal{E}_2(\eta_2) = \omega$ . To achieve equivalence in obtaining optimal solutions between the original problem in (25) and the modified problem in (27), we solve (27) for all feasible values of  $\eta_1$  and  $\eta_2$  and find the best solutions that minimize  $\mathcal{E}_1(\eta_1) + \mathcal{E}_2(\eta_2)$  while satisfying  $\bar{P} \leq P$ .

If  $\bar{P}$  is an optimal value of the problem in (27), at least one of the power constraints in (27) should be satisfied in equality, i.e.,  $\bar{P} = \max\{\mathbb{E}[\|\mathbf{x}_1\|^2], \mathbb{E}[\|\mathbf{x}_2\|^2]\}/N$ . If  $\bar{P} \neq \max\{\mathbb{E}[\|\mathbf{x}_1\|^2], \mathbb{E}[\|\mathbf{x}_2\|^2]\}/N$ ,  $\bar{P}$  is not an optimal solution since  $\max\{\mathbb{E}[\|\mathbf{x}_1\|^2], \mathbb{E}[\|\mathbf{x}_2\|^2]\}/N$  can be the smaller objective value in (27). This insight leads us to reformulate (27) equivalently to

$$\begin{aligned} & \underset{\mathbf{g}_1, \mathbf{F}_1, \mathbf{g}_2, \mathbf{F}_2}{\text{minimize}} && \max\{\mathbb{E}[\|\mathbf{x}_1\|^2], \mathbb{E}[\|\mathbf{x}_2\|^2]\} \\ & \text{subject to} && \text{SNR}_1 = \eta_1, \quad \text{SNR}_2 = \eta_2. \end{aligned} \quad (28)$$

We derive the following lemma, which is useful in solving (28).

**Lemma 1.** *The optimal value of  $\max\{\mathbb{E}[\|\mathbf{x}_1\|^2], \mathbb{E}[\|\mathbf{x}_2\|^2]\}$  in (28) is an increasing function of  $\eta_1$  when  $\eta_2$  is fixed.*

The proof of Lemma 1 is provided in Appendix C. The above lemma allows us to develop an efficient search method along  $\eta_1$ , which will be discussed in detail in Sec. III-F. Nevertheless, solving (28) is still intractable. As an approximation technique, we use the *weighted sum method*, which is a common choice in multi-objective optimization [21]. This method involves solving a weighted sum of the objective

functions, and then varying the weights to generate a set of solutions that lie on the Pareto front. The optimal solution is then selected from this set based on the original objective function. In our case, we select the solution that minimizes  $\max\{\mathbb{E}[\|\mathbf{x}_1\|^2], \mathbb{E}[\|\mathbf{x}_2\|^2]\}$ .

Based on the weighted sum method, we introduce a weighting coefficient  $\alpha \in (0, 1)$  and aim to minimize the weighted sum of the users' transmit powers under their SNR constraints. The corresponding optimization problem is given by

$$\begin{aligned} & \underset{\mathbf{g}_1, \mathbf{F}_1, \mathbf{g}_2, \mathbf{F}_2}{\text{minimize}} && \alpha \mathbb{E}[\|\mathbf{x}_1\|^2] + (1 - \alpha) \mathbb{E}[\|\mathbf{x}_2\|^2] \\ & \text{subject to} && \text{SNR}_1 = \eta_1, \quad \text{SNR}_2 = \eta_2. \end{aligned} \quad (29)$$

In summary, to achieve equivalence between the original sum-error minimization problem in (25) and the weighted sum-power minimization problem in (29) in terms of obtaining optimal solutions [21], [22], we solve (29) for every feasible solution sets of  $(\eta_1, \eta_2, \alpha)$  and find the best solutions of  $\mathbf{g}_1$ ,  $\mathbf{F}_1$ ,  $\mathbf{g}_2$ , and  $\mathbf{F}_2$ , that minimize  $\mathcal{E}_1(\text{SNR}_1) + \mathcal{E}_2(\text{SNR}_2)$  while satisfying  $\mathbb{E}[\|\mathbf{x}_1\|^2] \leq NP$  and  $\mathbb{E}[\|\mathbf{x}_2\|^2] \leq NP$ . Since the problem in (29) is more tractable, we first focus on solving it in Sec. III-D and III-E. Then, in Sec. III-F, we provide an efficient algorithm to find the solutions for our original problem in (25).

#### D. Optimization Problem for Weighted Sum-Power Minimization

In general, at time  $k \geq 2$ , User  $i$  feeds back a linear combination of the previously received symbols up to time  $k - 1$ , i.e.,  $\{y_i[\tau]\}_{\tau=1}^{k-1}$ , where  $i \in \{1, 2\}$ . This implies that the initially received symbols at the users are repetitively fed back to the other over a total of  $N$  channel uses, e.g., the information of  $y_2[1]$  at User 2 is fed back to User 1 over  $N - 1$  times from  $k = 2$  to  $N$ . This repetitive feedback in both ways would make the design of the encoding schemes more complicated because the encoding schemes of the users are coupled. To mitigate the complexity of designing the encoding schemes, we assume that User 2 only feeds back the recently received signal of  $y_2$  in (11). In other words, User 2 provides feedback only for  $y[k - 1]$  at time  $k$ . Consequently,  $\mathbf{F}_2$  should be in the following form:

$$\mathbf{F}_2 = \begin{bmatrix} 0 & 0 & 0 & \dots & 0 \\ f_{2,2} & 0 & 0 & \dots & 0 \\ 0 & f_{2,3} & 0 & \dots & 0 \\ \vdots & \vdots & \ddots & & 0 \\ 0 & 0 & \dots & f_{2,N} & 0 \end{bmatrix} \in \mathbb{R}^{N \times N}. \quad (30)$$

For convenience, we define a set  $\mathcal{F}_2$  as a solution space for  $\mathbf{F}_2$ , i.e.,  $\mathbf{F}_2 \in \mathcal{F}_2$ .

First, we will investigate the solution behavior for feedback of User 2. Specifically, we reveal in the following proposition that it is optimal for User 2 not to utilize the last channel use for feedback to User 1, i.e.,  $f_{2,N} = 0$ , regardless of the encoding schemes.

**Proposition 1.** *In (29) with  $\mathbf{F}_2 \in \mathcal{F}_2$ , it is optimal that  $f_{2,N} = 0$ .*

The proof of Proposition 1 is provided in Appendix D. We next look into the solution behavior of the message encoding vector for User 2,  $\mathbf{g}_2$ . To this end, we first formulate the optimization problem (29) only with respect to  $\mathbf{g}_2$  by using the expression in (16)-(17) as follows:

$$\begin{aligned} & \underset{\mathbf{g}_2}{\text{minimize}} && \alpha \|\mathbf{F}_1 \mathbf{g}_2\|^2 + (1 - \alpha) \|(\mathbf{I} + \mathbf{F}_2 \mathbf{F}_1) \mathbf{g}_2\|^2 \\ & \text{subject to} && \mathbf{g}_2^\top \mathbf{Q}_2^{-1} \mathbf{g}_2 = \eta_2. \end{aligned} \quad (31)$$

We first conduct a matrix decomposition on  $\mathbf{Q}_2$  and obtain  $\mathbf{Q}_2 = (\mathbf{Q}_2^{1/2})^2$  where  $\mathbf{Q}_2^{1/2} = (\mathbf{Q}_2^{1/2})^\top$ .<sup>2</sup> Defining  $\mathbf{q}_2 = \mathbf{Q}_2^{-1/2} \mathbf{g}_2$ , we can obtain an equivalent optimization problem as

$$\begin{aligned} & \underset{\mathbf{q}_2}{\text{minimize}} && \mathbf{q}_2^\top \mathbf{B} \mathbf{q}_2 \\ & \text{subject to} && \|\mathbf{q}_2\|^2 = \eta_2, \end{aligned} \quad (32)$$

where

$$\mathbf{B} = \alpha \mathbf{Q}_2^{1/2} \mathbf{F}_1^\top \mathbf{F}_1 \mathbf{Q}_2^{1/2} + (1 - \alpha) \mathbf{Q}_2^{1/2} (\mathbf{I} + \mathbf{F}_2 \mathbf{F}_1)^\top (\mathbf{I} + \mathbf{F}_2 \mathbf{F}_1) \mathbf{Q}_2^{1/2}. \quad (33)$$

We then introduce our conjecture on the objective function value of (32), based on which we find the optimal solution for  $\mathbf{g}_2$  in (31).

**Conjecture 1.** *For any  $\mathbf{F}_1$  and  $\mathbf{F}_2 \in \mathcal{F}_2$ ,*

$$\min\{\alpha\sigma_1^2, (1 - \alpha)\sigma_2^2\} \leq \nu_{\min}[\mathbf{B}] \leq (1 - \alpha)\sigma_2^2, \quad (34)$$

where  $\nu_{\min}[\mathbf{B}]$  denotes the smallest eigenvalue of  $\mathbf{B}$  in (32).

We have proved a special case of this conjecture when  $N = 3$  in Appendix E. We note that, for any  $N$ , we have not found any example that violates the conjecture in our extensive numerical simulations, where  $\mathbf{F}_1$  and  $\mathbf{F}_2 \in \mathcal{F}_2$  are randomly generated.

**Proposition 2.** *If Conjecture 1 is true,  $\mathbf{g}_2 = [0, \dots, 0, \sqrt{\eta_2} \sigma_2]^\top$  is optimal in (29) when  $\alpha \geq \frac{\sigma_2^2}{\sigma_1^2 + \sigma_2^2}$ .*

<sup>2</sup>If we conduct the singular value decomposition on  $\mathbf{Q}_2$ , we have  $\mathbf{Q}_2 = \mathbf{U} \Sigma \mathbf{U}^\top$  and obtain  $\mathbf{Q}_2^{1/2} = \mathbf{U} \Sigma^{1/2} \mathbf{U}^\top$ .



The proof of Proposition 2 is provided in Appendix F. The result of Proposition 2 shows that it is optimal for User 2 to transmit the message only over the last channel use when the weight coefficient in (29) satisfies  $\alpha \geq \frac{\sigma_2^2}{\sigma_1^2 + \sigma_2^2}$ .

We can extract further implications from Proposition 2. In the context of feedback utilization [6], [8]–[10], one user transmits its message *initially* and exchanges symbols containing the message and feedback information with the other user. However, given that User 2 only transmits its message in the last channel use from Proposition 2, User 2 does not utilize feedback. Consequently, User 1 does not function as a helper in providing feedback to User 2. Therefore, we can state the following remark.

**Remark 2.** *User 1 does not function as a helper when  $\alpha \geq \frac{\sigma_2^2}{\sigma_1^2 + \sigma_2^2}$  in (29).*

We further explore the implications of Remark 2 in the context of the relationship between the weight coefficient  $\alpha$  and the channel noise ratio  $\sigma_2^2/(\sigma_1^2 + \sigma_2^2)$  within the framework of weighted sum-power minimization in (29). We consider a scenario where the inequality is completely fulfilled –  $\sigma_1^2$  is comparatively larger than  $\sigma_2^2$ , and  $\alpha$  is close to 1. Under these conditions, User 1 would not provide feedback because delivering feedback across a noisy channel (characterized by the large  $\sigma_1^2$ ) demands significant power, subsequently leading to a substantial increase in the weighted sum-power (due to the large  $\alpha$ ) in (29). In such a scenario, refraining from providing feedback would be advantageous in achieving a lower weighted sum-power.

The authors in [6] introduced the concept of designating the user with lower channel noise as a helper and subsequently derived error exponents for GTWCs within this framework. It's important to note that assigning the user with lower channel noise as a helper may not always be the optimal strategy for addressing the weighted sum-power minimization problem. In this work, we investigate the relationship between the weight assigned in weighted sum-power minimization and the channel noise ratio. Our analysis reveals that even when a user (User 1) experiences lower channel noise (characterized by small  $\sigma_1^2$ ), designating it as a helper might not be suitable in (29) if the weight is larger than the channel noise ratio, i.e.,  $\alpha \geq \frac{\sigma_2^2}{\sigma_1^2 + \sigma_2^2}$ . Building upon the insights presented in [6], our work extends the understanding of the helper concept to encompass weighted sum problems.

Using Propositions 1 and 2, we next aim to simplify our optimization problem in (29). In our optimization, we consider  $\alpha \geq \frac{\sigma_2^2}{\sigma_1^2 + \sigma_2^2}$ . From Proposition 2, we have  $\mathbf{g}_2 = [0, \dots, 0, \sqrt{\eta_2}\sigma_2]^\top$  as an optimal solution, which always satisfies  $\text{SNR}_2 = \eta_2$  regardless of other variables. Thus, we can remove the dependency of the constraint for  $\text{SNR}_2$  in (29). Further, to make (29) more tractable, we first perform a matrix decomposition on  $\mathbf{Q}_1$  and obtain  $\mathbf{Q}_1 = (\mathbf{Q}_1^{1/2})^2$  where  $\mathbf{Q}_1^{1/2} = (\mathbf{Q}_1^{1/2})^\top$  in the same way for the decomposition on  $\mathbf{Q}_2$  as described below (31). Then, we define  $\mathbf{q}_1 = \mathbf{Q}_1^{-1/2} \mathbf{g}_1$  where  $\mathbf{Q}_1 = (\mathbf{Q}_1^{1/2})^2$ ,

which implies  $\text{SNR}_1 = \|\mathbf{q}_1\|^2$  and  $\|\mathbf{g}_1\|^2 = \mathbf{q}_1^\top \mathbf{Q}_1 \mathbf{q}_1$ . Consequently, we rewrite the transmit powers in (16) and (17) as

$$\begin{aligned} \mathbb{E}[\|\mathbf{x}_1\|^2] &= \mathbf{q}_1^\top \mathbf{Q}_1 \mathbf{q}_1 + \|\mathbf{F}_1 \mathbf{F}_2\|_F^2 \sigma_1^2 + \|\mathbf{F}_1\|_F^2 \sigma_2^2 \\ &= \|\mathbf{q}_1^\top (\mathbf{I} + \mathbf{F}_1 \mathbf{F}_2)\|^2 \sigma_1^2 + \|\mathbf{q}_1^\top \mathbf{F}_1\|^2 \sigma_2^2 + \|\mathbf{F}_1 \mathbf{F}_2\|_F^2 \sigma_1^2 + \|\mathbf{F}_1\|_F^2 \sigma_2^2, \end{aligned} \quad (35)$$

$$\mathbb{E}[\|\mathbf{x}_2\|^2] = \|\mathbf{g}_2\|^2 + \|\mathbf{F}_2 \mathbf{Q}_1^{1/2} \mathbf{q}_1\|^2 + \|\mathbf{F}_2 (\mathbf{I} + \mathbf{F}_1 \mathbf{F}_2)\|_F^2 \sigma_1^2 + \|\mathbf{F}_2 \mathbf{F}_1\|_F^2 \sigma_2^2, \quad (36)$$

where the fact that  $\mathbf{F}_1 \mathbf{g}_2 = \mathbf{0}$  is used. Finally, we simplify our optimization in (29) as

$$\begin{aligned} &\underset{\mathbf{q}_1, \mathbf{F}_1, \mathbf{F}_2 \in \mathcal{F}_2}{\text{minimize}} && \alpha \mathbb{E}[\|\mathbf{x}_1\|^2] + (1 - \alpha) \mathbb{E}[\|\mathbf{x}_2\|^2] \\ &\text{subject to} && \|\mathbf{q}_1\|^2 = \eta_1. \end{aligned} \quad (37)$$

### E. Optimization Solution for Weighted Sum-Power Minimization

To solve the problem in (37), we divide it into two sub-problems and solve them alternately through a series of iterations. The first sub-problem is to solve for  $\mathbf{q}_1$  and  $\mathbf{F}_1$  given that  $\mathbf{F}_2 \in \mathcal{F}_2$  is fixed, and the second sub-problem is to solve for  $\mathbf{F}_2 \in \mathcal{F}_2$  assuming  $\mathbf{q}_1$  and  $\mathbf{F}_1$  are fixed.

1) *First sub-problem for obtaining  $\mathbf{q}_1$  and  $\mathbf{F}_1$ :* We assume a fixed value for  $\mathbf{F}_2 \in \mathcal{F}_2$ . We first show that  $\mathbb{E}[\|\mathbf{x}_2\|^2]$  is upper bounded by the sum of the scaled version of  $\mathbb{E}[\|\mathbf{x}_1\|^2]$  and some constant terms as follows:

$$\begin{aligned} \mathbb{E}[\|\mathbf{x}_2\|^2] &\stackrel{(i)}{=} \|\mathbf{g}_2\|^2 + \|\mathbf{F}_2 \mathbf{Q}_1^{1/2} \mathbf{q}_1\|^2 + \|\mathbf{F}_2\|_F^2 \sigma_1^2 + \|\mathbf{F}_2 \mathbf{F}_1 \mathbf{F}_2\|_F^2 \sigma_1^2 + \|\mathbf{F}_2 \mathbf{F}_1\|_F^2 \sigma_2^2 \\ &\leq \|\mathbf{g}_2\|^2 + \|\mathbf{F}_2\|_F^2 \sigma_1^2 + f_{2,\max}^2 (\|\mathbf{Q}_1^{1/2} \mathbf{q}_1\|^2 + \|\mathbf{F}_1 \mathbf{F}_2\|_F^2 \sigma_1^2 + \|\mathbf{F}_1\|_F^2 \sigma_2^2) \\ &= \|\mathbf{g}_2\|^2 + \|\mathbf{F}_2\|_F^2 \sigma_1^2 + f_{2,\max}^2 \mathbb{E}[\|\mathbf{x}_1\|^2], \end{aligned} \quad (38)$$

where  $f_{2,\max}^2 = \max_{i=2,\dots,N-1} f_{2,i}^2$ . To obtain the equality (i) in (38), we use the fact that  $\text{tr}(\mathbf{F}_2 \mathbf{F}_1 \mathbf{F}_2 \mathbf{F}_1^\top) = 0$  for  $\mathbf{F}_2 \in \mathcal{F}_2$ . To derive the inequality in (38), we exploit the property that  $\|\mathbf{F}_2 \mathbf{y}\|^2 \leq f_{2,\max}^2 \|\mathbf{y}\|^2$  for any vector  $\mathbf{y} \in \mathbb{R}^{N \times 1}$  and  $\|\mathbf{F}_2 \mathbf{Y}\|_F^2 \leq f_{2,\max}^2 \|\mathbf{Y}\|_F^2$  for any matrix  $\mathbf{Y} \in \mathbb{R}^{N \times N}$  when  $\mathbf{F}_2 \in \mathcal{F}_2$ . Accordingly, we obtain an upper bound on the objective function in (37) as

$$(1 - \alpha) (\|\mathbf{g}_2\|^2 + \|\mathbf{F}_2\|_F^2 \sigma_1^2) + (\alpha + f_{2,\max}^2 (1 - \alpha)) \mathbb{E}[\|\mathbf{x}_1\|^2]. \quad (39)$$

In the first sub-problem, instead of solving (37) directly, we aim to minimize the upper bound of the objective function in (39). Since the other terms in (39) are constants except for  $\mathbb{E}[\|\mathbf{x}_1\|^2]$ , the first sub-problem is then reduced to

$$(\mathcal{P}_1) : \underset{\mathbf{q}_1, \mathbf{F}_1}{\text{minimize}} \quad \mathbb{E}[\|\mathbf{x}_1\|^2]$$

$$\text{subject to} \quad \|\mathbf{q}_1\|^2 = \eta_1. \quad (40)$$

We will solve  $\mathcal{P}_1$  via (i) obtaining the optimal solution form of  $\mathbf{F}_1$  in terms of  $\mathbf{q}_1$ , and then (ii) plugging the optimal solution form of  $\mathbf{F}_1$  in  $\mathbb{E}[\|\mathbf{x}_1\|^2]$  and solving the problem for  $\mathbf{q}_1$ .

**Solving for  $\mathbf{F}_1$ .** Note that  $\mathbf{F}_1 \in \mathbb{R}^{N \times N}$  is a strictly lower triangular matrix given by

$$\mathbf{F}_1 = \begin{bmatrix} 0 & 0 & \dots & 0 \\ f_{1,2,1} & 0 & \dots & 0 \\ \vdots & \ddots & \ddots & \vdots \\ f_{1,N,1} & \dots & f_{1,N,N-1} & 0 \end{bmatrix} = \begin{bmatrix} 0 & 0 & \dots & 0 \\ \mathbf{f}_{1,1} & 0 & \dots & 0 \\ & \ddots & \ddots & \vdots \\ & & \mathbf{f}_{1,N-1} & 0 \end{bmatrix},$$

where  $\mathbf{f}_{1,i} = [f_{1,i+1,i}, f_{1,i+2,i}, \dots, f_{1,N,i}]^\top \in \mathbb{R}^{(N-i) \times 1}$ ,  $i \in \{1, \dots, N-1\}$ . Considering  $\mathbf{q}_1 = [q_{1,1}, q_{1,2}, \dots, q_{1,N}]^\top$ , we define a vector that contains a portion of the entries of  $\mathbf{q}_1$  as

$$\mathbf{h}_i = [q_{1,i+1}, q_{1,i+2}, \dots, q_{1,N}]^\top \in \mathbb{R}^{(N-i) \times 1}, \quad (41)$$

where  $i \in \{0, \dots, N-1\}$ . With the defined vectors  $\{\mathbf{f}_{1,i}\}$  and  $\{\mathbf{h}_i\}$ , we can rewrite  $\mathbb{E}[\|\mathbf{x}_1\|^2]$  in (35) as

$$\mathbb{E}[\|\mathbf{x}_1\|^2] = \sum_{i=1}^{N-1} \Phi_i(\mathbf{f}_{1,i}) + \sigma_1^2 (q_{1,N-1}^2 + q_{1,N}^2), \quad (42)$$

where  $\Phi_1(\mathbf{f}_{1,1}) \triangleq (\mathbf{h}_1^\top \mathbf{f}_{1,1})^2 \sigma_2^2 + \mathbf{f}_{1,1}^\top \mathbf{f}_{1,1} \sigma_2^2$  and  $\Phi_i(\mathbf{f}_{1,i}) \triangleq (q_{1,i-1} + f_{2,i} \mathbf{h}_i^\top \mathbf{f}_{1,i})^2 \sigma_1^2 + (\mathbf{h}_i^\top \mathbf{f}_{1,i})^2 \sigma_2^2 + \mathbf{f}_{1,i}^\top \mathbf{f}_{1,i} (f_{2,i}^2 \sigma_1^2 + \sigma_2^2)$ ,  $i \in \{2, \dots, N-1\}$ . The detailed derivation of  $\Phi_i(\mathbf{f}_{1,i})$ ,  $i \in \{1, \dots, N-1\}$ , is presented in Appendix H.

Using (42), our problem of interest (i.e.,  $\min_{\mathbf{F}_1} \mathbb{E}[\|\mathbf{x}_1\|^2]$ ) can be decomposed into  $N-1$  independent sub-problems each in the form of  $\min_{\mathbf{f}_{1,i}} \Phi_i(\mathbf{f}_{1,i})$ ,  $i \in \{1, \dots, N-1\}$ . Since each independent sub-problem is convex with respect to  $\mathbf{f}_{1,i}$ , we find  $\mathbf{f}_{1,i}$  optimally by solving  $\frac{\partial \Phi_i(\mathbf{f}_{1,i})}{\partial \mathbf{f}_{1,i}} = \mathbf{0}^\top$ . Obviously, we have  $\mathbf{f}_{1,1} = \mathbf{0}$ . Also, for  $i \in \{2, \dots, N-1\}$ , we need to solve

$$\frac{\partial \Phi_i(\mathbf{f}_{1,i})}{\partial \mathbf{f}_{1,i}} = (q_{1,i-1} + f_{2,i} \mathbf{h}_i^\top \mathbf{f}_{1,i})^\top \mathbf{h}_i^\top f_{2,i} \sigma_1^2 + (\mathbf{h}_i^\top \mathbf{f}_{1,i})^\top \mathbf{h}_i^\top \sigma_2^2 + (f_{2,i}^2 \sigma_1^2 + \sigma_2^2) \mathbf{f}_{1,i}^\top = \mathbf{0}^\top. \quad (43)$$

We thus obtain

$$\mathbf{f}_{1,i} = -\frac{f_{2,i} \sigma_1^2}{f_{2,i}^2 \sigma_1^2 + \sigma_2^2} \frac{q_{1,i-1}}{1 + \|\mathbf{h}_i\|^2} \mathbf{h}_i, \quad i \in \{2, \dots, N-1\}. \quad (44)$$

For a detailed derivation of (44) from (43), refer to Appendix I.

**Solving for  $\mathbf{q}_1$ .** Putting the optimal solution of  $\{\mathbf{f}_{1,i}\}_{i=2}^{N-1}$  obtained in (44) back into (42), we get

$$\begin{aligned} \mathbb{E}[\|\mathbf{x}_1\|^2] = & \sum_{i=2}^{N-1} \left[ \left( q_{1,i-1} - \frac{f_{2,i}^2 \sigma_1^2}{f_{2,i}^2 \sigma_1^2 + \sigma_2^2} \frac{q_{1,i-1} \|\mathbf{h}_i\|^2}{1 + \|\mathbf{h}_i\|^2} \right)^2 \sigma_1^2 + \left( \frac{f_{2,i} \sigma_1^2}{f_{2,i}^2 \sigma_1^2 + \sigma_2^2} \frac{q_{1,i-1} \|\mathbf{h}_i\|^2}{1 + \|\mathbf{h}_i\|^2} \right)^2 \sigma_2^2 \right. \\ & \left. + \left( \frac{f_{2,i} \sigma_1^2}{f_{2,i}^2 \sigma_1^2 + \sigma_2^2} \frac{q_{1,i-1}}{1 + \|\mathbf{h}_i\|^2} \right)^2 \|\mathbf{h}_i\|^2 (f_{2,i}^2 \sigma_1^2 + \sigma_2^2) \right] + (q_{1,N-1}^2 + q_{1,N}^2) \sigma_1^2 \end{aligned}$$

$$= \sum_{i=2}^{N-1} \frac{\sigma_1^2 q_{1,i-1}^2 (f_{2,i}^2 \sigma_1^2 + \sigma_2^2 (1 + \|\mathbf{h}_i\|^2))}{(f_{2,i}^2 \sigma_1^2 + \sigma_2^2) (1 + \|\mathbf{h}_i\|^2)} + (q_{1,N-1}^2 + q_{1,N}^2) \sigma_1^2. \quad (45)$$

Then,  $\mathcal{P}_1$  can be reduced to the following optimization problem:

$$\begin{aligned} & \underset{\mathbf{q}_1}{\text{minimize}} && \sum_{i=1}^{N-2} \frac{\sigma_1^2 q_{1,i}^2 (f_{2,i+1}^2 \sigma_1^2 + \sigma_2^2 (1 + \|\mathbf{h}_{i+1}\|^2))}{(f_{2,i+1}^2 \sigma_1^2 + \sigma_2^2) (1 + \|\mathbf{h}_{i+1}\|^2)} + (q_{1,N-1}^2 + q_{1,N}^2) \sigma_1^2 \\ & \text{subject to} && \|\mathbf{q}_1\|^2 = \eta_1. \end{aligned} \quad (46)$$

Defining  $x_i = q_{1,i}^2 \geq 0$ , we rewrite the objective function in (46) as

$$\sum_{i=1}^{N-2} \frac{f_{2,i+1}^2 \sigma_1^4 x_i}{(f_{2,i+1}^2 \sigma_1^2 + \sigma_2^2) (1 + x_{i+2} + \dots + x_N)} + \sum_{i=1}^{N-2} \frac{\sigma_1^2 \sigma_2^2 x_i}{f_{2,i+1}^2 \sigma_1^2 + \sigma_2^2} + \sigma_1^2 (x_{N-1} + x_N), \quad (47)$$

and the constraint in (46) as  $\sum_{i=1}^N x_i = \eta_1$ . Using the vector form of  $\mathbf{x} = [x_1, \dots, x_N]^\top \in \mathbb{R}^{N \times 1}$ , we can formulate an equivalent optimization problem to (46) as

$$\begin{aligned} & \underset{\mathbf{x}}{\text{minimize}} && \sum_{i=1}^{N-1} \frac{\mathbf{u}_i^\top \mathbf{x}}{1 + \mathbf{m}_i^\top \mathbf{x}} \\ & \text{subject to} && \mathbf{1}^\top \mathbf{x} = \eta_1, \quad \mathbf{x} \geq \mathbf{0}, \end{aligned} \quad (48)$$

where  $\mathbf{1} = [1, \dots, 1]^\top \in \mathbb{R}^{N \times 1}$  and  $\mathbf{0} = [0, \dots, 0]^\top \in \mathbb{R}^{N \times 1}$ . In (48),  $\mathbf{u}_i \in \mathbb{R}^{N \times 1}$  and  $\mathbf{m}_i \in \mathbb{R}^{N \times 1}$ ,  $i \in \{1, \dots, N-1\}$ , are defined as

$$\begin{aligned} \mathbf{u}_i &= \left[ 0, \dots, 0, \underbrace{\frac{|f_{2,i+1}|^2 \sigma_1^4}{|f_{2,i+1}|^2 \sigma_1^2 + \sigma_2^2}}_{i\text{-th}}, 0, \dots, 0 \right]^\top, \quad i \in \{1, \dots, N-2\}, \\ \mathbf{u}_{N-1} &= \left[ \frac{\sigma_1^2 \sigma_2^2}{|f_{2,2}|^2 \sigma_1^2 + \sigma_2^2}, \dots, \frac{\sigma_1^2 \sigma_2^2}{|f_{2,N-1}|^2 \sigma_1^2 + \sigma_2^2}, \sigma_1^2, \sigma_1^2 \right]^\top, \\ \mathbf{m}_i &= [0, \dots, 0, \underbrace{1}_{i\text{-th}}, \dots, 1]^\top, \quad i \in \{1, \dots, N-2\}, \quad \mathbf{m}_{N-1} = [0, \dots, 0]^\top, \end{aligned}$$

where  $\mathbf{u}_i, \mathbf{m}_i \geq \mathbf{0}$ . Here,  $\mathbf{u}_{N-1}$  captures the last two terms in (47). The problem in (48) is a multi-objective linear fractional programming [23]. We thus can adopt commercial software [24] to solve this problem.

2) *Second sub-problem for obtaining  $\mathbf{F}_2$* : While fixing  $\mathbf{q}_1$  and  $\mathbf{F}_1$ , we formulate the second sub-problem as

$$(\mathcal{P}_2) : \underset{\mathbf{F}_2 \in \mathcal{F}_2}{\text{minimize}} \quad \alpha \mathbb{E}[\|\mathbf{x}_1\|^2] + (1 - \alpha) \mathbb{E}[\|\mathbf{x}_2\|^2]. \quad (49)$$

We aim to minimize the objective of  $\mathcal{P}_2$  for each  $f_{2,i}$ ,  $i \in \{2, \dots, N-1\}$  by setting the derivative with respect to  $f_{2,i}$  equal to zero. Our methodology would yield a sub-optimal solution given the non-convexity of the problem  $\mathcal{P}_2$ . We then obtain

$$\alpha \frac{\partial \mathbb{E}[\|\mathbf{x}_1\|^2]}{\partial f_{2,i}} + (1 - \alpha) \frac{\partial \mathbb{E}[\|\mathbf{x}_2\|^2]}{\partial f_{2,i}} = 2\alpha \sigma_1^2 q_{1,i-1} \mathbf{h}_i^\top \mathbf{f}_{1,i} + c_i f_{2,i}, \quad (50)$$

---

**Algorithm 1** Linear Encoding Schemes for Weighted Sum-Power Minimization in GTWC
 

---

- 1: **Input.** Power constraint  $NP$ , noise variances  $\sigma_1^2$  and  $\sigma_2^2$ , number of bits  $K_1$  and  $K_2$ , number of channel uses  $N$ , target SNRs  $\eta_1$  and  $\eta_2$ , weight value  $\alpha$ , and stopping value  $\epsilon$ .
  - 2: **Output.** Linear encoding schemes,  $\mathbf{g}_1$ ,  $\mathbf{F}_1$ ,  $\mathbf{g}_2$ , and  $\mathbf{F}_2$ .
  - 3: Obtain the optimal solutions,  $\mathbf{g}_2 = [0, 0, \dots, \sqrt{\eta_2 \sigma_2}]^\top$  and  $f_{2,N} = 0$ , from Propositions 1 and 2.
  - 4: Randomly generate  $\{f_{2,i}\}_{i=2}^{N-1}$ . Calculate the objective function value  $s_{\text{new}}$  of (29) with  $\mathbf{g}_1$ ,  $\mathbf{F}_1$ ,  $\mathbf{g}_2$ , and  $\mathbf{F}_2$ . Set  $s_{\text{old}} = 0$ .
  - 5: **while**  $|s_{\text{new}} - s_{\text{old}}| > \epsilon$  **do**
  - 6:   • **Sub-problem 1. Obtain  $\mathbf{g}_1$  and  $\mathbf{F}_1$**
  - 7:   Solve the problem in (48) for  $\mathbf{x} = [x_1, \dots, x_N]^\top$  and obtain  $q_{1,i} = \sqrt{x_i}$ ,  $i \in \{1, \dots, N\}$ .
  - 8:   Obtain the columns of  $\mathbf{F}_1$ ,  $\{\mathbf{f}_{1,i}\}_{i=1}^{N-1}$ , from (44), using the values of  $\{q_{1,i}\}_{i=1}^{N-1}$ .
  - 9:   Obtain  $\mathbf{g}_1 = \mathbf{Q}_1^{1/2} \mathbf{q}_1$  where  $\mathbf{Q}_1$  is given in (20).
  - 10:   • **Sub-problem 2. Obtain  $\mathbf{F}_2$**
  - 11:   Calculate the objective function value  $\nu_{\text{new}}$  of (29) with  $\mathbf{g}_1$ ,  $\mathbf{F}_1$ ,  $\mathbf{g}_2$ , and  $\mathbf{F}_2$ . Set  $\nu_{\text{old}} = 0$ .
  - 12:   **while**  $|\nu_{\text{new}} - \nu_{\text{old}}| > \epsilon$  **do**
  - 13:     Obtain  $f_{2,i}$  sequentially for  $i \in \{2, \dots, N-1\}$  by (51).  
 $\nu_{\text{old}} \leftarrow \nu_{\text{new}}$ .  
    Calculate the objective function value  $\nu_{\text{new}}$  of (29) with the updated  $\{f_{2,i}\}_{i=2}^{N-1}$ .
  - 14:   **end while**
  - 15:   • **Update values for stopping criterion**
  - 16:    $s_{\text{old}} \leftarrow s_{\text{new}}$ .
  - 17:   Calculate the objective function value  $s_{\text{new}}$  of (29) with the updated  $\mathbf{g}_1$ ,  $\mathbf{F}_1$ , and  $\mathbf{F}_2$ .
  - 18: **end while**
- 

where

$$\begin{aligned}
 c_i \triangleq & 2\alpha\sigma_1^2(\|\mathbf{h}_i^\top \mathbf{f}_{1,i}\|^2 + \|\mathbf{f}_{1,i}\|^2) + 2(1-\alpha)p_{i-1}^2 + 2(1-\alpha)\sigma_1^2 \\
 & + 2(1-\alpha)\sigma_1^2 \left( \sum_{j=i+1}^{N-1} f_{1,j,i}^2 f_{2,j+1}^2 + \sum_{k=2}^{i-2} f_{1,i-1,k}^2 f_{2,k}^2 \right) + 2\sigma_2^2(1-\alpha) \sum_{j=1}^{i-2} f_{1,i-1,j}^2.
 \end{aligned}$$

The details of derivations used for obtaining (50) are presented in Appendix J. By setting the right-hand side of the equality in (50) to zero, we obtain the solution for  $f_{2,i}$  as

$$f_{2,i} = -\frac{2\alpha\sigma_1^2 q_{1,i-1} \mathbf{h}_i^\top \mathbf{f}_{1,i}}{c_i}, \quad i \in \{2, \dots, N-1\}. \quad (51)$$

The pseudo-code of our iterative method to solve the overall optimization problem in (29) is summarized in Algorithm 1. We solve the two sub-problems alternatively through a series of *outer* iterations denoted in lines 5-17. In the *inner* iterations, lines 11-13, we solve the second sub-problem.

### F. Optimization Solution for Sum-Error Minimization

We solved the weighted sum-power (WSP) minimization problem (in (29)) in Sec. III-D, and presented the solution algorithm, Algorithm 1. We can express the input-output relationship of Algorithm 1 as

$$(\mathbf{g}_1, \mathbf{F}_1, \mathbf{g}_2, \mathbf{F}_2) = \text{Min-WSP}(\sigma_1^2, \sigma_2^2, N, \eta_1, \eta_2, \alpha), \quad (52)$$

where  $\eta_1$ ,  $\eta_2$ , and  $\alpha$  are given. We note that the objective value in (29) is the sum of the transmit powers, where the transmit powers,  $\mathbb{E}[\|\mathbf{x}_1\|^2]$  and  $\mathbb{E}[\|\mathbf{x}_2\|^2]$ , can be calculated from the obtained solutions,  $\mathbf{g}_1$ ,  $\mathbf{F}_1$ ,  $\mathbf{g}_2$ , and  $\mathbf{F}_2$ , by (16)-(17). To explicitly indicate the dependency of the powers,  $\mathbb{E}[\|\mathbf{x}_1\|^2]$  and  $\mathbb{E}[\|\mathbf{x}_2\|^2]$ , on the values of  $\eta_1$ ,  $\eta_2$ , and  $\alpha$ , we denote  $\mathbb{E}[\|\mathbf{x}_1\|^2]$  and  $\mathbb{E}[\|\mathbf{x}_2\|^2]$  as  $P_1(\eta_1, \eta_2, \alpha)$  and  $P_2(\eta_1, \eta_2, \alpha)$ , respectively.

Our next goal is to solve the sum-error minimization problem in (25) by using the solution algorithm for the WSP minimization problem in (29), i.e., Algorithm 1. A naive approach is to first run Algorithm 1 for every feasible set of  $(\eta_1, \eta_2, \alpha)$  and then find the best solution of  $(\mathbf{g}_1, \mathbf{F}_1, \mathbf{g}_2, \mathbf{F}_2)$  that minimizes the sum-error,  $\mathcal{E}_1(\eta_1) + \mathcal{E}_2(\eta_2)$ , and also satisfies the power constraints,  $P_i(\eta_1, \eta_2, \alpha) \leq NP$ ,  $i \in \{1, 2\}$ . However, the search space for  $(\eta_1, \eta_2, \alpha)$  would be prohibitively large since the search space is continuous and three-dimensional.

To mitigate such complexities, we propose a method that reduces the three-dimensional search to a one-dimensional search only over  $\eta_2$  through two distinct one-dimensional search methods: (i) the bisection method for finding  $\eta_1$  and (ii) the golden-section search method for searching over  $\alpha$ .

1) *Reducing the search space for  $\alpha$  via the golden-section search method [22]:* Given  $\eta_1$  and  $\eta_2$ , we consider solving (29) for various  $\alpha$  and obtaining the solution of (28) by selecting the best  $\alpha$ , denoted by  $\alpha^*$ , and its corresponding solution,  $(\mathbf{g}_1, \mathbf{F}_1, \mathbf{g}_2, \mathbf{F}_2)$ . However, searching over  $\alpha$  requires lots of computations since  $\alpha$  is continuous over the region  $(0, 1)$ . Therefore, we develop an approximate searching method by assuming that the objective function in (28),  $\max\{P_1(\eta_1, \eta_2, \alpha), P_2(\eta_1, \eta_2, \alpha)\}$ , is unimodal along  $\alpha \in (0, 1)$ . This assumption is motivated by our observation of unimodality through numerical experiments. Unimodal functions have a unique maximal or minimal point, for which the golden-section search method can be employed to find the point [22]. Thus, we adopt the golden-section search method and obtain

$$\alpha^*(\eta_1, \eta_2) = \min_{\alpha \in (0, 1)} \max\{P_1(\eta_1, \eta_2, \alpha), P_2(\eta_1, \eta_2, \alpha)\}. \quad (53)$$

where  $\alpha^*(\eta_1, \eta_2)$  is obtained depending on the values of  $\eta_1$  and  $\eta_2$ . In summary, we obtained the solution of (28) given  $\eta_1$  and  $\eta_2$  by applying the golden-section search method over  $\alpha$  to the problem (29) without requiring exhaustive search over  $\alpha$ .

---

**Algorithm 2** Linear Encoding and Decoding Schemes for Sum-Error Minimization in GTWC
 

---

- 1: **Input.** Power constraint  $NP$ , noise variances  $\sigma_1^2$  and  $\sigma_2^2$ , number of bits  $K_1$  and  $K_2$ , and number of channel uses  $N$ .
  - 2: **Output.** Linear encoding schemes  $\mathbf{g}_1, \mathbf{F}_1, \mathbf{g}_2$ , and  $\mathbf{F}_2$ , linear decoding schemes  $\mathbf{w}_1$  and  $\mathbf{w}_2$ , and SNR values  $\eta_1$  and  $\eta_2$ .
  - 3: Set a finite search space for  $\eta_2$  and pick a value for  $\eta_2$  from the set. Set a Boolean variable  $\text{SEARCH} = \text{True}$ .
  - 4: **while**  $\text{SEARCH}$  **do**
  - 5:   Apply the bisection method to find  $\eta_1^*(\eta_2)$  such that  $u(\eta_1^*(\eta_2)) = 0$ , where  $u(\eta_1) = \max\{P_1(\eta_1, \eta_2, \alpha^*(\eta_1, \eta_2)), P_2(\eta_1, \eta_2, \alpha^*(\eta_1, \eta_2))\} - NP$  in (54). Here,  $\alpha^*(\eta_1, \eta_2)$  is obtained by (53) through running Algorithm 1 over  $\alpha$ , i.e.,  $(\mathbf{g}_1, \mathbf{F}_1, \mathbf{g}_2, \mathbf{F}_2) = \text{Min-WSP}(\sigma_1^2, \sigma_2^2, N, \eta_1, \eta_2, \alpha)$ , and calculating  $P_1(\eta_1, \eta_2, \alpha)$  and  $P_2(\eta_1, \eta_2, \alpha)$  from (16)-(17) with the obtained solution  $(\mathbf{g}_1, \mathbf{F}_1, \mathbf{g}_2, \mathbf{F}_2)$ .
  - 6:   Set an unexplored point in the search space of  $\eta_2$ . Once all points are searched, set  $\text{SEARCH} = \text{False}$ .
  - 7: **end while**
  - 8: Find the tuple of  $(\mathbf{g}_1, \mathbf{F}_1, \mathbf{g}_2, \mathbf{F}_2, \eta_1, \eta_2)$  that minimizes  $\mathcal{E}_1(\eta_1) + \mathcal{E}_2(\eta_2)$ .
  - 9: Obtain the decoding schemes  $\mathbf{w}_1$  and  $\mathbf{w}_2$  by using  $\mathbf{g}_1, \mathbf{F}_1, \mathbf{g}_2$ , and  $\mathbf{F}_2$  from (22).
- 

2) *Reducing the search space for  $\eta_1$  via the bisection method [25]:* We recall that solving the original problem (25) is equivalent to solving (28) over all feasible region of  $(\eta_1, \eta_2)$  and finding the best solution. However, the computational complexity for searching over continuous two-dimensional space is prohibitive. Therefore, we use the fact that the objective function of (28) is increasing over  $\eta_1$  from Lemma 1, and utilize a one-dimensional search method for finding  $\eta_1$  given  $\eta_2$ . When seeking a particular functional value and its corresponding point in an increasing function, we can utilize the bisection method as an efficient one-dimensional search approach [25]. Hence, we apply the bisection method to find  $\eta_1^*(\eta_2)$ , which depends on the value of  $\eta_2$ , such that  $u(\eta_1^*(\eta_2)) = 0$ , where

$$u(\eta_1) = \max\{P_1(\eta_1, \eta_2, \alpha^*(\eta_1, \eta_2)), P_2(\eta_1, \eta_2, \alpha^*(\eta_1, \eta_2))\} - NP. \quad (54)$$

Note that  $u(\eta_1)$  is an increasing function with respect to  $\eta_1$  from Lemma 1. We then obtain  $\eta_1^*(\eta_2)$  such that  $\max\{P_1(\eta_1^*(\eta_2), \eta_2, \alpha^*(\eta_1^*(\eta_2), \eta_2)), P_2(\eta_1^*(\eta_2), \eta_2, \alpha^*(\eta_1^*(\eta_2), \eta_2))\} = NP$ .

For each value of  $\eta_2$  in the search space, we obtain the tuple  $(\eta_1^*(\eta_2), \eta_2, \alpha^*(\eta_1^*(\eta_2), \eta_2))$  and find the best case that yields the minimum sum-error. Overall, by adopting the bisection method and golden-section search method in obtaining the solution of (25), we reduced the three-dimensional search space to one-dimensional search only over  $\eta_2$  and mitigated the complexity. The overall algorithm is provided in Algorithm 2.

### G. Medium/Long Block-Lengths and Modulation Orders

We have focused on exchanging a message pair,  $m_1$  and  $m_2$ , between the two users, where the encoding/decoding schemes are obtained by Algorithm 2. We recall that the message  $m_i$  contains  $K_i$  bits via  $2^{K_i}$ -ary PAM,  $i \in \{1, 2\}$ . Let us define a long block-length as  $L_i$  to distinguish from a short

block-length  $K_i$ , where  $K_i$  denotes the number of *processing bits* contained per each message  $m_i$ . Given a total of  $L_i$  bits, User  $i$  has a total of  $M_i = L_i/K_i$  message symbols, each containing  $K_i$  bits and modulated with  $2^{K_i}$ -ary PAM. We define the total number of channel uses for exchanging  $L_1$  and  $L_2$  bits between the two users as  $N_L$  and the coding rate of User  $i$  as  $r_i = L_i/N_L$ . We consider that the values of  $L_i$  and  $N_L$  are fixed, while the value of  $K_i$  can be adjusted by User  $i$ . We assume the same number of messages at the users, i.e.,  $M = M_1 = M_2$ , by properly choosing  $K_i$  such that  $L_1/K_1 = L_2/K_2$ . The number of channel uses for exchanging a message pair is then  $N = N_L/M$ . Through this successive transmission, the users can exchange a total of  $M$  message pairs over  $N_L$  channel uses.

Depending on the value of  $K_i$ , there is a trade-off between the symbol distance and the feedback benefit in obtaining better SER in (24). If  $K_i$  is small, e.g.,  $K_i = 1$ , the users only use a small number of channel uses for exchanging a message pair, which leads us not to fully benefit from the feedback scheme and thus to have a low SNR in (23). On the other hand, as  $K_i$  becomes larger, the symbol error may easily occur since the distance between the quantized symbols decreases in signal space as the number of quantized symbols,  $2^{K_i}$ , increases. Therefore, a proper selection of  $K_i$  or the modulation order  $2^{K_i}$  is important to obtain better SER performance. We evaluate the error performance with different values of  $K_i$  in Sec. VI.

Our linear coding schemes can be straightforwardly extended to incorporating concatenated coding by using our schemes for inner coding in a similar way in feedback-enabled GOWCs proposed by [10]. In concatenated coding, outer coding can be implemented with any error correction codes, such as turbo codes or LDPC, where the  $L_i$  source bits are encoded to  $L_i^{(c)}$  bits with outer coding rate  $r_{\text{out}} = L_i/L_i^{(c)}$ . For inner coding, we consider modulating  $L_i^{(c)}$  bits to  $M_i = L_i^{(c)}/K_i$  messages each with  $2^{K_i}$ -ary PAM, and each message pair is exchanged with our linear coding schemes. Since this work focuses on proposing new frameworks for two-way coding, we evaluate our coding methodology with a simple coding setup without adopting concatenated coding.

We have so far explored the linear approach for two-way coding, which offer low computational complexity (further elaborated in Sec. V). However, the simplified linear coding approach may limit the flexibility in code design. To address this, we propose a non-linear coding scheme based on deep learning in Sec. IV.

#### IV. LEARNING-BASED CODING VIA RNNs

In this section, we propose a non-linear coding methodology based on deep learning frameworks which allow higher degrees of freedom in coding. First, we adopt a state propagation-based encoding (Sec. IV-A), and then, we discuss the composition of our learning-based coding structure in two parts: encoding



(Sec. IV-B) and decoding (Sec. IV-C). Afterwards, we discuss how to train our coding architecture and how to make an inference (Sec. IV-D), and finally in Sec. IV-E, we discuss a modulo-based approach to process long block-lengths of bits with the proposed RNN-based coding architecture.

#### A. State Propagation-Based Encoding

Recall the optimization problem (5)-(6), where the design variables are  $2N$  different encoding functions:  $\{f_{1,k}\}_{k=1}^N$  and  $\{f_{2,k}\}_{k=1}^N$ , and two decoding functions,  $g_1$  and  $g_2$ . It is expected that the  $N$  encoding functions at each user are correlated with one another, since the inputs used for encoding at each timestep in (3) overlap. Based on the correlation of encoding processes across time, we adopt a state propagation-based encoding technique [17], where only two functions are used for encoding at each user: (i) signal-generation and (ii) state-propagation. By designing only these two functions instead of the  $N$  encoding functions, the design complexity for encoding could be significantly reduced.

We first define the signal-generation function of User  $i$  as  $f_i : \mathbb{R}^{K_i+N_s+1} \rightarrow \mathbb{R}$ . We then re-write the encoding process in (3) as

$$x_i[k] = f_i(\mathbf{b}_i, y_i[k-1], \mathbf{s}_i[k]), \quad k \in \{1, \dots, N\}, \quad (55)$$

where we assume  $y_i[0] = 0$ . Here,  $\mathbf{s}_i[k] \in \mathbb{R}^{N_s}$  is the state vector, which propagates over time through the state-propagation function  $h_i : \mathbb{R}^{K_i+N_s+1} \rightarrow \mathbb{R}^{N_s}$ , which is given by

$$\mathbf{s}_i[k] = h_i(\mathbf{b}_i, y_i[k-1], \mathbf{s}_i[k-1]), \quad k \in \{1, \dots, N\}. \quad (56)$$

In (56), the current state  $\mathbf{s}_i[k]$  is updated from the prior state  $\mathbf{s}_i[k-1]$  by incorporating  $\mathbf{b}_i$  and  $y_i[k-1]$ . For the initial condition, we assume  $\mathbf{s}_i[0] = \mathbf{0}$ . We note that the functional form  $x_i[k] = f_{i,k}(\mathbf{b}_i, y_i[1], \dots, y_i[k-1])$  in (3) is represented by the two equations (55) and (56); The current state vector  $\mathbf{s}_i[k]$  as an input in (55) is a function of the previous state  $\mathbf{s}_i[k-1]$  in (56), where  $\mathbf{s}_i[k-1]$  contains  $y_i[k-2]$  as an input. By the recursive nature of the function  $h_i$  in (56), all previous receive signals,  $y_i[1], \dots, y_i[k-1]$  are captured for encoding as in (3). This encoding model in (55)-(56) can be seen as a general and non-linear extension of the state-space model used for linear encoding in feedback-enabled systems [12].

By using this technique, we only need to construct two encoding functions for each User  $i$ ,  $f_i$  and  $h_i$  – instead of  $N$  distinct functions  $\{f_{i,k}\}_{k=1}^N$  in (3) – and the decoding function  $g_i$ . We thus re-write the optimization problem in (5)-(6) as

$$\underset{f_1, f_2, h_1, h_2, g_1, g_2}{\text{minimize}} \quad \mathcal{E}_1(f_1, f_2, h_1, h_2, g_2) + \mathcal{E}_2(f_1, f_2, h_1, h_2, g_1) \quad (57)$$

$$\text{subject to} \quad \mathbb{E}_{\mathbf{b}_1, \mathbf{b}_2, \mathbf{n}_1, \mathbf{n}_2} \left[ \sum_{k=1}^N x_i^2[k] \right] \leq NP, \quad i \in \{1, 2\}, \quad (58)$$

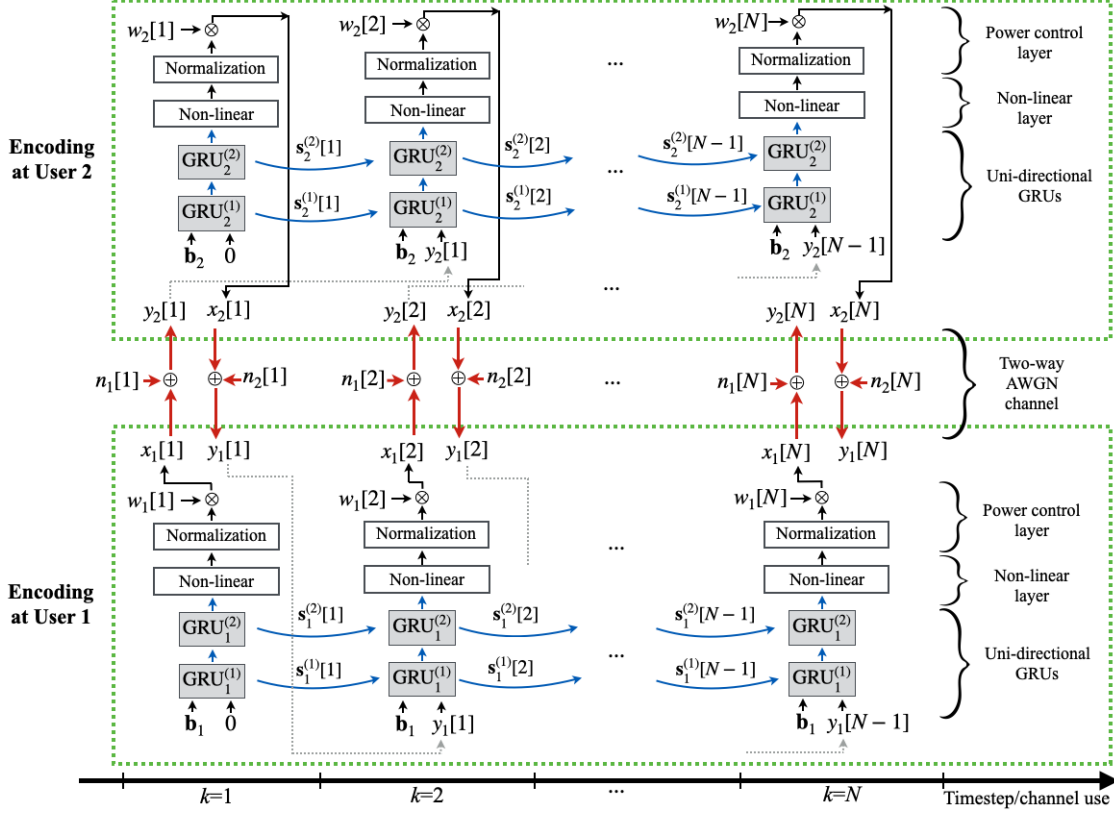


Fig. 2: Our proposed RNN-based encoding architecture for two-way channels. A pair of interactive RNNs captures the coupling effect caused by the encoding processes of the two users.

where the dependency on the error probability  $\mathcal{E}_i$ ,  $i \in \{1, 2\}$ , has been modified from (5) to (57) for state propagation-based encoding.

The problem (57)-(58) is still non-trivial since the encoding/decoding functions,  $f_i$ ,  $h_i$ , and  $g_i$ , can take arbitrary forms. A proper design of such non-linear functions can potentially provide higher degrees of flexibility in encoders' and decoders' behavior, as compared to the linear coding discussed in the previous section. To design such non-linear functions, in this section, we develop a learning-based coding architecture, which will be discussed in two parts: encoding (Sec. IV-B) and decoding (Sec. IV-C).

### B. Encoding

We follow the state propagation-based encoding approach discussed in Sec. IV-A. The concept of state propagation over time motivates us to employ RNNs as components of our learning architecture, similar to [17]. Specifically, we utilize gated recurrent units (GRUs), a type of RNNs, to effectively capture the long-term dependency of time-series information [26]. For User  $i$ ,  $i \in \{1, 2\}$ , the state-propagation function  $h_i$  in (56) consists of two layers of GRUs, while the signal-generation function  $f_i$  in (55) consists

of a non-linear layer and a power control layer in sequence. The overall encoding architecture of the two users and their interaction through the two-way channel are depicted in Fig. 2.

1) *GRUs for state propagation*: We adopt two layers of unidirectional GRUs at each user to capture the time correlation of the receive signals in a causal manner. Formally, we represent the input-output relationship at each layer at time  $k$  at User  $i$  as

$$\mathbf{s}_i^{(1)}[k] = \text{GRU}_i^{(1)}(\mathbf{b}_i, y_i[k-1], \mathbf{s}_i^{(1)}[k-1]), \quad (59)$$

$$\mathbf{s}_i^{(2)}[k] = \text{GRU}_i^{(2)}(\mathbf{s}_i^{(1)}[k], \mathbf{s}_i^{(2)}[k-1]), \quad (60)$$

where  $\text{GRU}_i^{(\ell)}$  represents a functional form of GRU processing at layer  $\ell$  of User  $i$  and  $\mathbf{s}_i^{(\ell)}[k] \in \mathbb{R}^{N_{i,\ell}^{(\text{enc})}}$  is the state vector obtained by  $\text{GRU}_i^{(\ell)}$  at time  $k$ , where  $i \in \{1, 2\}$ ,  $\ell \in \{1, 2\}$ , and  $k \in \{1, \dots, N\}$ . For the initial conditions, we assume  $\mathbf{s}_i^{(\ell)}[0] = \mathbf{0}$ ,  $i \in \{1, 2\}$ ,  $\ell \in \{1, 2\}$ .

Equations (59)-(60) can be represented as a functional form of the state propagation-based encoding in (56). By defining the overall state vector as  $\mathbf{s}_i[k] = [\mathbf{s}_i^{(1)}[k], \mathbf{s}_i^{(2)}[k]]$ , we obtain  $\mathbf{s}_i[k] = h_i(\mathbf{b}_i, y_i[k-1], \mathbf{s}_i[k-1])$ , where  $h_i$  denotes the process of two layers of GRUs in (59)-(60). Note that  $\mathbf{s}_i[k]$  propagates over time through the GRUs by incorporating the current input information into its state. Because the bit vector  $\mathbf{b}_i$  with length  $K_i$  is handled as a *block* to generate transmit signals with any length  $N$ , our method is flexible enough to support any coding rate  $r_i = K_i/N$ . Furthermore, the GRUs are interactive between the users since each user's GRU incorporates the previously received symbol as input, as shown in Fig. 2. The pair of interactive GRUs effectively captures the interplay of the users' encoding processes.

2) *Non-linear layer*: We adopt an additional non-linear layer at the output of the GRUs. The state vector at the last layer of the GRUs, i.e.,  $\mathbf{s}_i^{(2)}[k]$ , is taken as an input to this additional non-linear layer. Formally, we can represent the process of the non-linear layer at User  $i$  as

$$\tilde{x}_i[k] = \phi(\mathbf{w}_{\text{enc},i}^T \mathbf{s}_i^{(2)}[k] + b_{\text{enc},i}), \quad k \in \{1, \dots, N\}, \quad (61)$$

where  $\mathbf{w}_{\text{enc},i} \in \mathbb{R}^{N_{i,2}^{(\text{enc})}}$  and  $b_{\text{enc},i} \in \mathbb{R}$  are the trainable weights and biases, respectively, and  $\phi : \mathbb{R} \rightarrow \mathbb{R}$  is an activation function. In this work, we employ the hyperbolic tangent for  $\phi$  [26].

Since  $\tilde{x}[k]$  (as the output of the hyperbolic tangent) ranges in  $(-1, 1)$ , it is possible to use a scaled version of  $\tilde{x}[k]$ , i.e.,  $\sqrt{P}\tilde{x}[k]$ , as a transmit symbol that satisfies the power constraint  $\sum_{k=1}^N (\sqrt{P}\tilde{x}[k])^2 \leq NP$ . However, this does not ensure maximum or efficient utilization of the transmit power budget. Power control over the sequence of transmit signals is essential in the design of encoding schemes using feedback signals in order to achieve robust error performance, e.g., in feedback-enabled communications [8], [10], [14], [17].

3) *Power control layer*: We introduce a power control layer to optimize for the power distribution, while satisfying the power constraint in (58). This layer consists of two sequential modules: normalization and power-weight multiplication. The transmit symbol of User  $i$  at time  $k$  is then generated by

$$x_i[k] = w_i[k]\gamma_{i,k}^{(J)}(\tilde{x}_i[k]), \quad k \in \{1, \dots, N\}, \quad (62)$$

where  $w_i[k]$  is a trainable power weight satisfying  $\sum_{k=1}^N w_i^2[k] = NP$ ,  $i \in \{1, 2\}$ , and  $\gamma_{i,k}^{(J)} : \mathbb{R} \rightarrow \mathbb{R}$  is a normalization function applied to  $\tilde{x}_i[k]$  in a form of  $\gamma_{i,k}^{(J)}(x) = (x - m_{i,k}(J))/d_{i,k}(J)$ . Here,  $m_{i,k}(J)$  and  $d_{i,k}^2(J)$  are the sample mean and sample variance of  $x$  at User  $i$  at time  $k$  calculated from the data with size  $J$ .

Through the power control layer, the power weights  $\{w_i[k]\}_{i,k}$  are optimized via training in a way that minimizes the sum of errors in (57). At the same time, the power constraint in (58) should be satisfied. However, satisfying the power constraint in an (ensemble) average sense is non-trivial because the distributions of  $\{x_i[k]\}_{k=1}^N$  are unknown. Therefore, we approach it in an empirical sense as adopted in [17]: (i) During training, we use standard batch normalization; we normalize  $\tilde{x}_i[k]$  with the sample mean and sample variance calculated from each batch of data with size  $N_{\text{batch}}$  at each  $k$ . Note that  $N_{\text{batch}}$  denotes the size of batch used in a single iteration during training, and  $J$  represents the total available training data. (ii) After training, we calculate and save the sample mean  $m_{i,k}(J)$  and sample variance  $d_{i,k}^2(J)$  from the entire training data with size  $J$ . (iii) For inference, we use the saved mean and variance for normalization.

In the following lemma, we show that the above procedure guarantees satisfaction of the equality power constraint in an asymptotic sense with a large number of training data used for normalization.

**Lemma 2.** *Given the power control layer at User  $i$  in (62), the power constraint in (58) converges to  $NP$  almost surely, i.e.,  $\mathbb{E}_{\mathbf{b}_1, \mathbf{b}_2, \mathbf{n}_1, \mathbf{n}_2} \left[ \sum_{k=1}^N x_i^2[k] \right] \xrightarrow{a.s.} NP$ , as the number of training data  $J$  used for the normalization in (62) tends to infinity.*

The proof of Lemma 2 is provided in Appendix G.

### C. Decoding

The overall decoding architecture at User  $i$ ,  $i \in \{1, 2\}$ , is shown in Fig. 3. The decoding function  $g_i$  for User  $i$  in (4) consists of bi-directional GRUs, an attention layer, and a non-linear layer in sequence. We discuss each of them in detail below.

1) *Bi-directional GRUs*: At each user, we utilize two layers of bi-directional GRUs to capture the time correlation of the receive symbols both in the forward and backward directions over the sequence

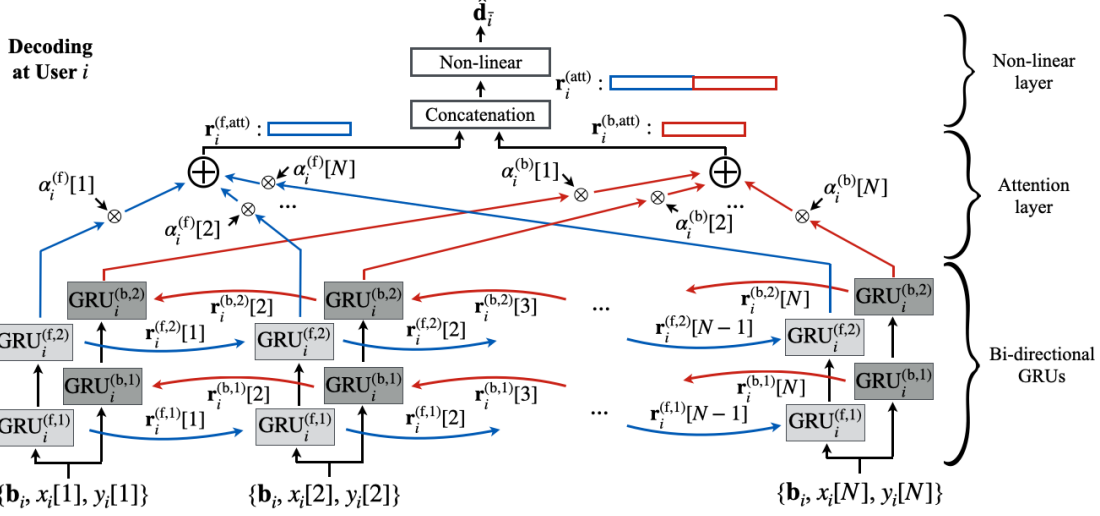


Fig. 3: Our proposed RNN-based decoding architecture at User  $i$ ,  $i \in \{1, 2\}$ . Bi-directional RNNs with the attention mechanism are introduced to exploit correlations among receive symbols in which the encoders' coupling behavior is captured. Here,  $\bar{i}$  denotes the index of the counterpart of User  $i$ , i.e.,  $\bar{i} = 2$  if  $i = 1$  while  $\bar{i} = 1$  if  $i = 2$ .

of the receive symbols. We represent the input-output relationship of the forward directional GRUs at time  $k$  of User  $i$  as

$$\begin{aligned} \mathbf{r}_i^{(f,1)}[k] &= \text{GRU}_i^{(f,1)}(\mathbf{b}_i, x_i[k], y_i[k], \mathbf{r}_i^{(f,1)}[k-1]), \\ \text{and } \mathbf{r}_i^{(f,2)}[k] &= \text{GRU}_i^{(f,2)}(\mathbf{r}_i^{(f,1)}[k], \mathbf{r}_i^{(f,2)}[k-1]), \end{aligned} \quad (63)$$

and that of the backward directional GRUs as

$$\begin{aligned} \mathbf{r}_i^{(b,1)}[k] &= \text{GRU}_i^{(b,1)}(\mathbf{b}_i, x_i[k], y_i[k], \mathbf{r}_i^{(b,1)}[k+1]), \\ \text{and } \mathbf{r}_i^{(b,2)}[k] &= \text{GRU}_i^{(b,2)}(\mathbf{r}_i^{(b,1)}[k], \mathbf{r}_i^{(b,2)}[k+1]), \end{aligned} \quad (64)$$

where  $\text{GRU}_i^{(f,\ell)}$  and  $\text{GRU}_i^{(b,\ell)}$  represent functional forms of GRU processing at layer  $\ell$  of User  $i$  in the forward and backward direction, respectively. Here,  $\mathbf{r}_i^{(f,\ell)}[k] \in \mathbb{R}^{N_{i,\ell}^{(\text{dec})}}$  and  $\mathbf{r}_i^{(b,\ell)}[k] \in \mathbb{R}^{N_{i,\ell}^{(\text{dec})}}$  are the state vectors obtained by  $\text{GRU}_i^{(f,\ell)}$  and  $\text{GRU}_i^{(b,\ell)}$ , respectively, at time  $k$ , where  $i \in \{1, 2\}$ ,  $\ell \in \{1, 2\}$ , and  $k \in \{1, \dots, N\}$ . For the initial conditions,  $\mathbf{r}_i^{(f,\ell)}[0] = \mathbf{0}$  and  $\mathbf{r}_i^{(b,\ell)}[N+1] = \mathbf{0}$ , where  $i \in \{1, 2\}$  and  $\ell \in \{1, 2\}$ .

2) *Attention layer*: We consider the forward/backward state vectors at the last layer, i.e.,  $\{\mathbf{r}_i^{(f,2)}[k]\}_{k=1}^N$  and  $\{\mathbf{r}_i^{(b,2)}[k]\}_{k=1}^N$ , as inputs to the attention layer. Each state vector contains different feature information depending on both its direction and timestep  $k$ : the forward state vector  $\mathbf{r}_i^{(f,2)}[k]$  captures the implicit correlation information of the input tuples of the previous timesteps, i.e.,  $\{\mathbf{b}_i, x_i[1], y_i[1]\}$ ,

...,  $\{\mathbf{b}_i, x_i[k], y_i[k]\}$ , while the backward state vector  $\mathbf{r}_i^{(b,2)}[k]$  captures that of the later timesteps, i.e.,  $\{\mathbf{b}_i, x_i[k], y_i[k]\}$ , ...,  $\{\mathbf{b}_i, x_i[N], y_i[N]\}$ . Although the state vectors at each end, i.e.,  $\mathbf{r}_i^{(f,2)}[N]$  and  $\mathbf{r}_i^{(b,2)}[1]$ , contain the information of all input data tuples, the long-term dependency cannot be fully captured [27]. Therefore, we adopt the attention layer [28], which merges the state vectors in the form of a summation. Formally,

$$\mathbf{r}_i^{(f,att)} = \sum_{k=1}^N \alpha_i^{(f)}[k] \mathbf{r}_i^{(f,2)}[k] \in \mathbb{R}^{N_{i,2}^{(dec)}}, \quad \text{and} \quad \mathbf{r}_i^{(b,att)} = \sum_{k=1}^N \alpha_i^{(b)}[k] \mathbf{r}_i^{(b,2)}[k] \in \mathbb{R}^{N_{i,2}^{(dec)}}, \quad (65)$$

where  $\alpha_i^{(f)}[k] \in \mathbb{R}$  and  $\alpha_i^{(b)}[k] \in \mathbb{R}$  are the trainable *attention weights* applied to the forward and backward state vectors, respectively,  $k \in \{1, \dots, N\}$ . We capture the forward and backward directional information separately by stacking the two vectors as

$$\mathbf{r}_i^{(att)} = [\mathbf{r}_i^{(f,att)}; \mathbf{r}_i^{(b,att)}] \in \mathbb{R}^{2N_{i,2}^{(dec)}}. \quad (66)$$

The attention mechanism enables the decoder at User  $i$  to fully capture the interaction between the two users over noisy channels by exploiting all timesteps' data tuples,  $\{\mathbf{b}_i, x_i[k], y_i[k]\}_{k=1}^N$ .

3) *Non-linear layer*: We utilize a non-linear layer to finally obtain the estimate of the other user's bit vector  $\hat{\mathbf{b}}_{\bar{i}}$ , by using the feature vector  $\mathbf{r}_i^{(att)}$  in (66), where  $\bar{i}$  denotes the index of the counterpart of User  $i$ , i.e.,  $\bar{i} = 2$  if  $i = 1$  while  $\bar{i} = 1$  if  $i = 2$ . The input-output relationship at the non-linear layer is given by

$$\hat{\mathbf{d}}_{\bar{i}} = \theta(\mathbf{W}_{\text{dec},i} \mathbf{r}_i^{(att)} + \mathbf{v}_{\text{dec},i}) \in (0, 1)^{M_{\bar{i}}} \quad (67)$$

where  $\mathbf{W}_{\text{dec},i} \in \mathbb{R}^{M_{\bar{i}} \times 2N_{i,2}^{(dec)}}$  and  $\mathbf{v}_{\text{dec},i} \in \mathbb{R}^{M_{\bar{i}}}$  are the trainable weights and biases, respectively, and  $\theta: \mathbb{R}^{M_{\bar{i}}} \rightarrow \mathbb{R}^{M_{\bar{i}}}$  is an activation function.

The dimension  $M_{\bar{i}}$  and the activation function  $\theta$  are chosen differently depending on the performance metric of interest. When BLER is considered for a metric, we utilize the softmax activation function and set  $M_{\bar{i}} = 2^{K_{\bar{i}}}$ . Then,  $\hat{\mathbf{d}}_{\bar{i}}$  in (67) denotes the probability distribution of  $2^{K_{\bar{i}}}$  possible outcomes of  $\hat{\mathbf{b}}_{\bar{i}}$ . Since the softmax function allows for classification with multiple classes, we can minimize the block error of the bit vectors, i.e.,  $\Pr[\{\mathbf{b}_i \neq \hat{\mathbf{b}}_i\}]$ , by treating each possible outcome of  $\mathbf{b}_i$  as a class. For example, if  $\mathbf{b}_i \in \{0, 1\}^2$ , there are four possible classes,  $[0, 0]$ ,  $[0, 1]$ ,  $[1, 0]$ , and  $[1, 1]$ . On the other hand, when BER is considered for a metric, we consider the sigmoid activation function and set  $M_{\bar{i}} = K_{\bar{i}}$ , where each entry of  $\hat{\mathbf{d}}_{\bar{i}}$  denotes the probability distribution of each entry of  $\hat{\mathbf{b}}_{\bar{i}}$ . Since the sigmoid function allows classification for binary classes, we can minimize the error of each bit, i.e.,  $\Pr[\{b_i[\ell] \neq \hat{b}_i[\ell]\}]$ , by conducting binary classification for each bit.

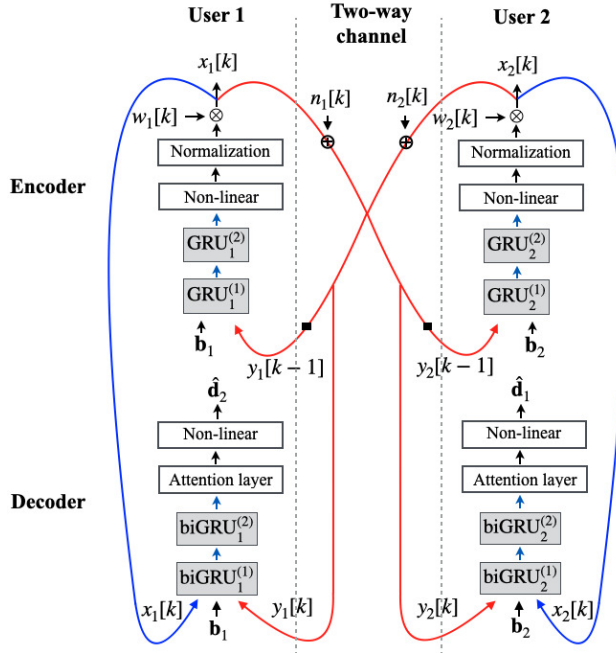


Fig. 4: Our proposed encoding/decoding architecture in a compact form for two-way channels.

#### D. Training and Inference

1) *Model training:* We consider different loss functions depending on the performance metric of interest. When BLER is considered for a metric, we have adopted the softmax function for multi-class classification, discussed in Sec. IV-C3. The commonly used loss function for training with the softmax function is cross-entropy (CE) loss. This loss function has been demonstrated to be effective in terms of the performance of multi-class classification tasks [26]. Therefore, for sum-BLER minimization, we consider the sum of CE loss defined by

$$\mathcal{L}_{\text{sum-BLER}} = \sum_{i=1}^2 \text{CE}(\mathbf{d}_i, \hat{\mathbf{d}}_i) = - \sum_{i=1}^2 \sum_{\ell=1}^{2^{K_i}} d_i[\ell] \log \hat{d}_i[\ell], \quad (68)$$

where  $d_i[\ell]$  and  $\hat{d}_i[\ell]$  are the  $\ell$ -th entry of  $\mathbf{d}_i \in \{0, 1\}^{2^{K_i}}$  and  $\hat{\mathbf{d}}_i \in (0, 1)^{2^{K_i}}$ , respectively. Here,  $\mathbf{d}_i$  is the target vector, which is a one-hot representation of  $\mathbf{b}_i \in \{0, 1\}^{K_i}$ . That is, only one entry of  $\mathbf{d}_i$  has a value of 1, while the rest entries are zero. Note that  $\hat{\mathbf{d}}_i$  is the inference output from the softmax function in (67). By treating the entire bit vector as a block through the use of one-hot vectors, we transform our problem of minimizing sum-BLER, i.e.,  $\sum_{i=1}^2 \Pr\{\mathbf{b}_i \neq \hat{\mathbf{b}}_i\}$ , into a *block-level* classification problem.

On the other hand, when BER is considered for a metric, we have adopted the sigmoid function for binary classification, discussed in Sec. IV-C3. Binary cross-entropy (BCE) loss is a commonly used loss function for training with sigmoid function and has been shown to be effective for binary

classification. [26]. Therefore, for sum-BER minimization, we consider the sum of binary cross entropy (BCE) loss defined by

$$\mathcal{L}_{\text{sum-BER}} = \sum_{i=1}^2 \text{BCE}(\mathbf{b}_i, \hat{\mathbf{d}}_i) = - \sum_{i=1}^2 \sum_{\ell=1}^{K_i} \left( b_i[\ell] \log(\hat{d}_i[\ell]) + (1 - b_i[\ell]) \log(1 - \hat{d}_i[\ell]) \right), \quad (69)$$

where  $b_i[\ell] \in \{0, 1\}$  is the  $\ell$ -th entry of  $\mathbf{b}_i \in \{0, 1\}^{K_i}$ . Note that  $\hat{\mathbf{d}}_i \in (0, 1)^{K_i}$  denotes the sigmoid output from (67). By treating each bit for training, we convert our problem of minimizing sum-BER, i.e.,  $\sum_{i=1}^2 (1/K_i) \sum_{\ell=1}^{K_i} \Pr[\{b_i[\ell] \neq \hat{b}_i[\ell]\}]$ , to a *bit-level* classification problem.

Either for sum-BLER or sum-BER minimization, we jointly train the encoders and decoders of both the users via autoencoder, where our overall coding architecture is provided in Fig. 4. The overall algorithm for training our RNN-based coding architecture is provided in Algorithm 3.

2) *Inference*: Once the coding architecture is trained, the goal of the decoder at each User  $i$  is to recover the other user's bit vector  $\hat{\mathbf{b}}_{\bar{i}} \in \{0, 1\}^{K_{\bar{i}}}$  from the decoding output  $\hat{\mathbf{d}}_{\bar{i}}$  in (67). We note that the recovery process is different depending on the performance metric of interest. First, for sum-BLER minimization, User  $i$  forces the entry with the largest value of  $\hat{\mathbf{d}}_{\bar{i}} \in (0, 1)^{2^{K_{\bar{i}}}}$  to 1, while setting the rest of the entries to 0, and then maps the obtained one-hot vector to a bit vector, which is then  $\hat{\mathbf{b}}_{\bar{i}}$ . For sum-BER minimization, User  $i$  obtains  $\hat{\mathbf{b}}_{\bar{i}}$  by rounding each entry of  $\hat{\mathbf{d}}_{\bar{i}} \in (0, 1)^{K_{\bar{i}}}$  to be either 0 or 1. That is,  $\hat{b}_{\bar{i}}[\ell]$  is a rounded version of  $\hat{d}_{\bar{i}}[\ell]$ .

### E. Modulo-Based Approach for Long Block-Lengths

A direct application of the proposed coding architecture for long block-lengths is not feasible, since the larger input/output sizes of the encoders and decoders result in a substantial increase in complexity. In particular, the larger input/output sizes lead to an increased number of computations at the non-linear layer in the decoder (in (67)) and potentially larger state vector sizes at the encoder (in (59)-(60)) and the decoder (in (63)-(64)), aiming to capture hidden features from the input data. To address this issue, we consider a modulo approach for processing long block-lengths of bits by successively applying our coding architecture built for short block-lengths [17].

In the long block-length regime, we define the entire block-length at User  $i$  as  $L_i > K_i$ , while  $K_i$  denotes the number of processing bits input to our coding architecture at a time,  $i \in \{1, 2\}$ . We consider that our two-way coding architecture has been trained for block-lengths  $K_1$  and  $K_2$ , i.e., for conveying  $K_1$  bits from User 1 to 2 and  $K_2$  bits from User 2 to 1 over  $N$  channel uses. To process the entire block-length  $L_1$  at User 1 and  $L_2$  at User 2, each User  $i$  first divides the  $L_i$  bits into  $\lceil L_i/K_i \rceil$  chunks each with length  $K_i$ . Note that when  $L_i$  is not a multiple of  $K_i$ , we can simply pad zeros following the



---

**Algorithm 3** Training for the proposed two-way coding architecture based on RNN autoencoder
 

---

**Input:** Training data  $\{\mathbf{b}_1^{(j)}, \mathbf{b}_2^{(j)}, \mathbf{n}_1^{(j)}, \mathbf{n}_2^{(j)}\}_{j=1}^J$ , number of epochs  $N_{\text{epoch}}$ , and batch size  $N_{\text{batch}}$ .

**Output:** Model parameters.

Initialize the model parameters.

**for**  $e = 1$  **to**  $N_{\text{epoch}}$  **do**

**for**  $t = 1$  **to**  $J/N_{\text{batch}}$  **do**

    Extract  $N_{\text{batch}}$  data tuples  $\{\mathbf{b}_1^{(j)}, \mathbf{b}_2^{(j)}, \mathbf{n}_1^{(j)}, \mathbf{n}_2^{(j)}\}_{j \in \mathcal{I}_{\text{batch}, t}}$  from the entire training data, where  $\mathcal{I}_{\text{batch}, t}$  denotes the indices of the extracted data tuples with  $|\mathcal{I}_{\text{batch}, t}| = N_{\text{batch}}$ .

    Update the model parameters using the gradient decent on the defined loss function;

    (i) For sum-BLER minization, we define the loss function as

$$\sum_{j \in \mathcal{I}_{\text{batch}, t}} \mathcal{L}_{\text{sum-BLER}, j} = - \sum_{j \in \mathcal{I}_{\text{batch}, t}} \sum_{i=1}^2 \sum_{\ell=1}^{2^{K_i}} d_i^{(j)}[\ell] \log \hat{d}_i^{(j)}[\ell], \quad (70)$$

    where  $d_i^{(j)}[\ell]$  and  $\hat{d}_i^{(j)}[\ell]$  are the  $\ell$ -th entry of  $\mathbf{d}_i^{(j)} \in \{0, 1\}^{2^{K_i}}$  and  $\hat{\mathbf{d}}_i^{(j)} \in (0, 1)^{2^{K_i}}$ , respectively. Here,  $\mathbf{d}_i^{(j)} = \text{one-hot}(\mathbf{b}_i^{(j)})$  is the target vector, and  $\hat{\mathbf{d}}_i^{(j)}$  is the block-level classification output obtained by the  $j$ -th data tuple passing through the overall encoder-decoder architecture in (59)-(67).

    (ii) For sum-BER minization, we define the loss function as

$$\sum_{j \in \mathcal{I}_{\text{batch}, t}} \mathcal{L}_{\text{sum-BER}, j} = - \sum_{j \in \mathcal{I}_{\text{batch}, t}} \sum_{i=1}^2 \sum_{\ell=1}^{K_i} \left( b_i^{(j)}[\ell] \log(\hat{d}_i^{(j)}[\ell]) + (1 - b_i^{(j)}[\ell]) \log(1 - \hat{d}_i^{(j)}[\ell]) \right), \quad (71)$$

    where  $b_i^{(j)}[\ell]$  and  $\hat{d}_i^{(j)}[\ell]$  are the  $\ell$ -th entry of  $\mathbf{b}_i^{(j)} \in \{0, 1\}^{K_i}$  and  $\hat{\mathbf{d}}_i^{(j)} \in (0, 1)^{K_i}$ , respectively. Here,  $\mathbf{b}_i^{(j)}$  is the target vector, and  $\hat{\mathbf{d}}_i^{(j)}$  is the bit-level classification output obtained by the  $j$ -th data tuple passing through (59)-(67).

**end for**

**end for**

---

residual bits in the last chunk. Then, the two users exchange their signals to convey their chunks of  $K_1$  and  $K_2$  bits by using our coding architecture in a time-division manner.

This modulo-based approach provides two benefits. First, it reduces the complexity of the network architecture by simplifying the encoding and decoding processes through successive applications of the neural networks trained for shorter block-lengths. Second, it allows generalization across various block-lengths (multiple of  $K_i$  bits) without necessitating re-training.

## V. COMPUTATIONAL COMPLEXITY OF LINEAR AND RNN-BASED CODING

In this section, we analyze the computational complexity of our proposed linear and RNN-based coding schemes. We first look into the case of linear coding. In Algorithm 2, we solve for the encoding schemes, i.e.,  $\mathbf{g}_1$ ,  $\mathbf{F}_1$ ,  $\mathbf{g}_2$ , and  $\mathbf{F}_2$ , given the fixed number of channel uses,  $N$ , and the noise variances,  $\sigma_1^2$  and  $\sigma_2^2$ . Subsequently, we obtain the decoding (combining) schemes,  $\mathbf{w}_1$  and  $\mathbf{w}_2$ , by (22) as functions of the encoding schemes. Once the encoding/decoding schemes are determined, they are used for encoding via

TABLE I: Linear coding complexity.

	User 1	User 2
Encoder	$\mathcal{O}(N^2)$	$\mathcal{O}(N)$
Decoder	$\mathcal{O}(N^2)$	$\mathcal{O}(N)$

TABLE II: RNN-based coding complexity.

	User $i, i \in \{1, 2\}$
Encoder	$\mathcal{O}(NN_i^{(\text{enc})}(N_i^{(\text{enc})}N_i^{(\text{enc,lay})} + K_i))$
Decoder with sigmoid	$\mathcal{O}(N_i^{(\text{dec,lay})}N(N_i^{(\text{dec})})^2 + K_{\bar{i}}NN_i^{(\text{dec})})$
Decoder with softmax	$\mathcal{O}(N_i^{(\text{dec,lay})}N(N_i^{(\text{dec})})^2 + K_{\bar{i}}NN_i^{(\text{dec})} + 2^{K_{\bar{i}}}N_i^{(\text{dec})})$

(10)-(11) and decoding described in Sec. III-B without being recalculated. Specifically, the complexity of encoding at User 1 is  $\mathcal{O}(N^2)$  from (10), where  $\mathbf{F}_1\mathbf{F}_2$  can be pre-calculated, while User 2 has the complexity of  $\mathcal{O}(N)$  in (11), where the computation of  $\mathbf{F}_2\mathbf{y}_2$  has  $\mathcal{O}(N)$  complexity since  $\mathbf{F}_2$  is in the form of (30). For decoding, User 1 has complexity of  $\mathcal{O}(N^2)$ , where the decoding process at User 1 consists of (i)  $\tilde{\mathbf{y}}_1 = (\mathbf{I} + \mathbf{F}_2\mathbf{F}_1)^{-1}(\mathbf{y}_1 - \mathbf{F}_2\mathbf{g}_1m_1)$  and (ii)  $\hat{m}_2 = \mathbf{w}_2^\top \tilde{\mathbf{y}}_1$ , described above (19). Here,  $(\mathbf{I} + \mathbf{F}_2\mathbf{F}_1)^{-1}$  and  $\mathbf{F}_2\mathbf{g}_1$  can be pre-computed. On the other hand, User 2 has  $\mathcal{O}(N)$  complexity, where the decoding process at User 2 is composed of (i)  $\tilde{\mathbf{y}}_2 = \mathbf{y}_2 - \mathbf{F}_1\mathbf{g}_2m_2$  and (ii)  $\hat{m}_1 = \mathbf{w}_1^\top \tilde{\mathbf{y}}_2$ , described above (21). Here,  $\mathbf{F}_1\mathbf{g}_2$  can be pre-computed.

We next investigate the computational complexity for RNN-based coding. In Algorithm 3, we obtain the model parameters for the non-linear coding architecture depicted in Fig. 4. The constructed architecture is then used for encoding and decoding with the fixed model parameters without further training. Although we implemented two layers of GRUs at the encoder (in Fig. 2) and decoder (in Fig. 3), we consider a general numbers of layers for complexity analysis, and define the number of GRU layers at the encoder and decoder of User  $i$  as  $N_i^{(\text{enc,lay})}$  and  $N_i^{(\text{dec,lay})}$ , respectively. Accordingly, we denote the number of neurons at each GRU layer at the encoder and decoder of User  $i$  as  $N_i^{(\text{enc})}$  and  $N_i^{(\text{dec})}$ , respectively, assuming the same number of neurons is applied to each GRU layer. For encoding, User  $i$  has the complexity of  $\mathcal{O}(NN_i^{(\text{enc})}(N_i^{(\text{enc})}N_i^{(\text{enc,lay})} + K_i))$ . For decoding, User  $i$  has the complexity of  $\mathcal{O}(N_i^{(\text{dec,lay})}N(N_i^{(\text{dec})})^2 + K_{\bar{i}}NN_i^{(\text{dec})})$  when the sigmoid function is used, while it has  $\mathcal{O}(N_i^{(\text{dec,lay})}N(N_i^{(\text{dec})})^2 + K_{\bar{i}}NN_i^{(\text{dec})} + 2^{K_{\bar{i}}}N_i^{(\text{dec})})$  when the softmax function is used, where  $\bar{i}$  denotes the index of the counterpart of User  $i$ , i.e.,  $\bar{i} = 2$  if  $i = 1$  while  $\bar{i} = 1$  if  $i = 2$ .

The encoding and decoding complexity at the users for linear coding and RNN-based coding are summarized in Tables I and II. Linear coding has a low coding complexity due to the simplified system model adopting linear operation for encoding and decoding in (10)-(11) and (22). While the RNN-based coding causes higher encoding/decoding complexity, it benefits from higher degrees of flexibility thanks to the non-linearity provided by deep neural networks, leading to better error performance under many practical noise scenarios (shown in Sec. VI).

## VI. EXPERIMENTAL RESULTS

In this section, we investigate both our linear and learning-based coding methodologies through numerical experiments. We first describe the simulation setup (Sec. VI-A) and validate our coding methodologies in a short block-length regime (Sec. VI-B). In addition, we discuss the enhancement of our linear coding scheme by thoroughly investigating its solution behavior (Sec. VI-C). We also show the effectiveness of our coding methodologies in a medium/long block-length regime (Sec. VI-D). Then, we analyze the benefits of two-way coding (Sec. VI-E), and show that the best coding strategy is different in SNR regimes (Sec. VI-F). Moreover, we investigate the error performance by varying the coding rates (Sec. VI-G) and provide information theoretic insights on power distribution of both linear and RNN-based coding (Sec. VI-H). Finally, we analyze the block-length gain of our RNN-based coding (Sec. VI-I).

### A. Simulation Parameters

We assume  $P = 1$ , i.e., the average power constraint per channel use is unity. We denote the average SNR for the channel of User  $i$  as  $\text{SNR}_i^{\text{ch}} = NP/(N\sigma_i^2) = 1/\sigma_i^2$ . We note that the channel SNR,  $\text{SNR}_i^{\text{ch}}$ , is different from the message SNR described in Sec. III, which is the post-processed SNR for message transmissions after the two-way linear encoding/decoding schemes are applied. In simulations, we consider  $\text{SNR}_1^{\text{ch}} \leq \text{SNR}_2^{\text{ch}}$  without loss of generality. For linear coding, we consider 30 different initializations of  $\{f_{2,i}\}_{i=2}^{N-1}$  with  $f_{2,i} \sim \mathcal{U}(0, 1)$ , and select the best solution for Algorithm 1. The threshold for the stopping criterion in lines 5 and 12 of Algorithm 1 is  $\epsilon = 10^{-3}$ . For Algorithm 2, we consider a finite search space for  $\eta_2$  over the region  $(0, \eta_{2,\max})$  where  $\eta_{2,\max} = NP/\sigma_2^2$ . The bisection method is carried out for  $\eta_1$  over  $(0, \eta_{1,\max})$  where  $\eta_{1,\max}$  is set to a scaled value of the maximum SNR of the feedback scheme as  $\eta_{1,\max} = 2NP(\sigma_1^2 + \sigma_2^2)/\sigma_2^2$  [10], while the golden-section search method is performed for  $\alpha$  over the range  $[\sigma_2^2/(\sigma_1^2 + \sigma_2^2), 1)$  to comply with the range of  $\alpha$  in Proposition 2.

For RNN-based coding, the number of training data samples that we used is  $J = 10^7$ , the batch size is  $N_{\text{batch}} = 2.5 \times 10^4$ , and the number of epochs is  $N_{\text{epoch}} = 100$ . We use Adam optimizer [26] and a decaying learning rate, where the initial rate is 0.01 and the decaying ratio is  $\gamma = 0.95$  applied for every epoch. We also use gradient clipping for training, where the gradients are clipped when the norm of gradients is larger than 1. We adopt two layers of uni-directional GRUs at the encoder and two layers of bi-directional GRUs at the decoder for each user, with  $N_{\text{neurons}} = N_i^{(\text{enc})} = N_i^{(\text{dec})} = 50$  neurons at each GRU. We initialize each neuron in a GRU with the uniform distribution  $U(-\zeta, \zeta)$ , where  $\zeta = 1/\sqrt{N_{\text{neurons}}}$ , and all the power weights and attention weights to 1. We train our neural network

model under particular noise scenarios, i.e.,  $\text{SNR}_1^{\text{ch}}$  and  $\text{SNR}_2^{\text{ch}}$ , and conduct inference under the same noise scenario. For inference, we consider  $10^{10}$  data tuples to calculate BER and BLER.

### B. Short Block-Length

We first investigate the performance of our coding strategies in a short block-length regime. We consider the same block-length of  $L_1 = L_2 = 6$  bits at the users and  $N_L = 18$  channel uses for exchanging  $L_1$  and  $L_2$  bits between the users. The coding rate is then  $r_1 = r_2 = 1/3$ . For baselines, we first consider repetition coding, where User  $i$  modulates each bit of  $\mathbf{b}_i \in \{0, 1\}^{L_i}$  with binary phase-shift keying (BPSK) and transmits each modulated symbol repetitively over  $N_L/L_i = 3$  channel uses. We consider tail-biting convolutional coding (TBCC) [29] as another baseline, adopted in LTE standards [30] for short block-length codes. We consider the trellis with  $(7, [133, 171, 165])$  of a constraint length of 7 and the generator  $[133, 171, 165]$  in octal representation, and BPSK modulation. For our linear and RNN-based coding, there are several ways to exchange  $L_1 = L_2 = 6$  bits between the users over  $N_L = 18$  channel uses by varying the value of  $K_i$ .<sup>3</sup> We consider the case of  $K = K_1 = K_2$  for both linear and RNN-based coding and investigate our coding schemes under different values of  $K$ .

Fig. 5 shows the sum-BLER performance under varying  $\text{SNR}_2^{\text{ch}}$ , where  $\text{SNR}_1^{\text{ch}} = 1\text{dB}$  in Fig. 5(a) and  $\text{SNR}_1^{\text{ch}} = -1\text{dB}$  in Fig. 5(b). In Fig. 5(a), the channel coding schemes, i.e., repetitive and TBCC, yield almost constant performance in sum-BLER, since sum-BLER is dominated by  $\text{BLER}_1$  because of the fact that  $\text{SNR}_1^{\text{ch}} < \text{SNR}_2^{\text{ch}}$ , and  $\text{BLER}_1$  is constant due to a constant value of  $\text{SNR}_1^{\text{ch}}$ . On the other hand, our two-way coding schemes, i.e., linear and RNN, yield better sum-BLER performance across different values of  $\text{SNR}_2^{\text{ch}}$ . The interactive exchange of information between the users allows User 2 under a better SNR condition to help User 1 under a worse SNR condition, which results in the performance improvement of  $\text{BLER}_1$ .

For linear coding, we adopt the successive transmission for exchanging multiple messages between the users discussed in Sec. III-G, denoted by ‘‘Linear (ST)’’. We also consider adopting an alternate channel use strategy for linear coding, denoted by ‘‘Linear’’, which will be discussed in detail in the next subsection, Sec. VI-C. Note that this strategy improves the error performance as shown in the plots of Fig. 5, and thus we adopt this strategy throughout simulations. In Fig. 5(a), linear coding with  $K_1 = K_2 = 3$  outperforms the other schemes when  $\text{SNR}_2^{\text{ch}}$  is high, due to its benefit of utilizing more channel uses per message, which is allowed by high-order modulation discussed in Sec. III-G. Under the

<sup>3</sup>For linear coding, User  $i$  modulates  $L_i$  bits to  $M_i = L_i/K_i$  messages with  $2^{K_i}$ -ary PAM, and  $M_i$  messages are exchanged between the users. For RNN-based coding, we construct a coding architecture that supports  $K_1$  and  $K_2$  bits at the users.

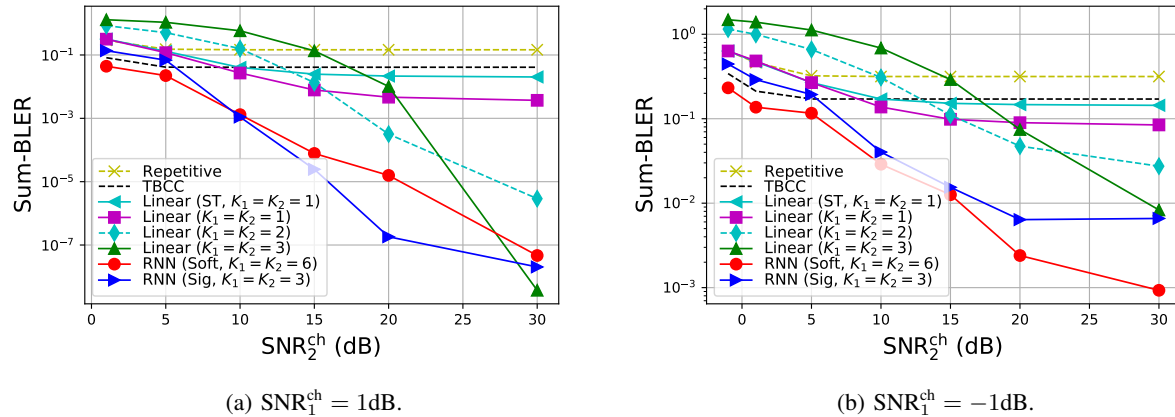


Fig. 5: Sum-BLER with short block-lengths of  $L_1 = L_2 = 6$  and  $N_L = 18$  channel uses with  $r_1 = r_2 = 1/3$ . RNN-based coding shows robustness to high channel noises, while linear coding performs well in very low noise scenarios. Here, sum-BLER of the channel coding schemes remains almost the same over  $\text{SNR}_2^{\text{ch}}$ , since sum-BLER is dominated by  $\text{BLER}_1$  and  $\text{BLER}_1$  is constant due to a constant value of  $\text{SNR}_1^{\text{ch}}$ . The proposed linear and RNN-based schemes benefit from interactive two-way coding and yield a significant performance improvement.

rest of the  $\text{SNR}_2^{\text{ch}}$  regions, RNN-based coding yields the best performance, where we used two different coding architectures: (i) the softmax function in (67) and  $K_1 = K_2 = 6$  processing bits and (ii) the sigmoid function and  $K_1 = K_2 = 3$  bits. In Fig. 5(a) with  $\text{SNR}_1^{\text{ch}} = 1\text{dB}$ , RNN-based coding with the softmax function and  $K_1 = K_2 = 6$  bits performs better when  $\text{SNR}_2^{\text{ch}} < 10\text{dB}$ , while RNN-based coding with the sigmoid function and  $K_1 = K_2 = 3$  bits performs better when  $\text{SNR}_2^{\text{ch}} > 10\text{dB}$ . This implies that using the softmax function for decoding provides robustness to channel noises due to the block-level classification of the bit vector, which is aligned with the result of feedback-enabled GOWCs [17]. In Fig. 5(b), where we consider a more noisy scenario with  $\text{SNR}_1^{\text{ch}} = -1\text{dB}$ , RNN-based coding with the softmax function yields the best performance over all the  $\text{SNR}_2^{\text{ch}}$  regions, showing its robustness to the high channel noises.

### C. Enhancement of the Linear Coding Scheme through Alternate Channel Uses

In this subsection, we introduce an efficient strategy to further enhance our linear coding scheme through alternate channel uses. We consider that the users exchange  $M = 2$  message pairs,  $(m_1, m_2)$  and  $(m'_1, m'_2)$ , over  $N_L = 6$  channel uses under power constraint  $N_L P = 6P$ , where  $\text{SNR}_1^{\text{ch}} = 1\text{dB}$  and  $\text{SNR}_2^{\text{ch}} = 20\text{dB}$ . We first consider the successive transmission discussed in Sec. III-G. Each message pair is exchanged over  $N = 3$  channel uses under power constraint  $3P$ , where the corresponding

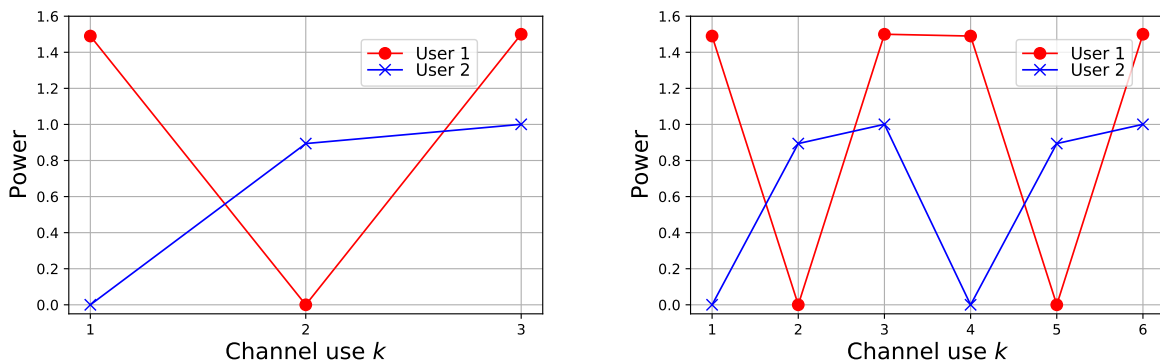
(a)  $M = 1$  message pair over  $N = 3$  channel uses.(b)  $M = 2$  message pairs over  $N_L = 6$  channel uses.

Fig. 6: Power distribution from linear coding along the channel uses. In (a), a pair of messages is exchanged over  $N = 3$  channel uses with power constraint  $NP = 3$ . In (b), two pairs of messages are exchanged with power  $N_L P = 6$  over  $N_L = 6$  channel uses via the successive transmission of the two message pairs. Some of the channel uses are not utilized by the users, which is a waste of channel uses.

encoding/decoding schemes are obtained via Algorithm 2. Fig. 6(a) shows the power distribution for exchanging a message pair over  $N = 3$  channel uses with the proposed linear coding scheme. The two message pairs are then exchanged via the successive transmission with the power distribution in Fig. 6(b). From the power distribution in Fig. 6(a) and Fig. 6(b), Users 1 and 2 only utilize about half of the channel uses, resulting in a waste of channel uses. More generally, when  $N$  is odd, it has been shown that User 1 uses only odd-numbered channel uses, while User 2 uses only even-numbered channel uses and the last channel use. It is interesting to see that although we do not impose any constraints on the separation of the channel usages between the two users, the separation of the channel usages is caused by solving the optimization problem. Specifically, the solution  $\mathbf{x}$  of the sub-problem (48) has non-zero and zero values in alternating positions.

Motivated by the alternate pattern of the channel uses at the users, we introduce the strategy of alternate channel uses so that the two users fully utilize the channel uses for exchanging multiple pairs of messages. We consider the same example of exchanging  $M = 2$  message pairs,  $(m_1, m_2)$  and  $(m'_1, m'_2)$ , over  $N_L = 6$  channel uses under power constraint  $N_L P = 6P$ .

**Step 1.** We first consider exchanging a pair of messages  $(m_1, m_2)$  over  $N = 2N_L/M - 1 = 5$  channel uses and power constraint  $(N_L/M)P = 3P$ . Then, we obtain the transmit signals as

$$\mathbf{x}_1 = [a_1, 0, b_1, 0, c_1], \quad \mathbf{x}_2 = [0, a_2, 0, b_2, c_2], \quad (72)$$

where  $a_i$ ,  $b_i$ , and  $c_i$ ,  $i \in \{1, 2\}$ , are non-zero values. To exchange another pair of messages  $(m'_1, m'_2)$

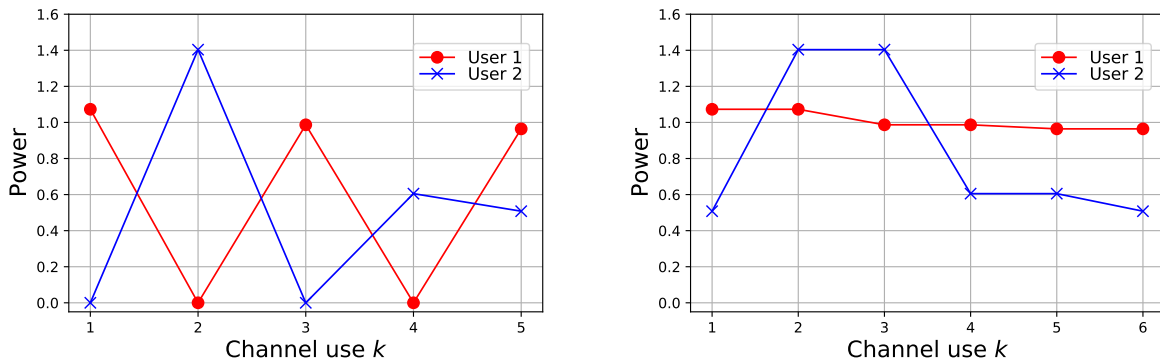
(a)  $M = 1$  message pair over  $N = 5$  channel uses.(b)  $M = 2$  message pairs over  $N_L = 6$  channel uses.

Fig. 7: Power distribution from linear coding along the channel uses. In (a), a pair of messages is exchanged over  $N = 5$  channel uses with power constraint  $3P$ . In (b), two pairs of messages are exchanged over  $N_L = 6$  channel uses with power constraint  $N_L P = 6$  where we adopt the strategy of alternate channel uses. Through this strategy, the users can fully utilize the channel uses.

over  $N = 5$  channel uses under power constraint  $3P$ , we have the transmit signals as

$$\mathbf{x}'_1 = [a'_1, 0, b'_1, 0, c'_1], \quad \mathbf{x}'_2 = [0, a'_2, 0, b'_2, c'_2], \quad (73)$$

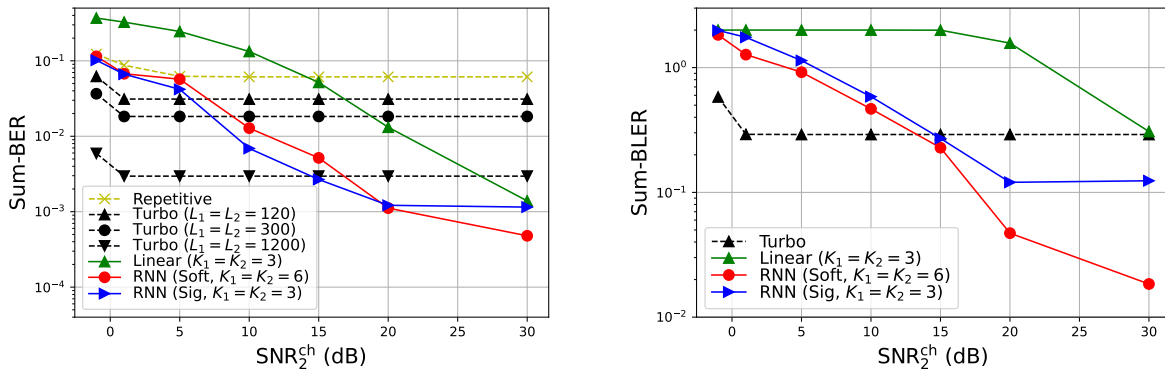
where  $a'_i$ ,  $b'_i$ , and  $c'_i$ ,  $i \in \{1, 2\}$ , are non-zero values. Note that there are zero-valued entries in (72) and (73), implying that the corresponding channel uses are not utilized.

**Step 2.** To fully utilize the channel uses, we consider that the users exchange the two message pairs via an alternate transmission of the transmit signals in (72) and (73). To this end, each User  $i$ ,  $i \in \{1, 2\}$ , transmits  $\mathbf{x}_i$  in (72) and  $\mathbf{x}'_i$  in (73) in an alternate manner over  $N_L = 6$  channel uses. Formally, User  $i$  generates  $\bar{\mathbf{x}}_i \in \mathbb{R}^{N+1}$  by putting the non-zero values of  $\mathbf{x}_i$  and  $\mathbf{x}'_i$  alternately in  $\bar{\mathbf{x}}_i$ . From the above example, we obtain

$$\bar{\mathbf{x}}_1 = [a_1, a'_1, b_1, b'_1, c_1, c'_1], \quad \bar{\mathbf{x}}_2 = [c'_2, a_2, a'_2, b_2, b'_2, c_2]. \quad (74)$$

Note that the transmit signals in (74) satisfy the power constraint  $N_L P = 6P$  while utilizing  $N_L = 6$  channel uses. This strategy also satisfies causality of the encoding process. We note that the transmit signal  $c'_2$  in  $\bar{\mathbf{x}}_2$  of (74) is not restricted to follow a causal processing since it is only composed of a scaled version of the message  $m'_2$  from Proposition 2, and thus it can be transmitted at any channel use.

Based on the alternate channel use strategy, we plot the power distribution in Fig. 7. Fig. 7(a) shows the power distribution for exchanging a pair of messages over  $N = 5$  channel uses discussed in **Step 1**, while Fig. 7(b) shows the power distribution for exchanging two pairs of messages over  $N_L = 6$  channel



(a) Sum-BER with medium/long block-lengths  $L_1, L_2$ . (b) Sum-BLER with medium block-length  $L_1 = L_2 = 120$ .

Fig. 8: Sum-error with medium/long block-lengths  $L_1, L_2$  where  $\text{SNR}_1^{\text{ch}} = -1\text{dB}$  and coding rate  $r_1 = r_2 = 1/3$ . Under the high noise scenario with  $\text{SNR}_1^{\text{ch}} = -1\text{dB}$ , RNN-based coding performs well in terms of balancing the communication reliability when the channel noises become more asymmetric.

uses when adopting the alternate channel use strategy discussed in **Step 2**. This alternate channel use strategy allows the users to fully utilize the channel uses within the same power constraint compared to the successive transmission in Fig. 6(b), and thus leads to the error performance improvement as shown in Fig. 5. Throughout simulations, we adopt this strategy for linear coding.

#### D. Medium/Long Block-Lengths

We next analyze a medium and long block-length regime, where we consider turbo coding [31] adopted in LTE standards as another baseline for medium/long block-length codes. We consider the trellis with  $(4, [13, 15])$ , BPSK modulation, and 10 decoding iterations. Fig. 8(a) shows sum-BER curves under varying  $\text{SNR}_2^{\text{ch}}$  where  $\text{SNR}_1^{\text{ch}} = -1\text{dB}$  and  $r_1 = r_2 = 1/3$ . Since turbo coding exploits the block-length gain, a longer block of bits leads to a better sum-BER performance. However, for given  $L_1$  and  $L_2$ , the sum-BER performances are almost constant over  $\text{SNR}_2^{\text{ch}}$  since sum-BER is dominated by a fixed value of  $\text{BER}_1$ . On the other hand, our proposed two-way coding schemes, i.e., linear and RNN-based coding, significantly improve  $\text{BER}_1$  as  $\text{SNR}_2^{\text{ch}}$  increases, due to the two-way interactions between the users, which leads to substantial improvements in the sum-BER.

Fig. 8(b) shows the sum-BLER performance for medium block-length  $L_1 = L_2 = 120$ , where  $\text{SNR}_1^{\text{ch}} = -1\text{dB}$  and rate  $r_1 = r_2 = 1/3$ . Since the SNR condition is poor, i.e.,  $\text{SNR}_1^{\text{ch}} = -1\text{dB}$ , turbo coding does not perform well, resulting in a performance degradation in terms of sum-BLER. However, the two-way coding schemes, in particular RNN-based coding, improve the error performance due to their



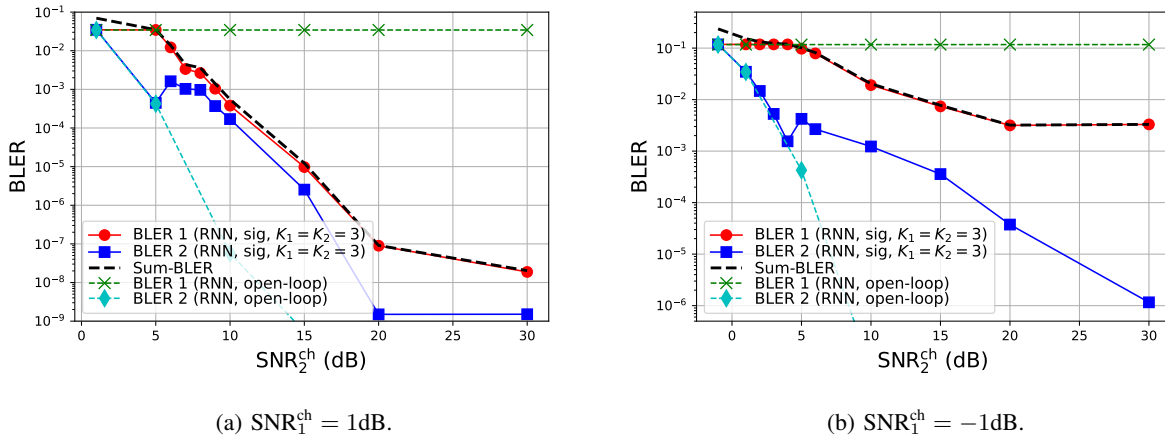


Fig. 9: Each of BLER curves with block-length  $L_1 = L_2 = 3$  obtained by RNN-based coding with the sigmoid function and  $K_1 = K_2 = 3$  bits. The users start to benefit from two-way coding when  $\text{SNR}_2^{\text{ch}}$  is larger than a threshold, which is 6dB in (a) and 5dB in (b), respectively.

robustness to channel noises, and ultimately balance the communication reliability, i.e., obtain much smaller sum-BLER values.

### E. Threshold for Two-Way Coding Benefits

We have so far observed that our two-way coding schemes significantly improve the sum-error performance when the channel conditions are asymmetric. In this subsection, we further investigate each error curve to analyze how communication reliability can be balanced by our two-way coding scheme. Fig. 9 shows the BLER curves obtained by our RNN-based coding scheme with the sigmoid function and  $K_1 = K_2 = 3$  bits, where BLER is measured over the block-length  $L_1 = L_2 = 3$  bits. We consider  $\text{SNR}_1^{\text{ch}} = 1\text{dB}$  in Fig. 9(a) and  $\text{SNR}_1^{\text{ch}} = -1\text{dB}$  in Fig. 9(b). To understand the interrelation between the two users through the proposed two-way coding, we introduce a baseline by modifying our RNN-based coding to generate two independent open-loop codes. Specifically, in Fig. 4, we provide  $x_i[k-1]$  as an input to the encoder of User  $i$  rather than  $y_i[k-1]$  to remove the dependency between the encoders of the users, which is denoted by “RNN, open-loop” in the plots. Under the asymmetric channels with  $\text{SNR}_1^{\text{ch}} < \text{SNR}_2^{\text{ch}}$ ,  $\text{BLER}_1$  and  $\text{BLER}_2$  obtained by “RNN, open-loop” is the upper and lower bound, respectively, of those obtained by our two-way coding scheme.

In the figures,  $\text{BLER}_1$  with open-loop coding yields a constant value, since  $\text{BLER}_1$  is only determined by the fixed value of  $\text{SNR}_1^{\text{ch}}$ , while  $\text{BLER}_2$  with open-loop coding decreases along  $\text{SNR}_2^{\text{ch}}$ . The results show that the two independent open-loop codes do not balance the communication reliability when the

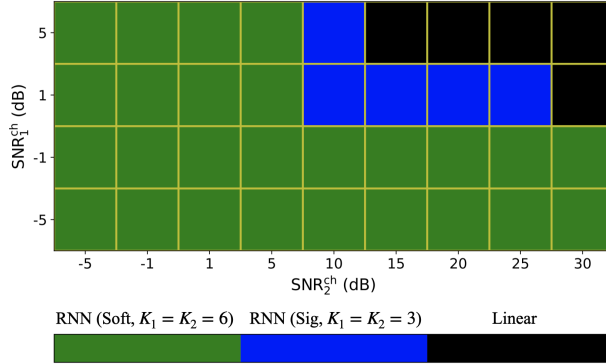


Fig. 10: The superior scheme in sum-BLER with block-lengths  $L_1 = L_2 = 6$  under various SNR scenarios. When SNRs are high and asymmetric, linear coding performs best, while RNN-based coding excels in low SNRs.

channels are asymmetric. However, our two-way coding scheme balances the communication reliability under asymmetric channels due to the interactive exchange of information between the users. In Fig. 9(a), when  $\text{SNR}_2^{\text{ch}} \geq 6\text{dB}$ ,  $\text{BLER}_1$  is improved relative to that of the open-loop codes, while  $\text{BLER}_2$  is sacrificed as compared to the open-loop coding. This is because User 2 (with higher SNR) helps User 1 (with lower SNR) through the interactive exchange of information to improve  $\text{BLER}_1$  by implicitly providing feedback information to User 1. This behavior is in line with the insight discussed in [6] that a user with lower channel noise can act as a helper. Furthermore, we can identify a threshold of  $\text{SNR}_2^{\text{ch}}$ , above which the users start to benefit from the two-way interaction of our coding scheme. When  $\text{SNR}_1^{\text{ch}} = 1\text{dB}$ , the threshold is  $\text{SNR}_2^{\text{ch}} = 6\text{dB}$  as indicated in Fig. 9(a), whereas, the threshold is  $\text{SNR}_2^{\text{ch}} = 5\text{dB}$  in Fig. 9(b) when  $\text{SNR}_1^{\text{ch}} = -1\text{dB}$ .

#### F. The Superior Scheme over Different SNR Regions

Next, we explore different coding scheme among repetitive coding, TBCC, linear coding, and RNN-based coding in terms of sum-BLER for block-lengths  $L_1 = L_2 = 6$  under various SNR scenarios. The results are demonstrated in Fig. 10. In high and asymmetric SNR regions, we observe that linear coding outperforms the other schemes. On the other hand, in low SNR regions, RNN-based coding with the softmax function and  $K_1 = K_2 = 6$  bits yields the best performance, demonstrating its robustness to channel noises. Specifically, under symmetric SNR scenarios ( $\text{SNR}_1^{\text{ch}} = \text{SNR}_2^{\text{ch}} = -5, -1, 1, 5\text{dB}$ ), RNN-based coding behaves like two independent open-loop coding when the channels are symmetric, as shown in Fig. 9, which outperforms TBCC. This result suggests that our learning architecture can be also utilized to develop error correction codes. While our study focuses on two-way coding behavior, the

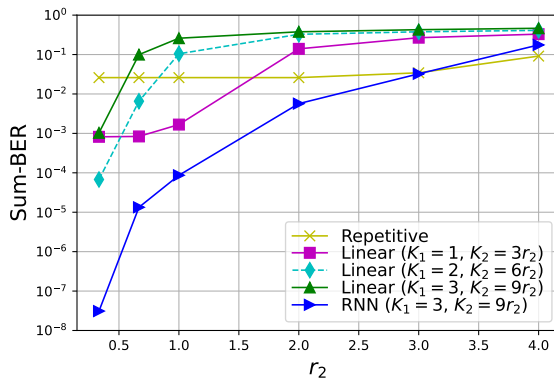


Fig. 11: Sum-BER with various coding rates of  $r_2$ , where  $\text{SNR}_1^{\text{ch}} = 1\text{dB}$ ,  $\text{SNR}_2^{\text{ch}} = 20\text{dB}$ , and  $r_1 = 1/3$ . RNN-based coding outperforms the counterparts in sum-BER even while supporting high coding rates.

construction of error correcting codes is a potential area for future research. Note that, for moderate and asymmetric SNRs, RNN-based coding with the sigmoid function performs the best among the schemes.

### G. Varying Coding Rates

We so far looked into the benefit of two-way coding in terms of improving sum-error performance when coding rates are fixed. However, when  $\text{SNR}_2^{\text{ch}}$  is high enough, while helping User 1 to improve sum-error, User 2 can increase its coding rate. To investigate the relationship between the coding rates and sum-error, we show the sum-BER performances with varying coding rates of  $r_2$  in Fig. 11, where  $r_1 = 1/3$ ,  $\text{SNR}_1^{\text{ch}} = 1\text{dB}$ , and  $\text{SNR}_2^{\text{ch}} = 20\text{dB}$ . For linear coding, we consider three different modulation bits at User 1,  $K_1 = 1, 2, 3$ . Correspondingly, we set the modulation bits at User 2 as  $K_2 = 3r_2, 6r_2, 9r_2$ . We consider the strategy of alternate channel uses discussed in Sec. VI-C for linear coding, where two message pairs are exchanged in an alternate manner. Specifically,  $2K_1$  and  $3K_1r_2$  bits are modulated to two messages at User 1 denoted by  $m_1, m'_1$  and at User 2 denoted by  $m_2, m'_2$ , respectively, and the two pairs of messages,  $(m_1, m_2)$  and  $(m'_1, m'_2)$ , are exchanged over  $6K_1$  channel uses in an alternate manner. For RNN-based coding, the number of bits input to the encoders of Users 1 and 2 are  $K_1 = 3$  and  $K_2 = 9r_2$ , respectively. From the figure, we observe that RNN-based coding outperforms the counterparts even under very high coding rates,  $r_2 \leq 3$ , while linear coding outperforms the repetitive coding when the coding rate is quite low,  $r_2 \leq 1.5$ .

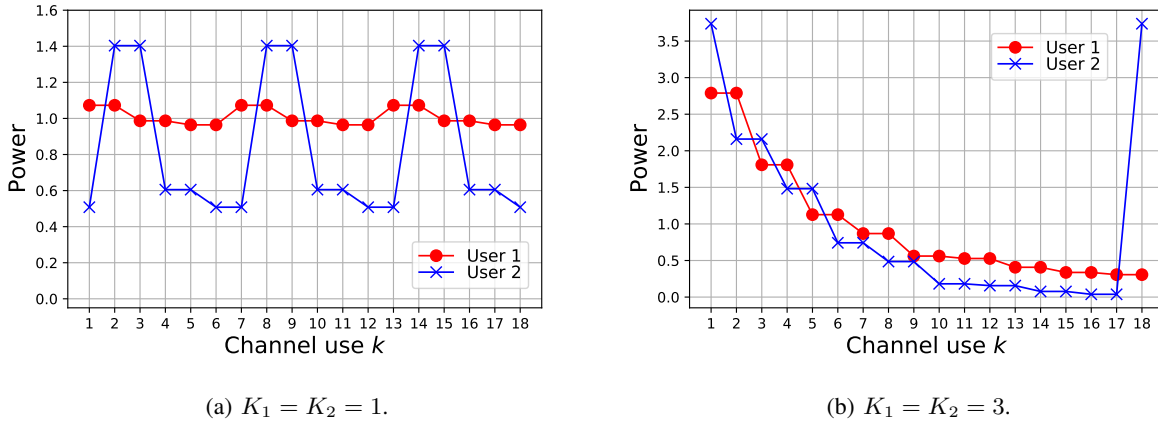


Fig. 12: Power distribution from linear coding along the channel uses when adopting the strategy of alternate channel uses, where  $L_1 = L_2 = 6$  and  $N_L = 18$ . In this way, the users can fully utilize the channel uses.

#### H. Power Distribution in Linear and RNN-Based Coding

We next investigate the power distribution from linear coding when adopting the strategy of alternate channel uses, where two users convey  $L_1 = L_2 = 6$  bits to one another over  $N_L = 18$  channel uses, where  $\text{SNR}_1^{\text{ch}} = 1\text{dB}$  and  $\text{SNR}_2^{\text{ch}} = 20\text{dB}$ . We consider two different modulation bits,  $K_1 = K_2 = 1$  in Fig. 12(a) and  $K_1 = K_2 = 3$  in Fig. 12(b). First, in Fig. 12(a), each User  $i$  has  $M_i = L_i/K_i = 6$  message symbols, where every two message pairs are transmitted over 6 channel uses through the alternate channel use strategy, as shown in Fig. 7(b). Specifically, for the first message pair, the 1st, 3rd and 5th channel uses at User 1 and the 2nd, 4th and 6th channel uses at User 2 are used, while for the second message pair, the 2nd, 4th and 6th channel uses at User 1 and the 1st, 3rd and 5th channel uses at User 2 are used, as discussed in (74). In Fig. 12(b), each User  $i$  has  $M_i = L_i/B_i = 2$  message symbols, and the two message pairs are transmitted over 18 channel uses via alternate channel uses. Overall, through this strategy, both the users can fully utilize all channel uses.

Fig. 13 shows the power distribution from RNN-based coding. We consider that the two users convey  $L_1 = L_2 = 6$  bits to one another over  $N_L = 18$  channel uses, where  $\text{SNR}_1^{\text{ch}} = 1\text{dB}$  and  $\text{SNR}_2^{\text{ch}} = 20\text{dB}$ . We consider two different coding architectures with different numbers of processing bits. First, in Fig. 13(a), we consider  $K_1 = K_2 = 3$  bits, where every pair of the three bits is the input to the RNN-based coding architecture with the sigmoid function at a time to generate transmit symbols for 9 channel uses. In Fig. 13(b), we consider  $K_1 = K_2 = 6$  bits, which are the input to the RNN-based coding architecture with the softmax function to generate transmit symbols for 18 channel uses.

For linear and RNN-based coding under this asymmetric SNR scenario, User 1 allocates more power

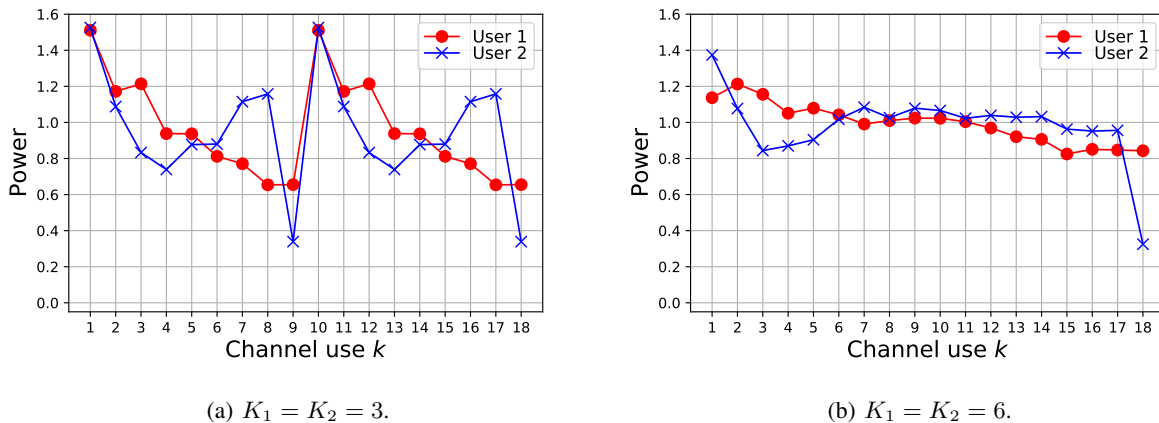


Fig. 13: Power distribution from RNN-based coding where  $L_1 = L_2 = 6$  and  $N_L = 18$ . Under this asymmetric channel ( $\text{SNR}_1^{\text{ch}} = 1\text{dB} < \text{SNR}_2^{\text{ch}} = 20\text{dB}$ ), User 1 allocates more power at the beginning to fully exploit the feedback information provided by User 2, in order to improve sum-error performance.

TABLE III: Block-length gain of RNN-based (two-way) coding along different numbers of processing bits  $K = K_1 = K_2$  when  $\text{SNR}_1^{\text{ch}} = 1\text{dB}$  and  $\text{SNR}_2^{\text{ch}} = 20\text{dB}$ .

	BER <sub>1</sub>	BER <sub>2</sub>	Sum-BER	BLER <sub>1,K</sub>	BLER <sub>2,K</sub>	Sum-BLER ( $L = 60$ )
$K = 6$	1.13E-6	3.04E-8	1.16E-6	4.65E-6	1.63E-7	4.81E-5
$K = 5$	1.91E-6	1.55E-8	1.93E-6	7.91E-6	5.7E-08	9.56E-5
$K = 4$	1.13E-6	1.93E-8	1.15E-6	4.08E-6	6.11E-8	6.21E-5
$K = 3$	3.03E-8	7.67E-10	<b>3.11E-8</b>	8.96E-8	1.50E-9	<b>1.82E-6</b>
$K = 2$	1.18E-7	1.50E-9	1.20E-7	2.35E-7	3.00E-9	7.14E-6
$K = 1$	8.00E-4	1.02E-6	8.01E-4	8.00E-4	1.02E-6	4.69E-2

at the beginning (over 6 channel uses in Fig. 12(a), 9 channel uses in Fig. 13(a), and 18 channel uses in Fig. 12(b) and Fig. 13(b)), which aligns with the result of using the feedback scheme in feedback-enabled GOWCs [10], [17]. This implies that User 1 exploits the feedback information provided by User 2, in order to improve  $\text{BLER}_1$  while sacrificing  $\text{BLER}_2$  as shown in Fig. 9. It is worth mentioning that, as compared with the one-way feedback coding in [9], [10], [14], [17], two-way coding requires that User 2 should (i) convey its own bit vector as well as the feedback information to User 1 and (ii) satisfy the power constraint. These additional aspects are the motivation of developing novel linear and RNN-based two-way coding schemes in this work.

TABLE IV: Block-length gain of RNN-based (two-way) coding along different numbers of processing bits

$$K = K_1 = K_2 \text{ when } \text{SNR}_1^{\text{ch}} = -1\text{dB} \text{ and } \text{SNR}_2^{\text{ch}} = 20\text{dB}.$$

	BER <sub>1</sub>	BER <sub>2</sub>	Sum-BER	BLER <sub>1,K</sub>	BLER <sub>2,K</sub>	Sum-BLER ( $L = 120$ )
$K = 8$	4.57E-3	2.55E-4	4.83E-3	1.08E-2	6.67E-4	1.60E-1
$K = 7$	1.57E-3	1.28E-4	1.70E-3	3.80E-3	3.42E-4	N/A
$K = 6$	9.96E-4	1.20E-4	1.12E-3	2.14E-3	2.60E-4	<b>4.71E-2</b>
$K = 5$	1.27E-3	8.87E-5	1.36E-3	2.90E-3	2.32E-4	7.29E-2
$K = 4$	7.10E-4	2.24E-5	<b>7.32E-4</b>	1.87E-3	5.89E-5	5.64E-2
$K = 3$	2.26E-3	3.53E-5	2.30E-3	4.45E-3	6.42E-5	1.66E-1
$K = 2$	4.54E-3	2.20E-5	4.56E-3	8.86E-3	3.26E-5	4.16E-1
$K = 1$	1.94E-2	2.92E-6	1.94E-2	1.94E-2	2.92E-6	9.05E-1

### I. Block-Length Gain of Two-Way Coding

Lastly, we investigate the block-length gain of two-way coding for GTWCs, where the block-length gain is measured as the sum-error, either sum-BLER or sum-BER. For two-way coding, we consider RNN-based coding with  $r_1 = r_2 = 1/3$ . We consider two different channel scenarios: (i)  $\text{SNR}_1^{\text{ch}} = 1\text{dB}$  and  $\text{SNR}_2^{\text{ch}} = 20\text{dB}$ , and (ii)  $\text{SNR}_1^{\text{ch}} = -1\text{dB}$  and  $\text{SNR}_2^{\text{ch}} = 20\text{dB}$ . First, in Table III, we investigate the sum-BER and sum-BLER performance under  $\text{SNR}_1^{\text{ch}} = 1\text{dB}$  and  $\text{SNR}_2^{\text{ch}} = 20\text{dB}$  by varying the numbers of processing bits  $K = K_1 = K_2$ . We consider the sigmoid function for RNN-based coding. In the table, we introduce the measure ‘‘Sum-BLER ( $L = 60$ )’’ to compare the BLER performances with different values of  $K$ , which is calculated as  $(1 - \text{BLER}_{1,K})^{L/K} + (1 - \text{BLER}_{2,K})^{L/K}$ , where  $\text{BLER}_{i,K}$  is the BLER of block-length  $K$  of User  $i$ . Both sum-BER and sum-BLER peak at  $K = 3$ , implying that our RNN-based coding exploits the block-length gain up to  $K = 3$ . We next investigate the different channel scenario,  $\text{SNR}_1 = -1\text{dB}$  and  $\text{SNR}_2 = 20\text{dB}$ , in Table IV, where the softmax function is considered for RNN-based coding. In the table, sum-BER peaks at  $K = 4$ , while sum-BLER peaks at  $K = 6$ .

We observe that in the low SNR scenario, i.e.,  $\text{SNR}_1 = -1\text{dB}$  in Table IV, more numbers of bits for coding yields better sum-error performance than the case with the higher SNR, i.e.,  $\text{SNR}_1 = 1\text{dB}$  in Table III. This is because two-way coding potentially benefits from noise-averaging effect by utilizing more numbers of channel uses under low SNR scenarios. Note that ‘‘Sum-BLER ( $L = 120$ )’’ in Table IV represents the sum of BLERs with  $L = 120$ , calculated similarly in Table III with  $L = 60$ . For simulations of RNN-based coding, we have considered the two representative coding architectures based on the results of Tables III and IV:  $K = 6$  bits with the softmax function and  $K = 3$  bits with the sigmoid function. It is important to note that, for specific SNR scenarios, the best sum-error performance is attained through

(i) the appropriate selection of  $K$  and (ii) a proper choice between sigmoid and softmax. As a result, given a certain channel environment, we can select the best-performing coding architecture from a set of pre-trained architectures that have been trained with various  $K$  and activation functions.

## VII. CONCLUSION

In this work, we focused on balancing the communication reliability between the two users in GTWCs by minimizing the sum of error probabilities of the users through the design of encoders/decoders for the users. We first provided general encoding/decoding functions, and formulated an optimization problem, aiming to minimize the sum-error of the users subject to users' power constraints. We proposed two coding strategies – linear coding and learning-based coding – to address the challenges of (i) the encoders' coupling effect, (ii) the requirement for effective decoding, and (iii) the need for efficient power management.

For linear coding, we adopted a linear processing for encoding/decoding, which mitigates the complex coupling effect in challenge (i). We then derived an optimal form of decoding as a function of encoding schemes, which addresses challenge (ii). Next, we solved the sum-error minimization problem subject to power constraints, which addresses challenge (iii). Furthermore, we provided new insights on user cooperation by analyzing the relationship between the channel noise ratio and the weight imposed in weighted sum-power minimization. For learning-based coding, we proposed an RNN-based coding architecture composed of multiple novel components. For encoding, we proposed interactive RNNs for addressing challenge (i) and a power control layer for addressing challenge (iii), while for decoding we incorporated bi-directional RNNs with an attention mechanism for addressing challenge (ii). To jointly address these challenges, we trained the encoder/decoders via auto-encoder. We then analyzed the computational complexity of both our linear and non-linear coding schemes.

Through simulations, we demonstrated that our two-way coding strategies outperform traditional channel coding schemes by wide margins in terms of sum-error performance. In addition, we examined our two-way coding schemes in terms of their power distribution, two-way coding benefit, different coding rates, and block-length gain. Our results highlighted the potential of our two-way coding methodologies to improve/balance the communication reliability in GTWCs.

## REFERENCES

- [1] J. Kim, S. Hosseinalipour, T. Kim, D. J. Love, and C. G. Brinton, "Linear coding for Gaussian two-way channels," in *58th Annual Allerton Conference on Communication, Control, and Computing (Allerton)*, Sep. 2022.
- [2] Z. Zhang, K. Long, A. V. Vasilakos, and L. Hanzo, "Full-duplex wireless communications: Challenges, solutions, and future research directions," *Proceedings of the IEEE*, vol. 104, no. 7, pp. 1369–1409, Feb. 2016.

- [3] D. Kim, H. Lee, and D. Hong, "A survey of in-band full-duplex transmission: From the perspective of PHY and MAC layers," *IEEE Communications Surveys & Tutorials*, vol. 17, no. 4, pp. 2017–2046, Feb. 2015.
- [4] C. E. Shannon, "Two-way communication channels," in *Proceedings of the Fourth Berkeley Symposium on Mathematical Statistics and Probability, Volume 1: Contributions to the Theory of Statistics*. University of California Press, Jan. 1961, pp. 611–644.
- [5] T. Han, "A general coding scheme for the two-way channel," *IEEE Transactions on Information Theory*, vol. 30, no. 1, pp. 35–44, Jan. 1984.
- [6] K. S. Palacio-Baus and N. Devroye, "Achievable error exponents of one-way and two-way AWGN channels," *IEEE Transactions on Information Theory*, vol. 67, no. 5, pp. 2693–2715, May 2021.
- [7] D. Vasal, "A dynamic program for linear sequential coding for two way Gaussian channel," *ResearchGate*, Dec. 2021.
- [8] J. Schalkwijk and T. Kailath, "A coding scheme for additive noise channels with feedback–I: No bandwidth constraint," *IEEE Transactions on Information Theory*, vol. 12, no. 2, pp. 172–182, Apr. 1966.
- [9] S. Butman, "A general formulation of linear feedback communication systems with solutions," *IEEE Transactions on Information Theory*, vol. 15, no. 3, pp. 392–400, May 1969.
- [10] Z. Chance and D. J. Love, "Concatenated coding for the AWGN channel with noisy feedback," *IEEE Transactions on Information Theory*, vol. 57, no. 10, pp. 6633–6649, Oct. 2011.
- [11] M. Agrawal, D. J. Love, and V. Balakrishnan, "An iteratively optimized linear coding scheme for correlated Gaussian channels with noisy feedback," in *IEEE 49th Annual Allerton Conference on Communication, Control, and Computing*, Sep. 2011, pp. 1012–1018.
- [12] N. Elia, "When Bode meets Shannon: Control-oriented feedback communication schemes," *IEEE Transactions on Automatic Control*, vol. 49, no. 9, pp. 1477–1488, Sep. 2004.
- [13] R. Mishra, D. Vasal, and H. Kim, "Linear coding for AWGN channels with noisy output feedback via dynamic programming," *IEEE Transactions on Information Theory*, Mar. 2023.
- [14] H. Kim, Y. Jiang, S. Kannan, S. Oh, and P. Viswanath, "Deepcode: Feedback codes via deep learning," *IEEE Journal on Selected Areas in Information Theory*, vol. 1, no. 1, pp. 194–206, Apr. 2020.
- [15] A. R. Safavi, A. G. Perotti, B. M. Popovic, M. B. Mashhadi, and D. Gunduz, "Deep extended feedback codes," *arXiv preprint arXiv:2105.01365*, May 2021.
- [16] E. Ozfatura, Y. Shao, A. G. Perotti, B. M. Popović, and D. Gündüz, "All you need is feedback: Communication with block attention feedback codes," *IEEE Journal on Selected Areas in Information Theory*, vol. 3, no. 3, pp. 587–602, Sep. 2022.
- [17] J. Kim, T. Kim, D. Love, and C. Brinton, "Robust non-linear feedback coding via power-constrained deep learning," *To appear at International Conference on Machine Learning (ICML)*, Jul. 2023.
- [18] J. G. Proakis, *Digital communications*. McGraw-Hill, Higher Education, Jan. 2008.
- [19] S. M. Kay, *Fundamentals of statistical signal processing: Estimation theory*. Prentice-Hall, Inc., Apr. 1993.
- [20] D. Tse and P. Viswanath, *Fundamentals of wireless communication*. Cambridge university press, Jul. 2005.
- [21] K. Deb, *Multi-objective optimisation using evolutionary algorithms: an introduction*. Springer, Jan. 2011.
- [22] E. K. Chong and S. H. Zak, *An introduction to optimization*. John Wiley & Sons, Jan. 2013, vol. 75.
- [23] R. W. Freund and F. Jarre, "Solving the sum-of-ratios problem by an interior-point method," *Journal of Global Optimization*, vol. 19, no. 1, pp. 83–102, Jan. 2001.
- [24] MathWorks, *MATLAB Optimization Toolbox*, Natick, MA, USA, 2021. [Online]. Available: <https://www.mathworks.com/help/optim/>
- [25] J. H. Ferziger, "Numerical methods for engineering applications," *New York, Wiley-Interscience*, Apr. 1998.



- [26] I. Goodfellow, Y. Bengio, and A. Courville, *Deep learning*. MIT press, 2016.
- [27] Y. Bengio, P. Frasconi, and P. Simard, “The problem of learning long-term dependencies in recurrent networks,” in *IEEE International Conference on Neural Networks*. IEEE, Mar. 1993, pp. 1183–1188.
- [28] D. Bahdanau, K. Cho, and Y. Bengio, “Neural machine translation by jointly learning to align and translate,” *arXiv preprint arXiv:1409.0473*, Sep. 2014.
- [29] H. Ma and J. Wolf, “On tail biting convolutional codes,” *IEEE Transactions on Communications*, vol. 34, no. 2, pp. 104–111, Feb. 1986.
- [30] 3GPP TS 36.212, “LTE: Evolved universal terrestrial radio access (E-UTRA): Multiplexing and channel coding,” vol. V8.8.0 Release 8, 2010.
- [31] C. Berrou and A. Glavieux, “Near optimum error correcting coding and decoding: Turbo-codes,” *IEEE Transactions on communications*, vol. 44, no. 10, pp. 1261–1271, Oct. 1996.
- [32] P. Billingsley, *Probability and measure*. John Wiley & Sons, Feb. 2012.

## APPENDIX A

DERIVATION FOR  $\mathbf{g}_1$ ,  $\mathbf{F}_1$ ,  $\mathbf{g}_2$ , AND  $\mathbf{F}_2$  AS FUNCTIONS OF  $\tilde{\mathbf{g}}_1$ ,  $\tilde{\mathbf{F}}_1$ ,  $\tilde{\mathbf{g}}_2$ , AND  $\tilde{\mathbf{F}}_2$ 

First, we will derive the functional forms of  $\mathbf{g}_2$  and  $\mathbf{F}_2$  in (11) by starting from (9). We move all terms including  $\mathbf{x}_2$  in (9) to the left-hand side and obtain  $(\mathbf{I} + \tilde{\mathbf{F}}_2\tilde{\mathbf{F}}_1)\mathbf{x}_2 = \tilde{\mathbf{g}}_2m_2 + \tilde{\mathbf{F}}_2\mathbf{y}_2$ . We take the inverse of  $(\mathbf{I} + \tilde{\mathbf{F}}_2\tilde{\mathbf{F}}_1)$  on both sides and obtain

$$\mathbf{x}_2 = (\mathbf{I} + \tilde{\mathbf{F}}_2\tilde{\mathbf{F}}_1)^{-1}\tilde{\mathbf{g}}_2m_2 + (\mathbf{I} + \tilde{\mathbf{F}}_2\tilde{\mathbf{F}}_1)^{-1}\tilde{\mathbf{F}}_2\mathbf{y}_2. \quad (75)$$

By comparing (11) and (75), we find  $\mathbf{g}_2 = (\mathbf{I} + \tilde{\mathbf{F}}_2\tilde{\mathbf{F}}_1)^{-1}\tilde{\mathbf{g}}_2$  and  $\mathbf{F}_2 = (\mathbf{I} + \tilde{\mathbf{F}}_2\tilde{\mathbf{F}}_1)^{-1}\tilde{\mathbf{F}}_2$ .

We will then derive the functional expressions of  $\mathbf{g}_1$  and  $\mathbf{F}_1$  in (10) by starting from (8). As a first step, we rewrite (8) as

$$\begin{aligned} \mathbf{x}_1 &= \tilde{\mathbf{g}}_1m_1 + \tilde{\mathbf{F}}_1(\mathbf{y}_1 - \tilde{\mathbf{F}}_2\mathbf{x}_1 + \mathbf{F}_2\mathbf{x}_1 - \mathbf{F}_2\mathbf{x}_1) \\ &= (\mathbf{I} - \tilde{\mathbf{F}}_1(\mathbf{F}_2 - \tilde{\mathbf{F}}_2))^{-1}\tilde{\mathbf{g}}_1m_1 + (\mathbf{I} - \tilde{\mathbf{F}}_1(\mathbf{F}_2 - \tilde{\mathbf{F}}_2))^{-1}\tilde{\mathbf{F}}_1(\mathbf{y}_1 - \mathbf{F}_2\mathbf{x}_1). \end{aligned} \quad (76)$$

To obtain the equality in the first line in (76), we add the term  $\mathbf{F}_2\mathbf{x}_1 - \mathbf{F}_2\mathbf{x}_1$ , which is a zero vector, inside the parenthesis in (8). To obtain the equality in the second line in (76), we first move the term of  $\tilde{\mathbf{F}}_1(-\tilde{\mathbf{F}}_2\mathbf{x}_1 + \mathbf{F}_2\mathbf{x}_1)$  (in the first line) to the left-hand side, and accordingly obtain  $(\mathbf{I} - \tilde{\mathbf{F}}_1(\mathbf{F}_2 - \tilde{\mathbf{F}}_2))\mathbf{x}_1 = \tilde{\mathbf{g}}_1m_1 + \tilde{\mathbf{F}}_1(\mathbf{y}_1 - \mathbf{F}_2\mathbf{x}_1)$ . We take the inverse of  $(\mathbf{I} - \tilde{\mathbf{F}}_1(\mathbf{F}_2 - \tilde{\mathbf{F}}_2))$  on both sides and finally obtain the equality in the second line in (76). By comparing (10) and (76), we find  $\mathbf{g}_1 = \mathbf{A}^{-1}\tilde{\mathbf{g}}_1$  and  $\mathbf{F}_1 = \mathbf{A}^{-1}\tilde{\mathbf{F}}_1$ , where  $\mathbf{A} = \mathbf{I} - \tilde{\mathbf{F}}_1(\mathbf{F}_2 - \tilde{\mathbf{F}}_2)$ . Here, we put the obtained result of  $\mathbf{F}_2 = (\mathbf{I} + \tilde{\mathbf{F}}_2\tilde{\mathbf{F}}_1)^{-1}\tilde{\mathbf{F}}_2$  in  $\mathbf{A}$ , and obtain  $\mathbf{A} = \mathbf{I} - \tilde{\mathbf{F}}_1((\mathbf{I} + \tilde{\mathbf{F}}_2\tilde{\mathbf{F}}_1)^{-1} - \mathbf{I})\tilde{\mathbf{F}}_2$ .

In summary, we have

$$\mathbf{g}_2 = (\mathbf{I} + \tilde{\mathbf{F}}_2\tilde{\mathbf{F}}_1)^{-1}\tilde{\mathbf{g}}_2, \quad (77)$$

$$\mathbf{F}_2 = (\mathbf{I} + \tilde{\mathbf{F}}_2\tilde{\mathbf{F}}_1)^{-1}\tilde{\mathbf{F}}_2, \quad (78)$$

$$\mathbf{g}_1 = (\mathbf{I} - \tilde{\mathbf{F}}_1((\mathbf{I} + \tilde{\mathbf{F}}_2\tilde{\mathbf{F}}_1)^{-1} - \mathbf{I})\tilde{\mathbf{F}}_2)^{-1}\tilde{\mathbf{g}}_1, \quad (79)$$

$$\mathbf{F}_1 = (\mathbf{I} - \tilde{\mathbf{F}}_1((\mathbf{I} + \tilde{\mathbf{F}}_2\tilde{\mathbf{F}}_1)^{-1} - \mathbf{I})\tilde{\mathbf{F}}_2)^{-1}\tilde{\mathbf{F}}_1. \quad (80)$$

We observe that  $\mathbf{F}_1$  and  $\mathbf{F}_2$  in (80) and (78), respectively, are strictly lower triangular matrices. We first demonstrate how  $\mathbf{F}_1$  in (80) becomes strictly lower triangular. Since  $\tilde{\mathbf{F}}_1$  and  $\tilde{\mathbf{F}}_2$  are strictly lower triangular matrices (as discussed in Sec. III-A), the term  $(\mathbf{I} - \tilde{\mathbf{F}}_1((\mathbf{I} + \tilde{\mathbf{F}}_2\tilde{\mathbf{F}}_1)^{-1} - \mathbf{I})\tilde{\mathbf{F}}_2)^{-1}$  in (80) is lower triangular given that (i) the multiplication of lower triangular matrices yields a lower triangular matrix and (ii) the inverse of a lower triangular matrix is also lower triangular. Consequently,  $\mathbf{F}_1$  in (80) is strictly lower triangular, as the multiplication of the lower triangular matrix  $(\mathbf{I} - \tilde{\mathbf{F}}_1((\mathbf{I} + \tilde{\mathbf{F}}_2\tilde{\mathbf{F}}_1)^{-1} - \mathbf{I})\tilde{\mathbf{F}}_2)^{-1}$  and

the strictly lower triangular matrix  $\tilde{\mathbf{F}}_1$  results in a strictly lower triangular matrix. Similarly,  $\mathbf{F}_2$  becomes strictly lower triangular.

## APPENDIX B

### VALIDITY OF REMARK 1 WITHIN OUR LINEAR CODING FRAMEWORK

Let  $(\mathbf{g}_1, \mathbf{F}_1, \mathbf{g}_2, \mathbf{F}_2)$  be the solution tuple of the optimization in (25). Let's consider  $\tilde{P} > P$ . We can always find  $\tilde{\mathbf{g}}_1 = (1 + \epsilon)\mathbf{g}_1$ , where  $\epsilon > 0$  can be chosen to satisfy both  $\mathbb{E}[\|\mathbf{x}_1\|^2] \leq N\tilde{P}$  and  $\mathbb{E}[\|\mathbf{x}_2\|^2] \leq N\tilde{P}$  in (16)-(17). Then, the solution tuple  $(\tilde{\mathbf{g}}_1, \mathbf{F}_1, \mathbf{g}_2, \mathbf{F}_2)$  yields larger  $\text{SNR}_1$  in (23), leading to smaller  $\mathcal{E}_1(\text{SNR}_1)$ . However,  $\mathcal{E}_2(\text{SNR}_2)$  remains the same here since  $\text{SNR}_2$  is not a function of  $\tilde{\mathbf{g}}_1$ . Thus,  $\mathcal{E}_1(\text{SNR}_1) + \mathcal{E}_2(\text{SNR}_2)$  decreases.

## APPENDIX C

### PROOF OF LEMMA 1

*Proof.* We first define the optimal value of  $\max\{\mathbb{E}[\|\mathbf{x}_1\|^2], \mathbb{E}[\|\mathbf{x}_2\|^2]\}$  in (28) with the constraints,  $\text{SNR}_1 = \delta$  and  $\text{SNR}_2 = \eta_2$ , as  $h(\delta, \eta_2)$ . We want to show that  $h(\delta, \eta_2)$  is an increasing function of  $\delta$ .

We show this by contradiction. Suppose that  $h(\delta, \eta_2)$  is not an increasing function of  $\delta$ . This implies that there exist  $\delta_1$  and  $\delta_2$ , such that  $\delta_1 < \delta_2$  and  $h(\delta_1, \eta_2) \geq h(\delta_2, \eta_2)$ . Let us denote the optimal solution tuple that yields  $h(\delta_2, \eta_2)$  and satisfies the constraints,  $\text{SNR}_1 = \delta_2$  and  $\text{SNR}_2 = \eta_2$ , as  $(\mathbf{g}_1, \mathbf{F}_1, \mathbf{g}_2, \mathbf{F}_2)$ . Assuming that  $\mathbf{F}_1, \mathbf{g}_2$ , and  $\mathbf{F}_2$  are fixed, we can find  $\tilde{\mathbf{g}}_1 = (1 - \epsilon)\mathbf{g}_1$ , where  $\epsilon > 0$  is chosen to satisfy  $\text{SNR}_1 = \delta_1 < \delta_2$  in (23). The tuple  $(\tilde{\mathbf{g}}_1, \mathbf{F}_1, \mathbf{g}_2, \mathbf{F}_2)$  satisfies  $\text{SNR}_2 = \eta_2$  since  $\text{SNR}_2$  is not a function of  $\mathbf{g}_1$ . Furthermore, this tuple  $(\tilde{\mathbf{g}}_1, \mathbf{F}_1, \mathbf{g}_2, \mathbf{F}_2)$  yields smaller  $\mathbb{E}[\|\mathbf{x}_1\|^2]$  in (16) and  $\mathbb{E}[\|\mathbf{x}_2\|^2]$  in (17), since  $\|\tilde{\mathbf{g}}_1\|^2 < \|\mathbf{g}_1\|^2$  and  $\|\mathbf{F}_2\tilde{\mathbf{g}}_1\|^2 < \|\mathbf{F}_2\mathbf{g}_1\|^2$ . That is, the tuple  $(\tilde{\mathbf{g}}_1, \mathbf{F}_1, \mathbf{g}_2, \mathbf{F}_2)$  yields a smaller objective value of  $\max\{\mathbb{E}[\|\mathbf{x}_1\|^2], \mathbb{E}[\|\mathbf{x}_2\|^2]\}$ , say  $\nu$ , than the one obtained by  $(\mathbf{g}_1, \mathbf{F}_1, \mathbf{g}_2, \mathbf{F}_2)$ , i.e.,  $\nu < h(\delta_2, \eta_2)$ .

We observe that the tuple  $(\tilde{\mathbf{g}}_1, \mathbf{F}_1, \mathbf{g}_2, \mathbf{F}_2)$  is a feasible solution for the problem in (28) with the constraints,  $\text{SNR}_1 = \delta_1$  and  $\text{SNR}_2 = \eta_2$ , yielding an objective value of  $\nu$ . As  $h(\delta_1, \eta_2)$  defines the optimal (or smallest) objective value for this problem,  $h(\delta_1, \eta_2)$  must be less than or equal to  $\nu$ , i.e.,  $h(\delta_1, \eta_2) \leq \nu$ . Combining with the previous result,  $\nu < h(\delta_2, \eta_2)$ , we then have  $h(\delta_1, \eta_2) \leq \nu < h(\delta_2, \eta_2)$ . This contradicts the statement of  $h(\delta_1, \eta_2) \geq h(\delta_2, \eta_2)$ . Thus,  $h(\delta, \eta_2)$  is an increasing function of  $\delta$ .  $\square$

## APPENDIX D

## PROOF OF PROPOSITION 1

*Proof.* We let  $(\mathbf{g}_1, \mathbf{F}_1, \mathbf{g}_2, \mathbf{F}_2)$  be any feasible solution of (29) with  $\mathbf{F}_2 \in \mathcal{F}_2$ . We want to show that it is optimal that  $f_{2,N} = 0$  in  $\mathbf{F}_2 \in \mathcal{F}_2$  for any feasible solution  $(\mathbf{g}_1, \mathbf{F}_1, \mathbf{g}_2, \mathbf{F}_2)$ . That is, we will show that the objective value obtained from the solution with  $f_{2,N} = 0$  is always smaller than or equal to that with any  $f_{2,N}$ .

First, we let  $\bar{\mathbf{F}}_2$  be equal to  $\mathbf{F}_2$ , except that the last entry of  $\bar{\mathbf{F}}_2$  is zero, i.e.,  $\bar{f}_{2,N} = 0$ . We will show that (i) the solution  $(\mathbf{g}_1, \mathbf{F}_1, \bar{\mathbf{g}}_2, \bar{\mathbf{F}}_2)$  is a feasible solution where  $\bar{\mathbf{g}}_2 = (1 - \epsilon)\mathbf{g}_2$  with some  $\epsilon \in [0, 1)$ , and (ii) the solution  $(\mathbf{g}_1, \mathbf{F}_1, \bar{\mathbf{g}}_2, \bar{\mathbf{F}}_2)$  results in an objective value smaller than or equal to that obtained by  $(\mathbf{g}_1, \mathbf{F}_1, \mathbf{g}_2, \mathbf{F}_2)$ . By showing the two statements above, we show that the feasible solution  $(\mathbf{g}_1, \mathbf{F}_1, \bar{\mathbf{g}}_2, \bar{\mathbf{F}}_2)$  with  $\bar{f}_{2,N} = 0$  always yields a smaller objective value than that obtained by any feasible solution  $(\mathbf{g}_1, \mathbf{F}_1, \mathbf{g}_2, \mathbf{F}_2)$ , implying that it is optimal that  $f_{2,N} = 0$  in  $\mathbf{F}_2 \in \mathcal{F}_2$  in (29).

**Proof of Statement (i):** Since  $(\mathbf{g}_1, \mathbf{F}_1, \mathbf{g}_2, \mathbf{F}_2)$  is a feasible solution, it satisfies the constraints for  $\text{SNR}_1$  and  $\text{SNR}_2$  in (29). First, for  $\text{SNR}_2$ , using (23) and (18), we get

$$\begin{aligned} \text{SNR}_2 = \eta_2 &= \mathbf{g}_2^\top (\mathbf{F}_2 \mathbf{F}_2^\top \sigma_1^2 + \sigma_2^2 \mathbf{I})^{-1} \mathbf{g}_2 \\ &\leq \mathbf{g}_2^\top (\bar{\mathbf{F}}_2 \bar{\mathbf{F}}_2^\top \sigma_1^2 + \sigma_2^2 \mathbf{I})^{-1} \mathbf{g}_2. \end{aligned} \quad (81)$$

In (81), we can always choose  $\bar{\mathbf{g}}_2 = (1 - \epsilon)\mathbf{g}_2$  with  $\epsilon \in [0, 1)$  that satisfies  $\bar{\mathbf{g}}_2^\top (\bar{\mathbf{F}}_2 \bar{\mathbf{F}}_2^\top \sigma_1^2 + \sigma_2^2 \mathbf{I})^{-1} \bar{\mathbf{g}}_2 = \eta_2$ . This implies that  $(\mathbf{g}_1, \mathbf{F}_1, \bar{\mathbf{g}}_2, \bar{\mathbf{F}}_2)$  satisfies the constraint for  $\text{SNR}_2$ . The constraint for  $\text{SNR}_1$  is also satisfied with  $(\mathbf{g}_1, \mathbf{F}_1, \bar{\mathbf{g}}_2, \bar{\mathbf{F}}_2)$  since  $\text{SNR}_1$  relies on  $\mathbf{Q}_1$  in (20) and we have  $\mathbf{F}_1 \mathbf{F}_2 = \mathbf{F}_1 \bar{\mathbf{F}}_2$ . Therefore,  $(\mathbf{g}_1, \mathbf{F}_1, \bar{\mathbf{g}}_2, \bar{\mathbf{F}}_2)$  is a feasible solution of (29).

**Proof of Statement (ii):** First,  $(\mathbf{g}_1, \mathbf{F}_1, \bar{\mathbf{g}}_2, \bar{\mathbf{F}}_2)$  yields a smaller or an equal transmit power of  $\mathbb{E}[\|\mathbf{x}_2\|^2]$  since

$$\begin{aligned} \mathbb{E}[\|\mathbf{x}_2\|^2] &= \|(\mathbf{I} + \mathbf{F}_2 \mathbf{F}_1) \mathbf{g}_2\|^2 + \|\mathbf{F}_2 \mathbf{g}_1\|^2 + \|\mathbf{F}_2 (\mathbf{I} + \mathbf{F}_1 \mathbf{F}_2)\|_F^2 \sigma_1^2 + \|\mathbf{F}_2 \mathbf{F}_1\|_F^2 \sigma_2^2 \\ &\geq \|(\mathbf{I} + \bar{\mathbf{F}}_2 \mathbf{F}_1) \bar{\mathbf{g}}_2\|^2 + \|\bar{\mathbf{F}}_2 \mathbf{g}_1\|^2 + \|\bar{\mathbf{F}}_2 (\mathbf{I} + \mathbf{F}_1 \bar{\mathbf{F}}_2)\|_F^2 \sigma_1^2 + \|\bar{\mathbf{F}}_2 \mathbf{F}_1\|_F^2 \sigma_2^2. \end{aligned} \quad (82)$$

Note that  $\mathbb{E}[\|\mathbf{x}_1\|^2]$  in (16) are not dependent on  $f_{2,N}$  since  $\mathbf{F}_1 \mathbf{F}_2$  does not include  $f_{2,N}$ .

Therefore, when  $f_{2,N} = 0$ , we can always obtain a smaller or an equal objective value of  $\alpha \mathbb{E}[\|\mathbf{x}_1\|^2] + (1 - \alpha) \mathbb{E}[\|\mathbf{x}_2\|^2]$  in (29), while satisfying the SNR constraints. It is thus optimal to set  $f_{2,N} = 0$  in (29) with  $\mathbf{F}_2 \in \mathcal{F}_2$ .  $\square$

## APPENDIX E

PROOF OF CONJECTURE 1 WHEN  $N = 3$ 

*Proof for  $N = 3$ .* We note that  $\min\{\alpha\sigma_1^2, (1-\alpha)\sigma_2^2\} \leq (1-\alpha)\sigma_2^2$  for any  $\alpha \in (0, 1)$ . In the special case with  $N = 3$ , we will show that  $\nu_{\min}[\mathbf{B}] = (1-\alpha)\sigma_2^2$  for any  $\mathbf{F}_1$  and  $\mathbf{F}_2 \in \mathcal{F}_2$  (in the form of (30)). We first rewrite  $\mathbf{B} = (1-\alpha)\sigma_2^2\mathbf{I} + \mathbf{C}$  where  $\mathbf{C} = (1-\alpha)\sigma_1^2\mathbf{F}_2\mathbf{F}_2^\top + \mathbf{Q}_2^{1/2}(\alpha\mathbf{F}_1^\top\mathbf{F}_1 + (1-\alpha)(\mathbf{F}_2\mathbf{F}_1 + \mathbf{F}_1^\top\mathbf{F}_2^\top + \mathbf{F}_1^\top\mathbf{F}_2^\top\mathbf{F}_2\mathbf{F}_1))\mathbf{Q}_2^{1/2}$ . Then, showing  $\nu_{\min}[\mathbf{B}] = (1-\alpha)\sigma_2^2$  is equivalent to showing  $\nu_{\min}[\mathbf{C}] = 0$ . First, since  $\mathbf{F}_2\mathbf{F}_1 = \mathbf{0}$  due to  $f_{2,3} = 0$  from Proposition 1, we have

$$\mathbf{C} = (1-\alpha)\sigma_1^2\mathbf{F}_2\mathbf{F}_2^\top + \alpha\mathbf{Q}_2^{1/2}\mathbf{F}_1^\top\mathbf{F}_1\mathbf{Q}_2^{1/2}. \quad (83)$$

In (83),  $\mathbf{F}_2\mathbf{F}_2^\top$  and  $\mathbf{Q}_2^{1/2}\mathbf{F}_1^\top\mathbf{F}_1\mathbf{Q}_2^{1/2}$  are positive semidefinite (PSD), respectively, since each of them is a form of a matrix multiplied with its own transpose. Since  $(1-\alpha)\sigma_1^2 > 0$  and  $\alpha > 0$ ,  $(1-\alpha)\sigma_1^2\mathbf{F}_2\mathbf{F}_2^\top$  and  $\alpha\mathbf{Q}_2^{1/2}\mathbf{F}_1^\top\mathbf{F}_1\mathbf{Q}_2^{1/2}$  in (83) are PSD, respectively. Thus, the summation of the two PSD matrices is also PSD, i.e.,  $\mathbf{C}$  is PSD. This implies that  $\nu_{\min}[\mathbf{C}] \geq 0$ . The remaining part to claim  $\nu_{\min}[\mathbf{C}] = 0$  is to show that  $\mathbf{C}$  has an eigenvalue of 0. Since the last ( $N$ -th) column of  $\mathbf{C}$  is a zero vector,  $\mathbf{C}$  has an eigenvalue of 0 with the corresponding eigenvector  $[0, 0, 1]^\top$ , i.e.,  $\mathbf{C}[0, 0, 1]^\top = 0 \cdot [0, 0, 1]^\top$ . We then have  $\nu_{\min}[\mathbf{C}] = 0$ , which leads to  $\nu_{\min}[\mathbf{B}] = (1-\alpha)\sigma_2^2$ .  $\square$

## APPENDIX F

## PROOF OF PROPOSITION 2

*Proof.* We have a lower bound of the objective function in (32) as  $\mathbf{q}_2^\top\mathbf{B}\mathbf{q}_2 \geq \nu_{\min}[\mathbf{B}]\|\mathbf{q}_2\|^2$ . From Conjecture 1, we have  $\nu_{\min}[\mathbf{B}] = (1-\alpha)\sigma_2^2$  when  $\alpha \geq \frac{\sigma_2^2}{\sigma_1^2 + \sigma_2^2}$ . Then, we have the lower bound as  $\mathbf{q}_2^\top\mathbf{B}\mathbf{q}_2 \geq (1-\alpha)\sigma_2^2\|\mathbf{q}_2\|^2$ . Here,  $\mathbf{q}_2^* = [0, \dots, 0, \sqrt{\eta_2}]^\top$  satisfies the lower bound with  $\|\mathbf{q}_2^*\|^2 = \eta_2$ , which can be easily shown by the fact that all the entries in the last column and row of  $\mathbf{B}$  are zeros except the last diagonal entry is  $(1-\alpha)\sigma_2^2$  due to  $f_{2,N} = 0$  from Proposition 1. In other words,  $\mathbf{q}_2^*$  is an optimal solution of (32). We then have the optimal solution for (31) as  $\mathbf{g}_2^* = \mathbf{Q}_2^{1/2}\mathbf{q}_2^* = [0, \dots, 0, \sqrt{\eta_2}\sigma_2]^\top$ , since  $f_{2,N} = 0$  from Proposition 1.  $\square$

## APPENDIX G

## PROOF OF LEMMA 2

*Proof.* We extend the proof of the one-way coding architecture in [17] to the two-way coding architecture. Define the training data tuples as  $\{\mathcal{T}_j\}_{j=1}^J$ , where  $\mathcal{T}_j = \{\mathbf{b}_1^{(j)}, \mathbf{b}_2^{(j)}, \mathbf{n}_1^{(j)}, \mathbf{n}_2^{(j)}\}$  is the  $j$ -th tuple of the training data. Let us denote  $\tilde{\eta}_i^{(j)}[k]$  as the output at timestep  $k$  generated by data  $j$ ,  $\mathcal{T}_j$ , through the User  $i$ 's encoding process of (59)-(61),  $k = 1, \dots, N$ . It is obvious that  $\tilde{\eta}_i^{(j)}[k]$  is independent and identically

distributed (i.i.d.) over  $j$  assuming the data tuples  $\{\mathcal{T}_j\}_{j=1}^J$  are i.i.d. from each other. We define the mean and variance of  $\tilde{\eta}_i^{(j)}[k]$  as  $\mu_{i,k}$  and  $\delta_{i,k}^2$ , respectively. With the sample mean  $m_{i,k}(J) = \frac{1}{J} \sum_{j=1}^J \tilde{\eta}_i^{(j)}[k]$  and the sample variance  $d_{i,k}^2(J) = \frac{1}{J} \sum_{j=1}^J (\tilde{\eta}_i^{(j)}[k] - m_{i,k}(J))^2$ , we define the normalization function as  $\gamma_{i,k}^{(J)}(x) = (x - m_{i,k}(J))/d_{i,k}(J)$ .

Let us define  $\tilde{x}_i[k]$  as the output at timestep  $k$  at User  $i$ , generated by the data tuple for inference,  $\{\mathbf{b}_1, \mathbf{b}_2, \mathbf{n}_1, \mathbf{n}_2\}$ . Assuming the training and inference data tuples are extracted from the same distribution, the mean and variance of  $\tilde{x}_i[k]$  are then  $\mu_{i,k}$  and  $\delta_{i,k}^2$ , respectively. We then have  $\mathbb{E}_{\mathbf{b}_1, \mathbf{b}_2, \mathbf{n}_1, \mathbf{n}_2} [(\gamma_{i,k}^{(J)}(\tilde{x}_i[k]))^2] = \frac{\delta_{i,k}^2 + (m_{i,k}(J) - \mu_{i,k})^2}{d_{i,k}^2(J)}$ . By the strong law of large number (SLLN) [32],  $m_{i,k}(J) \rightarrow \mu_{i,k}$  and  $d_{i,k}^2(J) \rightarrow \delta_{i,k}^2$  almost surely (a.s.) as  $J \rightarrow \infty$ . Then, by continuous mapping theorem [32],  $\mathbb{E}_{\mathbf{b}_1, \mathbf{b}_2, \mathbf{n}_1, \mathbf{n}_2} [(\gamma_{i,k}^{(J)}(\tilde{x}_i[k]))^2] \rightarrow 1$  a.s. as  $J \rightarrow \infty$ . Then,  $\mathbb{E}_{\mathbf{b}_1, \mathbf{b}_2, \mathbf{n}_1, \mathbf{n}_2} [\sum_{k=1}^N x_i^2[k]] = \sum_{k=1}^N w_i^2[k] \mathbb{E}_{\mathbf{b}_1, \mathbf{b}_2, \mathbf{n}_1, \mathbf{n}_2} [(\gamma_{i,k}^{(J)}(\tilde{x}_i[k]))^2] \rightarrow NP$  a.s. as  $J \rightarrow \infty$ .  $\square$

## APPENDIX H

### DERIVATION FOR $\Phi_i(\mathbf{f}_{1,i})$ IN (42)

We express each of the terms of  $\mathbb{E}[\|\mathbf{x}_1\|^2]$  in (35) as follows:

$$\|\mathbf{q}_1^\top (\mathbf{I} + \mathbf{F}_1 \mathbf{F}_2)\|^2 \sigma_1^2 = \sigma_1^2 \left( \sum_{i=2}^{N-1} (q_{1,i-1} + f_{2,i} \mathbf{h}_i^\top \mathbf{f}_{1,i})^2 + q_{1,N-1}^2 + q_{1,N}^2 \right) \quad (84)$$

where  $\mathbf{q}_1^\top (\mathbf{I} + \mathbf{F}_1 \mathbf{F}_2) = [q_{1,1} + f_{2,2} \mathbf{h}_2^\top \mathbf{f}_{1,2}, q_{1,2} + f_{2,3} \mathbf{h}_3^\top \mathbf{f}_{1,3}, \dots, q_{1,N-2} + f_{2,N-1} \mathbf{h}_{N-1}^\top \mathbf{f}_{1,N-1}, q_{1,N-1}, q_{1,N}]$ ,

$$\|\mathbf{q}_1^\top \mathbf{F}_1\|^2 \sigma_2^2 = \sigma_2^2 \sum_{i=1}^{N-1} (\mathbf{h}_i^\top \mathbf{f}_{1,i})^2, \quad (85)$$

$$\|\mathbf{F}_1 \mathbf{F}_2\|_F^2 \sigma_1^2 = \sigma_1^2 \text{tr}((\mathbf{F}_1 \mathbf{F}_2)^\top \mathbf{F}_1 \mathbf{F}_2) = \sigma_1^2 \sum_{i=2}^{N-1} f_{2,i}^2 \mathbf{f}_{1,i}^\top \mathbf{f}_{1,i}, \quad (86)$$

$$\|\mathbf{F}_1\|_F^2 \sigma_2^2 = \sigma_2^2 \text{tr}(\mathbf{F}_1^\top \mathbf{F}_1) = \sigma_2^2 \sum_{i=1}^{N-1} \mathbf{f}_{1,i}^\top \mathbf{f}_{1,i}. \quad (87)$$

With (84)-(87), we represent  $\mathbb{E}[\|\mathbf{x}_1\|^2]$  as

$$\begin{aligned} \mathbb{E}[\|\mathbf{x}_1\|^2] &= \sigma_1^2 \left( \sum_{i=2}^{N-1} (q_{1,i-1} + f_{2,i} \mathbf{h}_i^\top \mathbf{f}_{1,i})^2 + q_{1,N-1}^2 + q_{1,N}^2 \right) \\ &\quad + \sigma_2^2 \sum_{i=1}^{N-1} (\mathbf{h}_i^\top \mathbf{f}_{1,i})^2 + \sigma_1^2 \sum_{i=2}^{N-1} f_{2,i}^2 \mathbf{f}_{1,i}^\top \mathbf{f}_{1,i} + \sigma_2^2 \sum_{i=1}^{N-1} \mathbf{f}_{1,i}^\top \mathbf{f}_{1,i} \end{aligned} \quad (88)$$

$$\begin{aligned} &= (\mathbf{h}_1^\top \mathbf{f}_{1,1})^2 \sigma_2^2 + \sum_{i=2}^{N-1} \left( (q_{1,i-1} + f_{2,i} \mathbf{h}_i^\top \mathbf{f}_{1,i})^2 \sigma_1^2 + (\mathbf{h}_i^\top \mathbf{f}_{1,i})^2 \sigma_2^2 + \mathbf{f}_{1,i}^\top \mathbf{f}_{1,i} (f_{2,i}^2 \sigma_1^2 + \sigma_2^2) \right) \\ &\quad + \sigma_1^2 (q_{1,N-1}^2 + q_{1,N}^2). \end{aligned} \quad (89)$$

We note that equation (89) is equivalent to equation (42).

## APPENDIX I

## DERIVATION OF (44) FROM (43)

To satisfy the equality in (43), we must have

$$(f_{2,i}^2\sigma_1^2 + \sigma_2^2)(\mathbf{h}_i\mathbf{h}_i^\top + \mathbf{I})\mathbf{f}_{1,i} = -q_{1,i-1}f_{2,i}\sigma_1^2\mathbf{h}_i. \quad (90)$$

Finally, the optimal solution form of  $\mathbf{f}_{1,i}$ ,  $i \in \{2, \dots, N-1\}$ , is given in terms of the entries of  $\mathbf{q}_1$  (encapsulated in  $\mathbf{h}_i$  according to (41)) as follows:

$$\begin{aligned} \mathbf{f}_{1,i} &= -\frac{q_{1,i-1}f_{2,i}\sigma_1^2}{f_{2,i}^2\sigma_1^2 + \sigma_2^2}(\mathbf{h}_i\mathbf{h}_i^\top + \mathbf{I})^{-1}\mathbf{h}_i \\ &\stackrel{(i)}{=} -\frac{q_{1,i-1}f_{2,i}\sigma_1^2}{f_{2,i}^2\sigma_1^2 + \sigma_2^2}\left(\mathbf{I} - \frac{\mathbf{h}_i\mathbf{h}_i^\top}{1 + \|\mathbf{h}_i\|^2}\right)\mathbf{h}_i \\ &= -\frac{f_{2,i}\sigma_1^2}{f_{2,i}^2\sigma_1^2 + \sigma_2^2}\frac{q_{1,i-1}}{1 + \|\mathbf{h}_i\|^2}\mathbf{h}_i, \end{aligned} \quad (91)$$

where the Sherman–Morrison formula is used to obtain equality (i) in (91).

## APPENDIX J

DERIVATION FOR  $\alpha\frac{\partial\mathbb{E}[\|\mathbf{x}_1\|^2]}{\partial f_{2,i}} + (1-\alpha)\frac{\partial\mathbb{E}[\|\mathbf{x}_2\|^2]}{\partial f_{2,i}}$  IN (50)

From the equation of  $\mathbb{E}[\|\mathbf{x}_1\|^2]$  in (42), we can readily obtain

$$\frac{\partial\mathbb{E}[\|\mathbf{x}_1\|^2]}{\partial f_{2,i}} = 2q_{1,i-1}\mathbf{h}_i^\top\mathbf{f}_{1,i}\sigma_1^2 + 2\sigma_1^2(|\mathbf{h}_i^\top\mathbf{f}_{1,i}|^2 + \|\mathbf{f}_{1,i}\|^2)f_{2,i}, \quad i \in \{2, \dots, N-1\}. \quad (92)$$

For  $\mathbb{E}[\|\mathbf{x}_2\|^2]$ , we first express each of the terms including  $\mathbf{F}_2$  in  $\mathbb{E}[\|\mathbf{x}_2\|^2]$  of (36) as a sum of entries of  $\mathbf{F}_2$ , i.e.,  $\{f_{2,i}\}_{i=2}^{N-1}$ . First, revisiting the second term in (36), we obtain

$$\|\mathbf{F}_2\mathbf{Q}_1^{1/2}\mathbf{q}_1\|^2 = \mathbf{q}_1^\top\mathbf{Q}_1^{1/2}\mathbf{F}_2^\top\mathbf{F}_2\mathbf{Q}_1^{1/2}\mathbf{q}_1 = \mathbf{p}^\top\mathbf{F}_2^\top\mathbf{F}_2\mathbf{p} = \sum_{i=2}^N p_{i-1}^2 f_{2,i}^2, \quad (93)$$

where we assumed that  $\mathbf{p} \triangleq \mathbf{Q}_1^{1/2}\mathbf{q}_1 = [p_1, \dots, p_N]^\top$  is fixed for tractability although  $\mathbf{Q}_1^{1/2}$  depends on  $\mathbf{F}_2$ . We then express the third term in (36) as

$$\|\mathbf{F}_2(\mathbf{I} + \mathbf{F}_1\mathbf{F}_2)\|_F^2\sigma_1^2 = \sigma_1^2\sum_{i=2}^N f_{2,i}^2 + \sigma_1^2\sum_{i=2}^{N-2}\sum_{j=i+1}^{N-1} f_{1,j,i}^2 f_{2,i}^2 f_{2,j+1}^2. \quad (94)$$

Also, the last term in (36) can be expressed as

$$\|\mathbf{F}_2\mathbf{F}_1\|_F^2\sigma_2^2 = \sigma_2^2\sum_{i=3}^N f_{2,i}^2\sum_{j=1}^{i-2} f_{1,i-1,j}^2. \quad (95)$$

We take the derivative to the terms (93)-(95) with respect to  $f_{2,i}$ . Accordingly, we obtain

$$\frac{\partial\mathbb{E}[\|\mathbf{x}_2\|^2]}{\partial f_{2,i}} = 2p_{i-1}^2 f_{2,i} + 2\sigma_1^2 f_{2,i} + 2\sigma_1^2\left(\sum_{j=i+1}^{N-1} f_{1,j,i}^2 f_{2,j+1}^2 + \sum_{k=2}^{i-2} f_{1,i-1,k}^2 f_{2,k}^2\right) + 2\sigma_2^2\sum_{j=1}^{i-2} f_{1,i-1,j}^2, \quad (96)$$

for  $i \in \{2, \dots, N-1\}$ . Using (92) and (96), we obtain  $\alpha\frac{\partial\mathbb{E}[\|\mathbf{x}_1\|^2]}{\partial f_{2,i}} + (1-\alpha)\frac{\partial\mathbb{E}[\|\mathbf{x}_2\|^2]}{\partial f_{2,i}}$  in (50).